THE GRADUATE COLLEGE
WESTERN MICHIGAN UNIVERSITY
KALAMAZOO, MICHIGAN

Date 6-21-83

WE HEREBY APPROVE THE THESIS SUBMITTED BY

Steven James Hoin

ENTITLED A HIGH RESOLUTION GROUND MAGNETIC STUDY OF PART OF THE ALBION-SCIPIO TREND

AS PARTIAL FULFILLMENT OF THE REQUIREMENTS FOR THE DEGREE OF Master of Science

Geology
(Department)

William A. Sauck
Major Thesis Adviser

W. Thomas Straw
Thesis Committee Member

Christopher Schmidt
Thesis Committee Member

APPROVED

Laurel Kotzmacher
Dean of The Graduate College

Date August 1983

A HIGH RESOLUTION GROUND MAGNETIC STUDY OF PART OF THE ALBION-SCIPIO TREND

By

Steven James Hoin

A Thesis
Submitted to the
Faculty of the Graduate College
in partial fulfillment
of the
requirements for the
Degree of Master of Science
Department of Geology

Western Michigan University
Kalamazoo, Michigan
August, 1983

ACKNOWLEDGEMENTS

This project was funded with a grant from the Hunt Energy Corporation, and was conducted in cooperation with the Michigan Department of Natural Resources, Geological Survey Division. I would like to thank Dr. William A. Sauck for his enthusiastic support throughout the duration of the project. He organized and developed many of the ideas and techniques used in the study. I would also like to thank Dr. Thomas Straw, and Dr. Christopher Schmidt for their advice and recommendations. Special thanks are extended to David Snyder who initiated the project while with the Michigan Department of Natural Resources, Geologic Survey Division. Boyd K. Parker donated much of his time and expertise during the data collection stage while working for the Michigan Geologic Survey. I would also like to thank Stan Leja and Mark Parrish, fellow students, who helped in the task of data collection. Last but certainly not least, I would like to express my deepest appreciation to my wife Paulette. Her care and patience were crucial during all aspects of the study.

Steven James Hoin

TABLE OF CONTENTS

TABLE OF CONTENTS (cont'd)

TABLE OF CONTENTS (cont'd)

LIST OF FIGURES

LIST OF ENCLOSURES

Enclosure

1. Base map of field area showing magnetometer base stations
2. Residual ground magnetic map of the Albion-Scipio Trend
3. Interpretive residual ground magnetic map of the Albion Scipio Trend

LIST OF TABLES

INTRODUCTION

The Albion-Scipio Trend is Michigan's most productive oil field. Annual production during 1979 amounted to 1,409,306 BBL of oil, and 6,673,294 MCF of gas (Ells, 1980). Of the total production in Michigan through 1979, the Albion-Scipio Trend has yielded 14.6% of all oil, and 12.2% of all gas. The trend consists of several linear separate oil fields with a cumulative length of about 35 miles (57 km.), and an average width of less than one mile (1.6 km.).

Published geophysical and geological investigations have met with limited success in delineating the trend. Many authors (Ells, 1962; Merritt, 1968; Buehner and Davis, 1968; Shaw, 1975; Harding, 1974) suggest, on the basis of various data, basement faulting as the controlling factor in the trend formation.

The objective of this investigation was to develop an inexpensive geophysical method that would be capable of detecting the presence of basement structure associated with the Albion-Scipio Trend. For this reason, and because of the relatively shallow, and structurally simple sedimentary cover in this portion of the Michigan Basin, a magnetic survey was chosen as the method of investigation. A ground magnetic survey was chosen in preference to an aeromagnetic survey because of inherent advantages in ground surveys, when compared to aeromagnetic surveys. Some of the advantages are:

1) Ground surveys over small areas can be considerably cheaper than aeromagnetic surveys when coverage is dense, and 2) Assuming a small body, anomaly amplitude decreases according to the inverse cube of the distance from the body. Thus, a ground survey will have a significant increase in resolution. This should aid in detecting the subtle structures expected in the area.

Some of the disadvantages are: 1) Increased noise caused by the proximity of cultural objects and magnetic material in the glacial cover, 2) Decreased speed because of ground transportation, and 3) Erratic coverage caused by the inaccessability of private land.

The investigation used a technique whereby two magnetometers, one mobile, and one stationary, were employed. Radio communication was maintained between the magnetometer stations, and simultaneous readings were taken at each station. More detailed information on field procedures will be given in the appropriate section.

Location and History

The survey covered an area of roughly 426 square miles (1100 sq. km.) in portions of Calhoun, Jackson, Hillsdale, and Branch Counties (Figure 1). The first commercially successful well in the Albion-Scipio Trend was the Perry-Houseknecht No. 1. This well was completed in 1957 flowing at 150 BOPD (Ives and Ells, 1958).

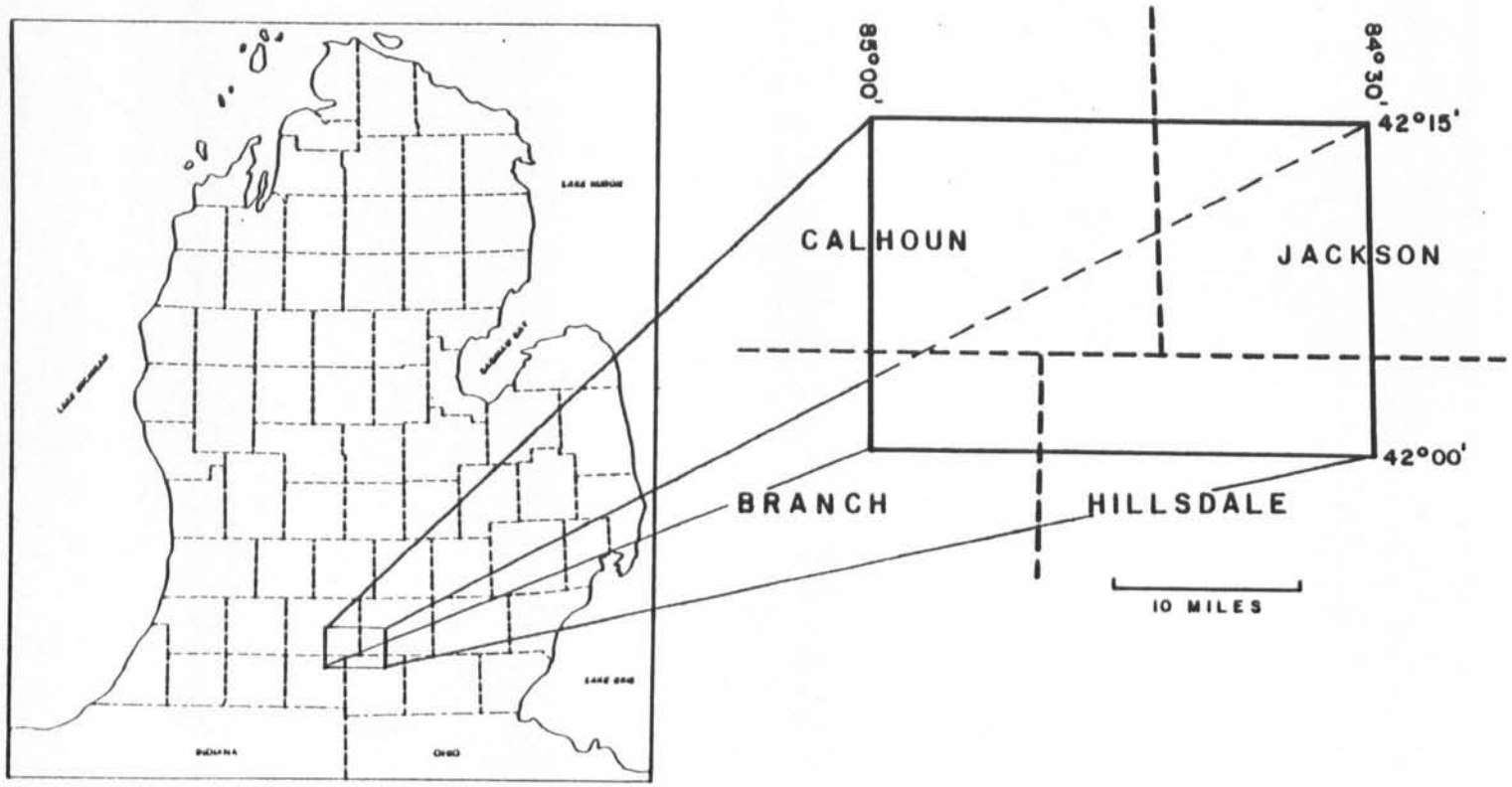

Fig. 1. Location map of the study area.

The fourth well following the discovery well was the Stephens No. 1. This well flowed out of control for 25 hours, losing an estimated 4000 BBL of oil. The gusher stimulated drilling and the Scipio Field was established. In late 1958 a new commercial well was discovered about 12 miles to the northwest of the Scipio Field. This new discovery, along with subsequent wells were designated the Albion Field. At about the same time a new well was discovered in Pulaski Township midway between the Albion and the Scipio Fields. The excellent alignment of wells was noticed and stepout drilling on 20 acre parcels began (Beghini and Conroy, 1966). This 'on trend drilling' (Ells, 1962) led to the eventual development of the present day Albion-Scipio Trend.

Physiography

The elevations in the survey area range from just over 900 feet in the northwest corner to over 1200 feet above mean sea level (MSL) in the southeast. The relief is typical of most of the central southern peninsula of Michigan, and other glaciated areas. Smooth rolling hills dominate the central and southern portions of the area, with more level topography toward the southwest and west. Nearly all of the land is used for agriculture, with small lakes, wetlands, and wooded areas interspersed among the farms.

Previous Work

Considering the economic importance of the Albion-Scipio trend, little published work exists pertaining to the area. Ells has been

the principle author, following the field development from the first discovery in 1957 up to a recently published article (Ives and Ells, 1958; Ells and Layton 1968; Ells and Champion, 1975; Ells, 1980). The first detailed study of the area was published by Ells (1962). It consisted of isopach maps of the major formations in the area along with other valuable data. Beghini and Conroy, (1966), gave a detailed description of reservior characteristics. Shaw (1975) completed a comprehensive study of the area. He analyzed well logs and cores, and found evidence for vertical displacement associated with the trend. There have been many ideas proposed regarding faulting. Harding (1974) and Buehner and Davis (1968) attribute field structures to wrench faulting. Ells (1962) also mentions the possibility of some strike-slip displacement. Merritt (1968), Ells (1969), Hinze et al. (1975), and Hinze and Merritt (1969) suggest that the trend is controlled by vertical faulting. Hinze et al. (1971) compiled Bouguer gravity (Figure 2) and residual aeromagnetic (Figure 3) maps of the Michigan Basin. A detailed study of the basement structure in southern Michigan was completed by Kellogg (1971). The aeromagnetic map produced during this study reveals some regional anomalies within the study area. Published geophysical work pertaining directly to the trend is lacking. A detailed gravity survey across the trend was carried out by Merritt (1968). The results show a change in Bouguer gravity gradient coincident with the trend. A ground magnetic map of a major portion of the trend was produced by Jenny (1961).

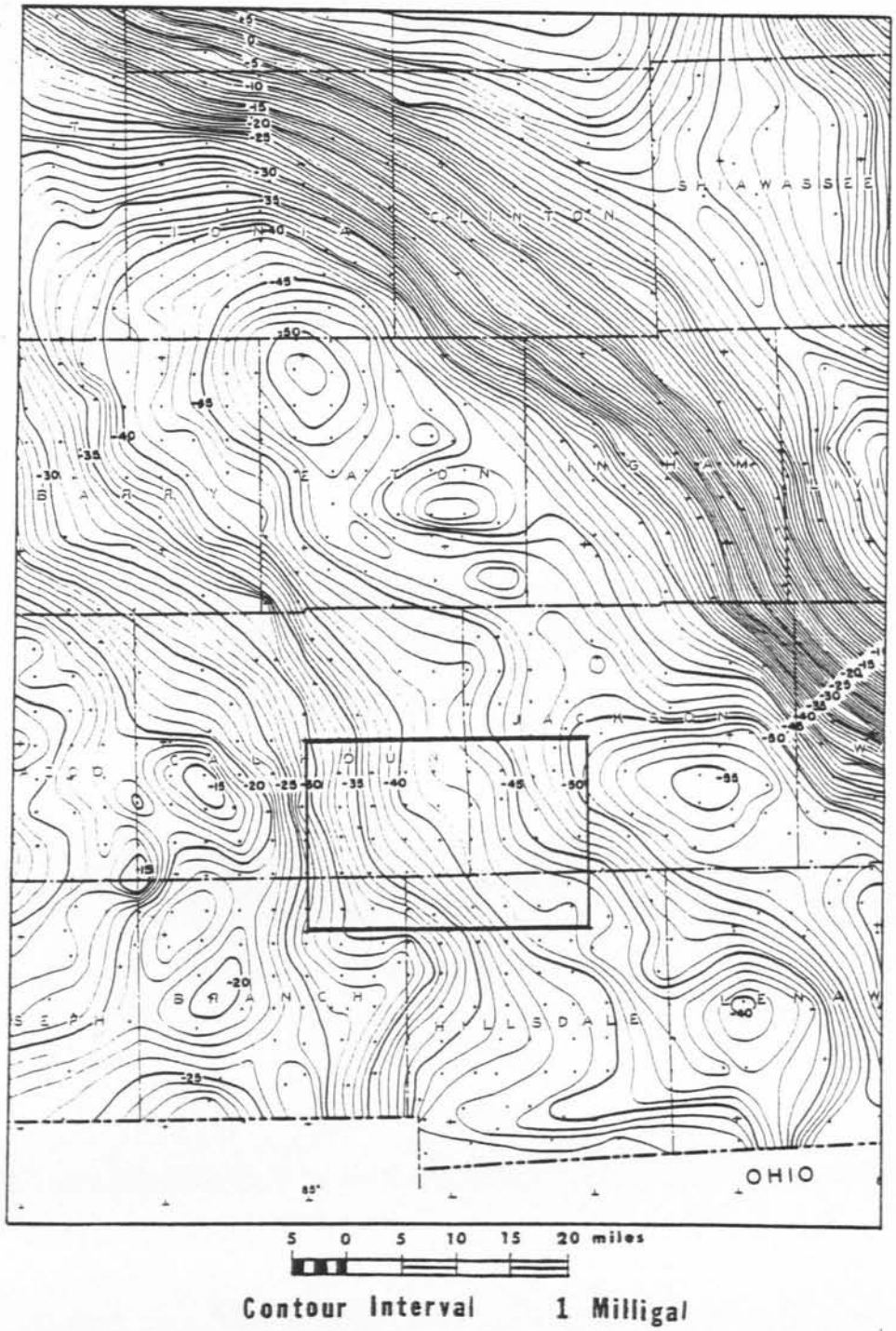

Fig. 2. Portion of the Bouger Gravity Anomaly Map of the Southern Peninsula of Michigan, including the survey area, after Hinze et al. (1971).

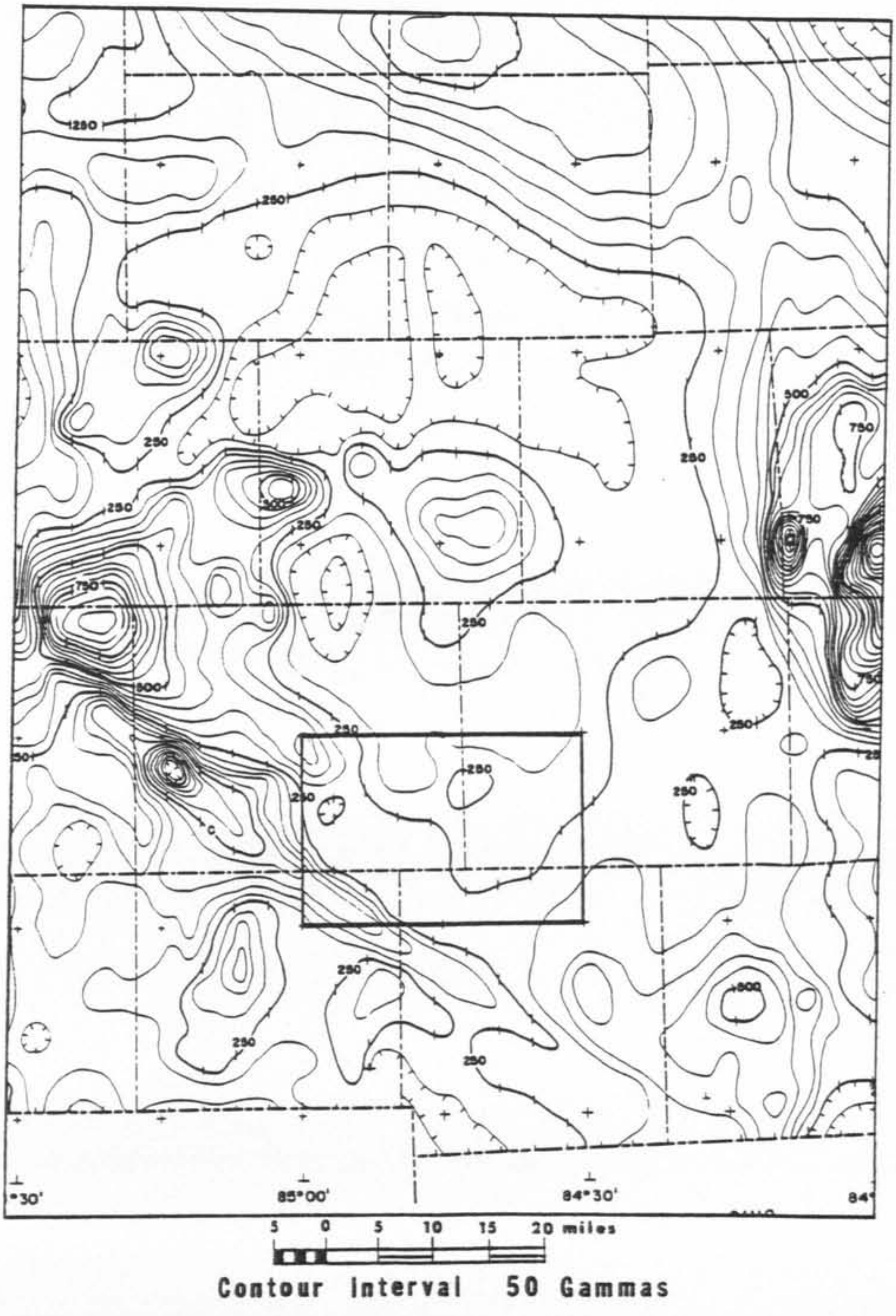

Fig. 3. Portion of the Total Magnetic Intensity Anomaly Map of Michigan, showing the survey area, after Hinze et al. (1971).

Ground Magnetic Surveys

With the advent of the total field magnetometer and accurately controlled flight, the ground magnetic method as a petroleum industry exploration tool has been all but eliminated. Dobrin (1960), documented some examples of ground magnetic surveys for petroleum exploration. These cases involve the use of a vertical component magnetometer, and most examples involve unconventional or rare geologic situations, such as porous serpentine plugs or large displacement faults. The map produced by Jenny (1961) was contoured using a 25 gamma contour interval, and it lacks the detail needed to discern trend structures. More recently Shaw (1971) completed a mobile ground magnetic survey across the lower peninsula of Michigan. He was able to delineate some regional susceptibility contrasts.

GENERAL GEOLOGY

Regional Geology

The Michigan basin is part of a large stable area located in the midwestern United States. The structural basin is surrounded by major geologic features which define the basin framework (Cohee and Landes, 1958). The northern boundary is formed by the complex Pre-Cambrian rocks of the Lake Superior syncline, which are part of the mid-continent rift system (Halls, 1978). The western boundary of the basin is the Wisconsin arch. This structure continues through nearly all of central Wisconsin. The south is defined by the Kankakee Arch in Indiana, and the Findlay Arch in northwestern Ohio. The Algonquin Axis, which may be fault controlled (Fisher, 1969), marks the eastern border in Ontario, Canada. This arch is separated from the Findlay Arch by the Chatam Sag. Figure 4 shows the tectonic framework of the basin. Lockett (1947) suggests that the surrounding positive structural features are underlain by Pre-Cambrian mountain cores. Rudmann et al. (1965) concluded on the basis of seismic data that the Ohio Platform is a basement high separating the Michigan and Indiana basins.

Based on the structure map of the top of the Trenton Limestone (Cohee and Landes, 1958), the Phanerozoic basin can be described as an elliptical sedimentary basin, with a slight northwest elongation, The sediments of the basin dip toward multiple deponcenters (where

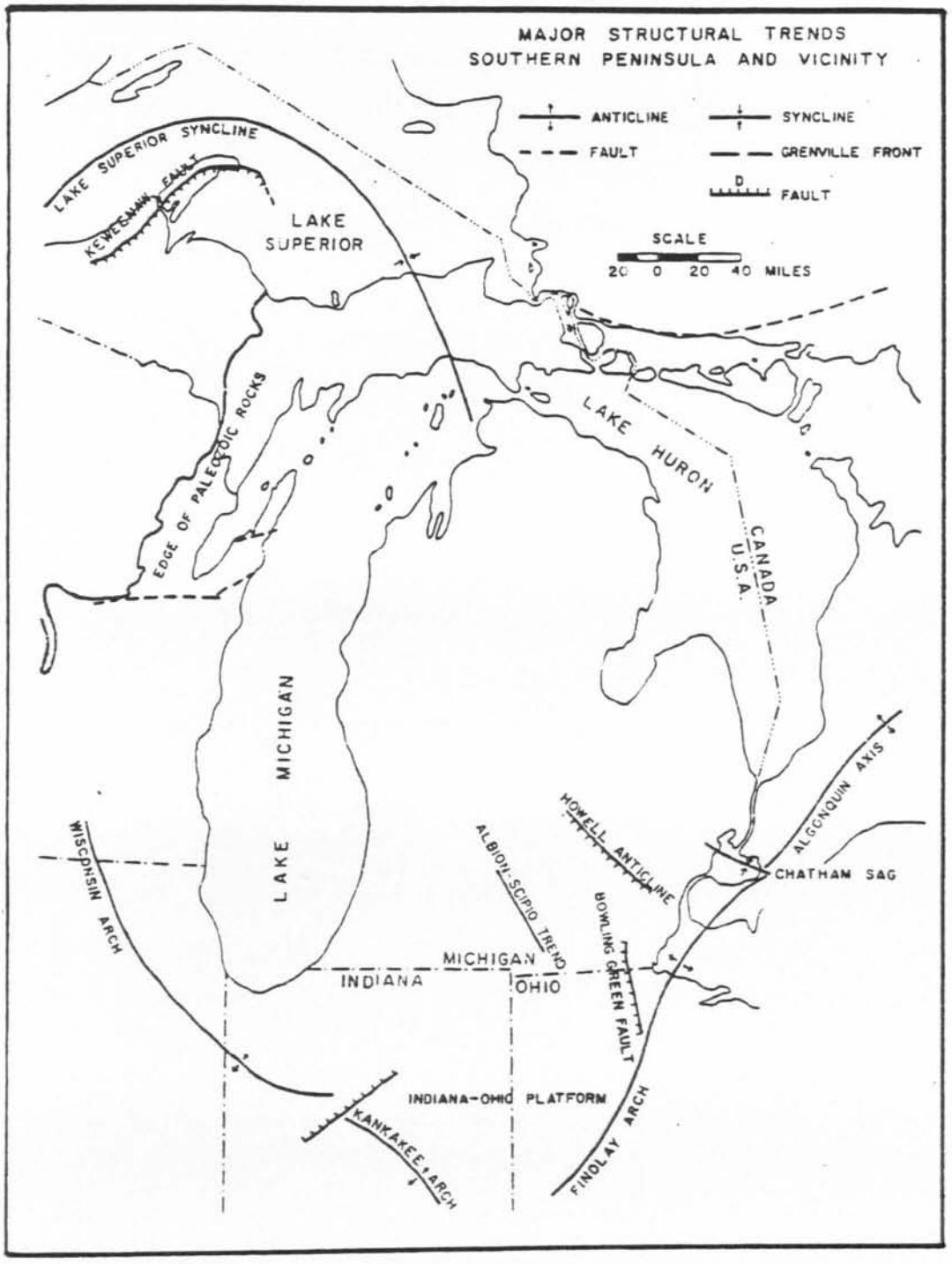

Fig. 4. Tectonic framework of the Michigan Basin, after Kellogg(1971).

most rocks are thickest) at a rate of 25 to 60 feet per mile (Ells, 1969). The Paleozoic rocks of the basin consist of a thick Cambrian sandstone sequence, a lower Ordovician to Mid-Devonian carbonate and evaporite sequence, an Upper Devonian-Mississippian sandstone and shale sequence, and a Pennsylvanian coal sequence (Shaw, 1975).

A dominance of Middle Ordovician to Mississippian northwest-southeast trending folds and faults was noted very early by Newcombe (1933), and Pirtle (1932). The Washtenaw Anticlinorium as defined by Ells (1969), is located in the southeastern corner of Michigan. This structure includes many prominent northwest-southeast trending structures, such as the Howell and the Freedom Anticlines and the Lucas Monocline. In southwestern Michigan the Albion-Scipio Trend is a very conspicuous northwest-southeast trending structure. Regional geophysical data also confirms the northwest-southeast trend (Hinze and Merritt, 1969). Several authors (Cohee and Landes, 1958; Hinze, 1963; Hinze and Merritt, 1969) suggest basement control of the folds and faults.

Basement Geology

The most recent basement configuration map was produced by Hinze et al. (1975). It is based on 19 poorly distributed basement drill holes and depths interpreted from a total magnetic intensity anomaly map (Hinze et al., 1971). The basement map (Figure 5) depicts the Pre-Cambrian basement as a rather uniform oval depression,

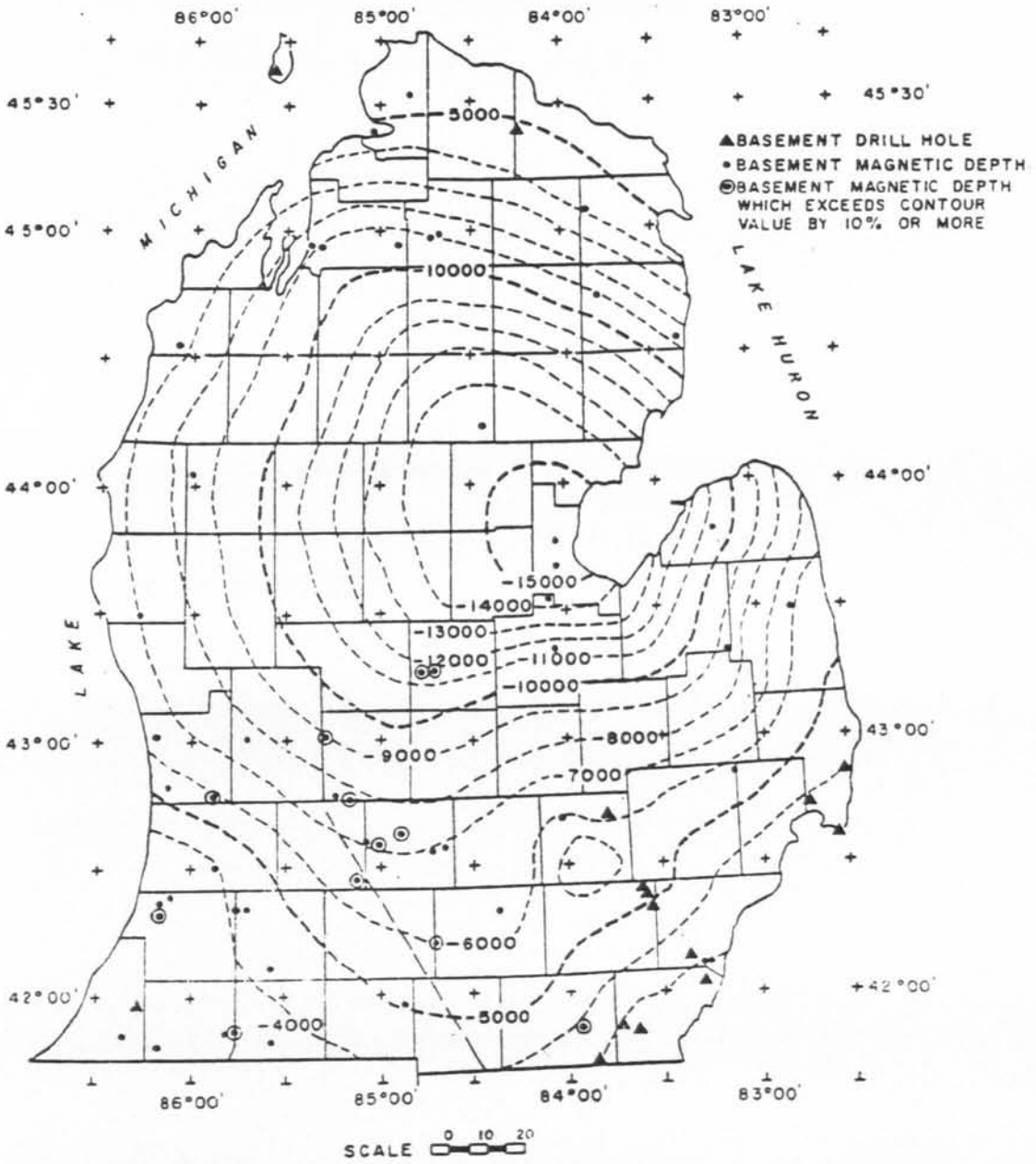

Fig. 5. Basement configuration of Michigan, from Hinze et al. (1971).

with a maximum depth of 15,000 feet (4.5 km.) below MSL near the center of Bay County. A recent Gratiot County drill hole penetrated slightly over 12,000 feet (3700 meters) of Paleozoic sediments, and this value is compatible with the map produced by Hinze et al. (1975). The few existing basement drill holes encountered granite, granite gneiss, granite regolith, some mafic gneisses, and a few holes penetrated metasediments. The few mafic rocks drilled tend to occur within the Mid-Michigan positive Bouguer gravity anomaly. This gravity map was prepared by Hinze et al. (1971). The McLure-Sparks et al. #1-8 Gratiot County drill hole encountered a Metabasic rock at 17,224 feet (5.3 km.), which has been identified as an altered lava flow with Keweenawan affinites (Vander Voo and Watts, 1978). A drill hole on Presque Isle County bottomed in a metamorphosed lava (greenstone) (Hinze et al., 1975).

Gravity (Hinze, 1963) and magnetic (Kellogg, 1971) studies indicate that basement lithologies in the Michigan Basin are more complex than represented by drill holes. The Mid-Michigan Bouguer gravity anomaly transects the basin from Grand Traverse Bay to Lake St. Clair, with a positive Bouguer gravity anomaly in excess of 15 milligals in the center of the state. The total magnetic intensity anomaly map is characterized by numerous high amplitude and/or steep gradient anomalies. A basement province map (Figure 6) was constructed by Kellogg (1971) using magnetic and gravity data along with geophysical trend maps and isotopic age dates. The Albion-Scipio

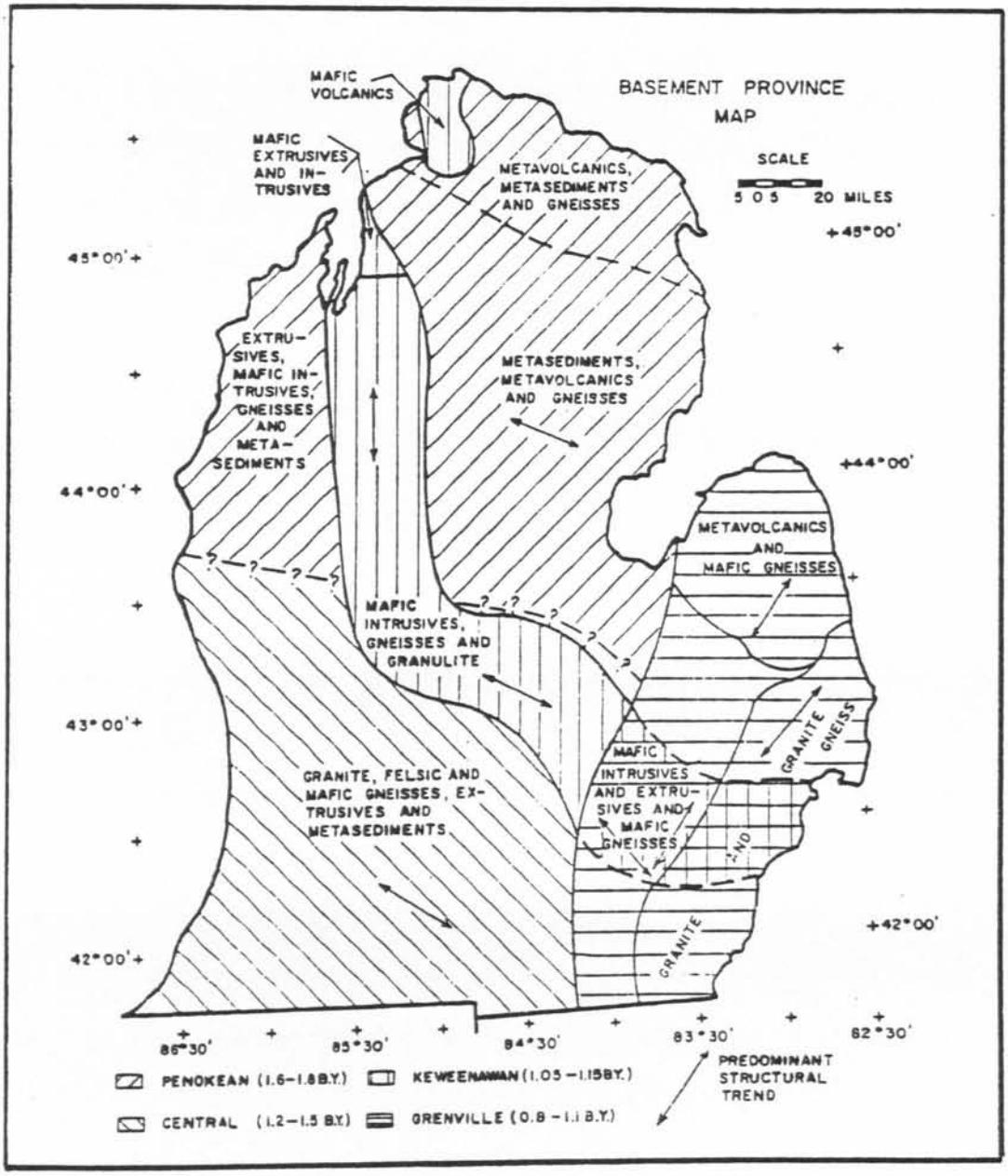

Fig. 6. Basement Province Map of Michigan, from Kellogg, (1971).

Trend is located in the central province of this map. This province occupies the southern half of the Michigan Basin along with much of the Midwestern United States (Engel, 1963). It is characterized by age dates of 1.2-1.5 BY., and rocks of granitic and rhyolitic composition (O'Hara nad Hinze, 1972). The Keweenawan province is mapped coincident with the gravity anomaly, and is terminated in the southeast by the Grenville province. The Keweenawan province has been identified as a paleo rift by many authors (Hinze, et al. 1975; Halls, 1978; Kellogg, 1971). Hinze et al. (1975) noted some significant complications associated with the rift zone. He noted a lack of basaltic rock from drill holes within the Mid-Michigan gravity high. He also noticed the variation of the magnetic intensity anomaly map within the rift zone. The magnetic anomalies do not follow the gravity high as clearly as in the Mid-Continent rift zone. Drill holes within the flanking gravity minima have not encountered thick clastic wedges. He proposed a number of models to explain the rift zone. One of the models shows the rift composed of high grade metamorphic rocks as a result of crustal deformation of mafic intrusives. The other models characterize the rift as basalt-filled grabens, with or without downwarping of the Mohorovicic discontinuity. A more recent model (Fowler and Kuenzi, 1978) depicts the basement as a foundered protoceanic basin with thick clastic wedges and central basaltic through. This interpretation is based on the sedimentary analysis of Pre-Cambrian red mudstones and sandstone from the Gratiot County deep drill hole. The COCORP deep

reflection seismic study across the central rift system (Jensen et al., 1979) clearly reveals the rift zone. The rift zone appears as a broad synform approximately 37 miles (60 km.) wide. Discontinuities and seismic velocities suggest normal faulting flanking a sequence of interbedded clastics and volcanics, and underlying horizons.

Keweenawan rifting in Michigan is associated with the similar well documented rifting event in the Central United States (Thiel, 1956; King and Zeitz, 1971). Cambray, (1979) suggested that the Mid-Continent rift system, the Mid-Michigan rift and a third suspected paleo rift, the Kapuskasing Horst system of Canada, may be part of an ancient (RRR) type triple junction.

Tectonic History

The tectonic history of the Michigan Basin is not yet clarified. A simple subsidence of the basin in the response to thermal contraction following rifting as proposed by Hinze and Merritt (1969), seems unlikely. Sleep and Sloss (1978) postulated at least two thermal events, based on paleomagnetic dates (Vander Voo and Watts, 1978) and petrology (Honnorez, 1978) of rocks in the Gratiot County drill hole. Catacosinos (1973) documents major Cambrian uplift, indicating some tectonic or thermal event. Further subsidence events have been postulated by Cohee and Landes (1958), and Sleep and Sloss (1978) because of variations in sedimentary thickness in the basin.

Albion-Scipio Geology

The Albion-Scipio Trend reservoir consists of a dolomitized zone of the limestone portion of the Trenton-Black River interval (Figure 7) of the Michigan Basin (Ells, 1962). The interval is approximately 600 feet (183 meters) thick within the trend. Isopach maps of the interval indicate that the thickness of the interval does not deviate at the trend.

Trend structures are subtle. A shallow depression (Shaw, 1975), or syncline (Ells, 1962) is directly related to the producing zone, and discontinuities in the depression correlate to non-producing zones. The average relief along the depression is only 50 feet (15.2 meters), thus the structure is not easily detected using seismic methods. The depression is attributed to collapse following dolomitization (Shaw, 1975). He also dated the collapse of the producing zone as Devonian. Many authors have suggested faulting as the structural control for the trend. Ells (1962) listed some indirect evidence for faulting associated with the trend. These are: 1) lineation of the oil fields, 2) varying degrees of fracturing and brecciation, which are typical of faulting, 3) variable reservoir characteristics, which are typical of fracture pools. Merritt (1968) concluded on the basis of a gravity survey that a fault-line scarp with approximately 800 feet (244 meters) of relief may be present in the basement below the fault. Shaw (1975) suggested that the gravity anomaly was caused by Mississippi Valley

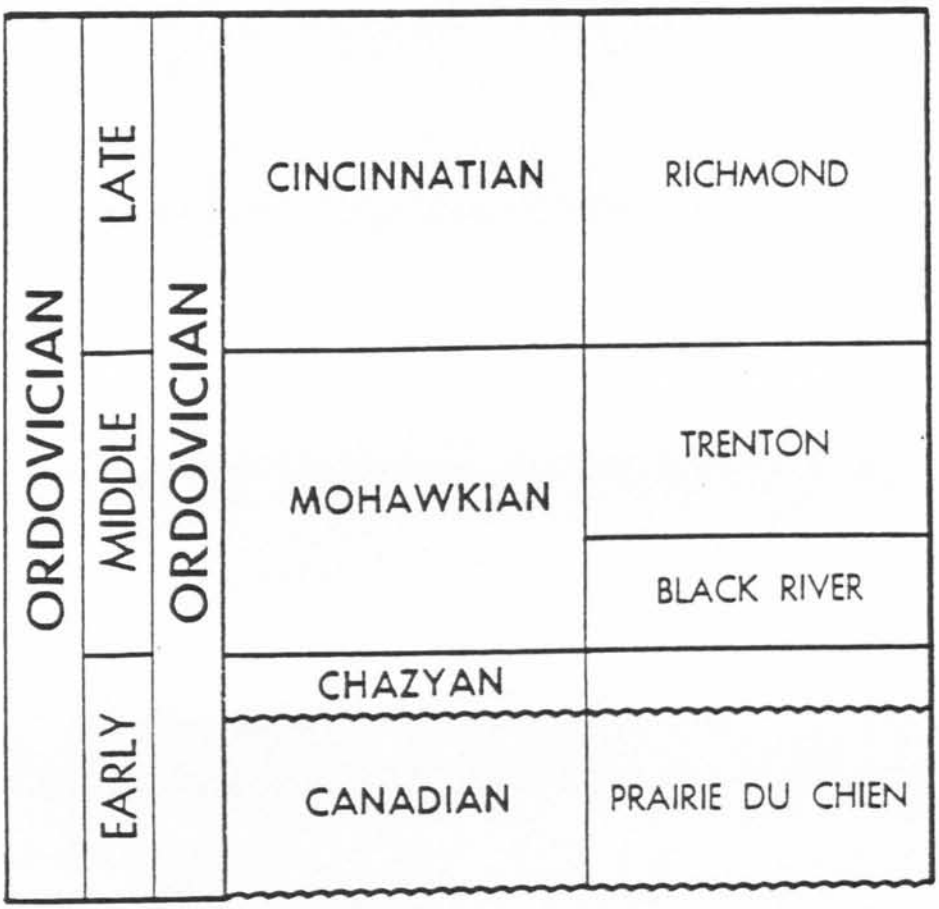

Fig. 7. Ordovician stratigraphy of the Michigan Basin.

type mineralization, since no stratigraphic evidence for faulting of this magnitude exists. He also compared Niagaran (Middle Silurian) reefs in the northern end of the trend, and correlated a difference in reef facies across the trend with trenton structure. He calculated a 50 to 100 ft. (15 to 31 meters) vertical fault displacement, with the eastern end upthrown. Shearing forces and movement along pre-existing basement faults is indicated by the presence of small en-echelon synclines and anticlines at small angles to the trend (Ells, 1962). Harding (1974) suggested deep-seated slight left lateral strike slip displacement along a pre-existing basement fault. He also proposed that an oblique, divergent component was present, and opened the fractures, thus facilitating dolomitization.

Glacial Geology

The bedrock surface of the field area is covered by a highly variable thickness of glacial drift. The drift thickness map (Figure 8) shows that the drift thickness in the survey area ranges from 10 feet (3 meters) to over 200 feet (60 meters). The map of the surface formations (Figure 9) also exhibits variability. Lovan (1977) studied the heavy mineral composition in the 120-230 mesh sand till fraction in parts of southwestern Michigan. He found that the source of these heavy minerals was most likely the Canadian Shield, and magnetite accounted for 7-28% of the heavy minerals. He noted a high degree of

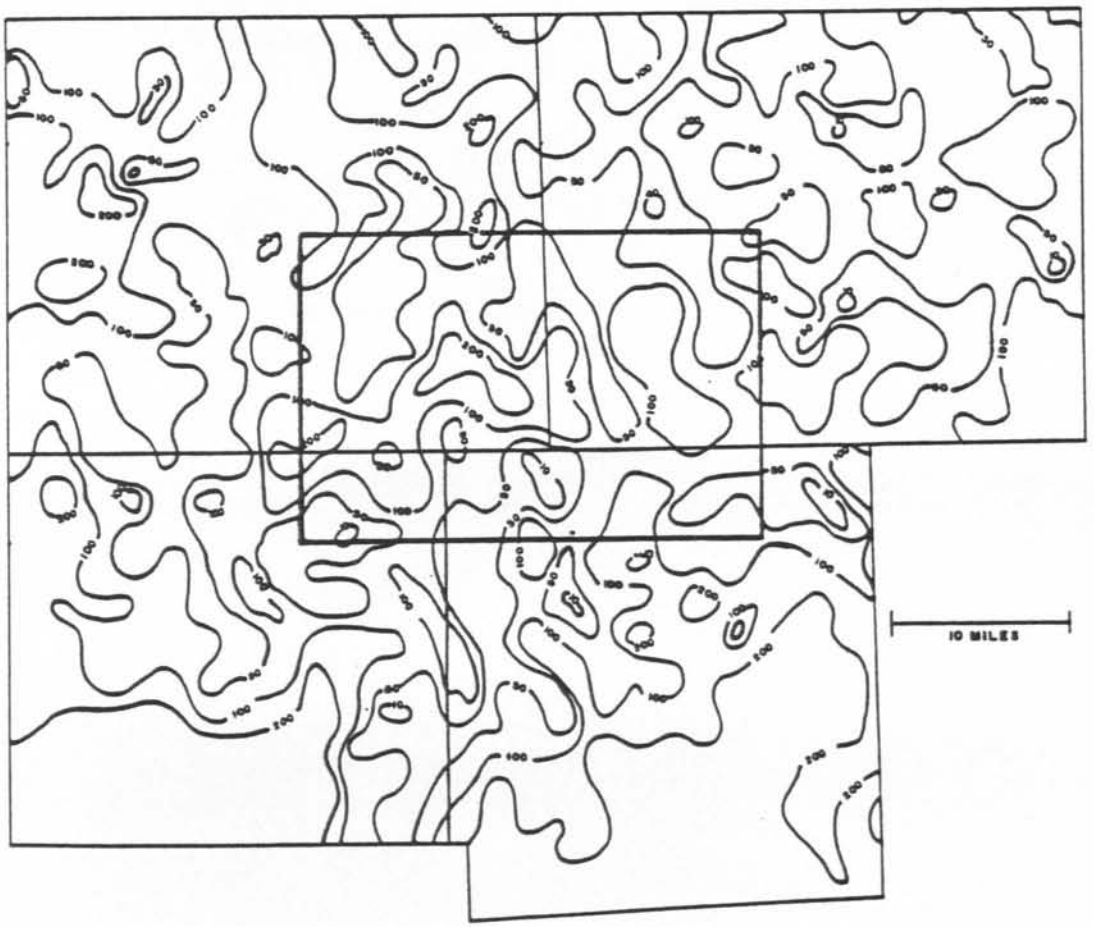

Fig. 8. Glacial drift thickness of part of South Central Michigan, showing the survey area, modified from Passero et al. (1981).

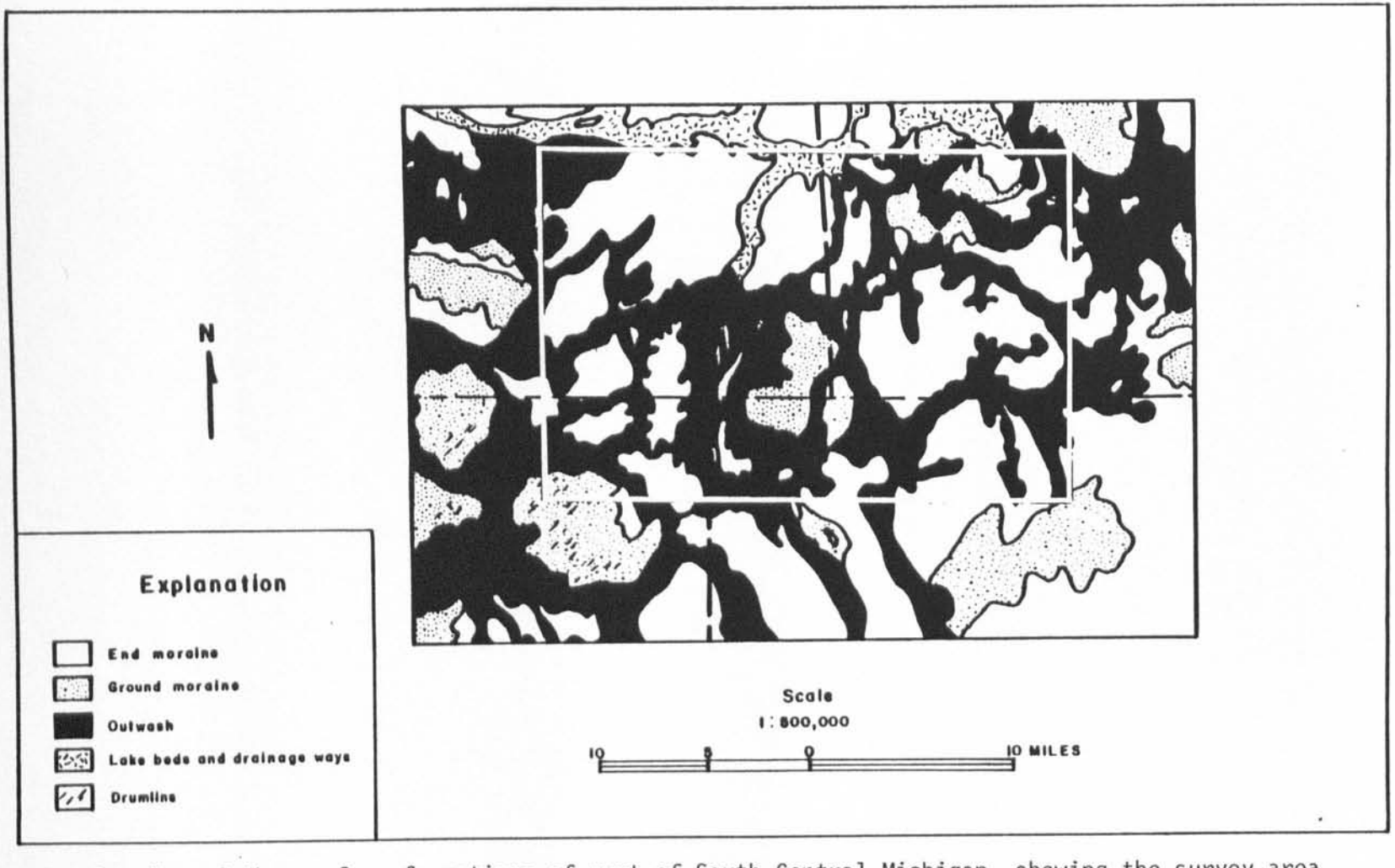

Fig. 9. Map of the surface formations of part of South Central Michigan, showing the survey area, modified from Martin el al. (1955).

variability in magnetic susceptibilities for the tills studied, and calculated a mean susceptibility of .0003 CGS units. This susceptibility translates into approximately 1% magnetite by volume (Lindsley et al., 1966).

DATA COLLECTION

Instrumentation and Equipment

Two Geometrics Proton Precession magnetometers, model G816, were used in the study. The instrument is designed to be rugged and lightweight, and is accurate within one gamma over a range of 20,000 to 90,000 gammas. The accuracy of each measurement is independent of sensor leveling, temperature, humidity, and battery conditions (Geometrics, 1979).

Sharma and Biswas (1966) gave a good description of proton precession magmetometer operation. The principle of operation is quite simple. An organic fluid, usually a petroleum derivative, surrounds and fills a magetizing coil. The coil is commonly a toroid or cylinder, the toroid being more independent of sensor orientation. A strong DC current is applied to the coil for a time on the order of the spin lattice relaxation time. This polarizes the protons in the sample in the direction of the magnetizing field. The current is then removed and the protons precess around the earth's magnetic field direction at a frequency given by $f = \delta pF/2\pi$ where δp is the gyromagnetic ratio of a proton. Thus by measuring f, the frequency of precession, F the total field value of the earth's magnetic field can be determined.

The sensor head of the Geometrics magnetometer consists of a coil surrounded by a well-sealed quart-sized plastic container.

The sensor is basically independent of orientation, but in areas where the magnetic field is greater than 40,000 gammas, the north arrow on the sensor should be pointed roughly north for optimum signal output. The sensor head is mounted on an eight ft. staff, and is connected to the magnetometer console with a shielded cable. The console is carried in a shoulder harness, and contains the batteries and the controlling, measuring, and display components of the instrument. The readout is a simple 5 digit numeric display, and the total field is displayed in gammas (or nanoteslas). The instrument also has signal strength and battery strength lights. The magnetometer must be field tuned to the tuning position which yields the maximum signal strength. A deviation of 3 or 4 tuning positions in either direction will not reduce accuracy in areas where the magnetic gradient is not excessive. During the survey, it was never necessary to retune the instruments after the initial tuning.

Two automobiles were used along with the two magnetometers. Each station operator used a citizens band radio, with exterior speakers. Two digital watches were needed to maintain synchronization between the mobile and base stations. The mobile car was equipped with a roof rack which allowed the sensor and staff to be rapidly attached and removed from the car exterior. Small pole stands were designed to be staked into the ground and act as staff holders at some base station locations.

Field Testing

A field test was conducted in April of 1980. The test was performed to determine the effect of variations in glacial terrain on the magnetometer readings. These tests were conducted in Kalamozoo County by Varga and Samuelson (1980). Two types of glacial terrain were investigated. These were outwash plain and bouldery end moraine. The stations were located on a 5 foot grid, and the time variation of the magnetic field was removed using a synchronized base station magnetometer. Figure 10 shows the results of this test. The bouldery end moraine shows a total magnetic relief of 56 gammas over a 750 sq. ft. area, while the outwash plain exhibits a magnetic relief of 15 gammas over an area of the same size. The bouldery end moraine site has a total standard deviation of 11.2 gammas, and the outwash plain site has a total standard deviation of 2.78 gammas. The bouldery end moraine site had boulders of various lithologies at the surface. This site represents an extreme case, and during the survey a station located in similar terrain would be abandoned. From these tests a field reading method was devised. A 'T' pattern was determined to be most effective in detecting the presence of lateral variations and gradients of the magnetic field. This pattern included 16 readings made along the 3 legs of the 'T' pattern. Each leg was started on an even minute and readings were taken at 20 second intervals. The method was standardized, because this minimized communications with the base

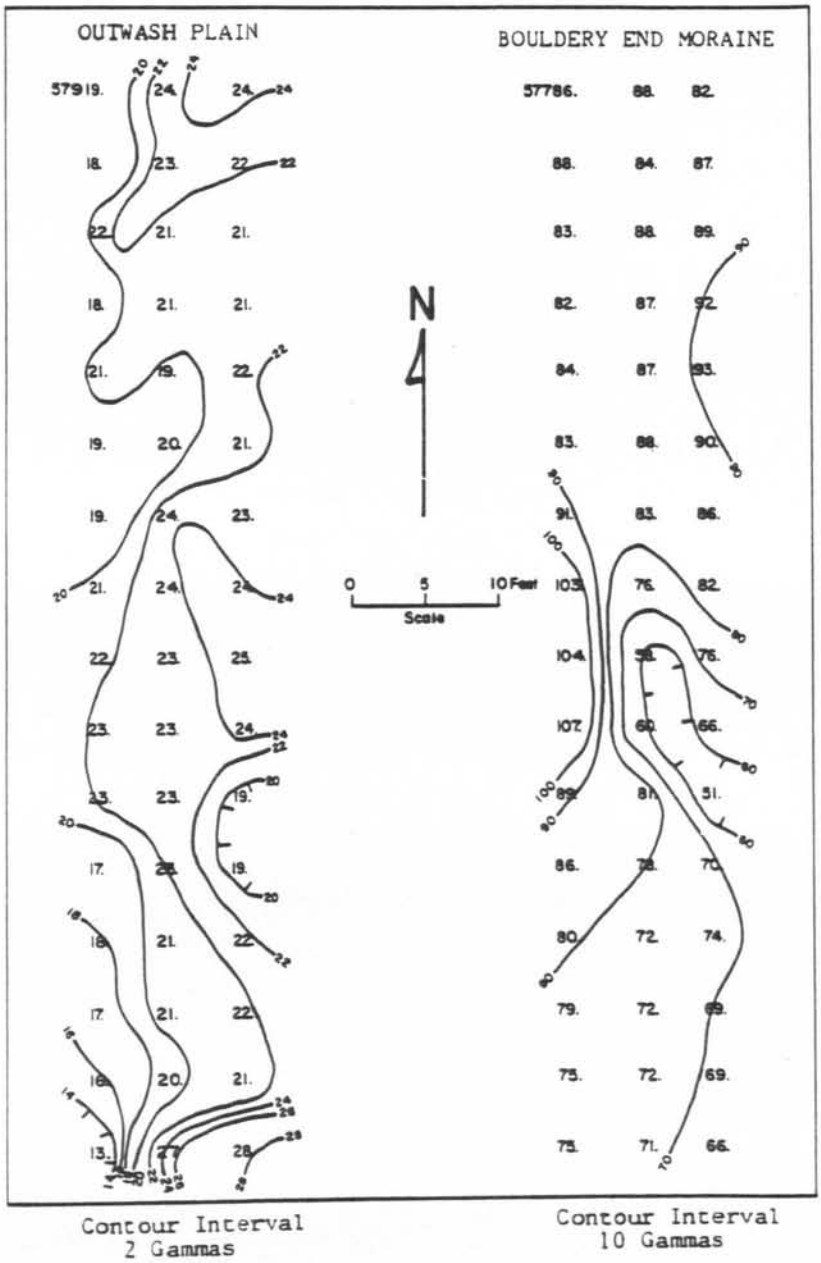

Fig. 10. Total magnetic intensity test grids on various glacial lithologies. (after Varga and Samuelson, 1980)

stations. Figure 11 is a representation of the 'T' pattern. The number of readings was set at 16, as a 'T' pattern with this number of readings would safely detect any of the anomalies present on the test grid.

Periodic field tests were carried out to check the comparability of the two instruments. These tests consisted of placing the two magnetometer sensor heads together, and then taking alternate readings with each instrument. The instruments proved to be accurate, and normally matched within one gamma.

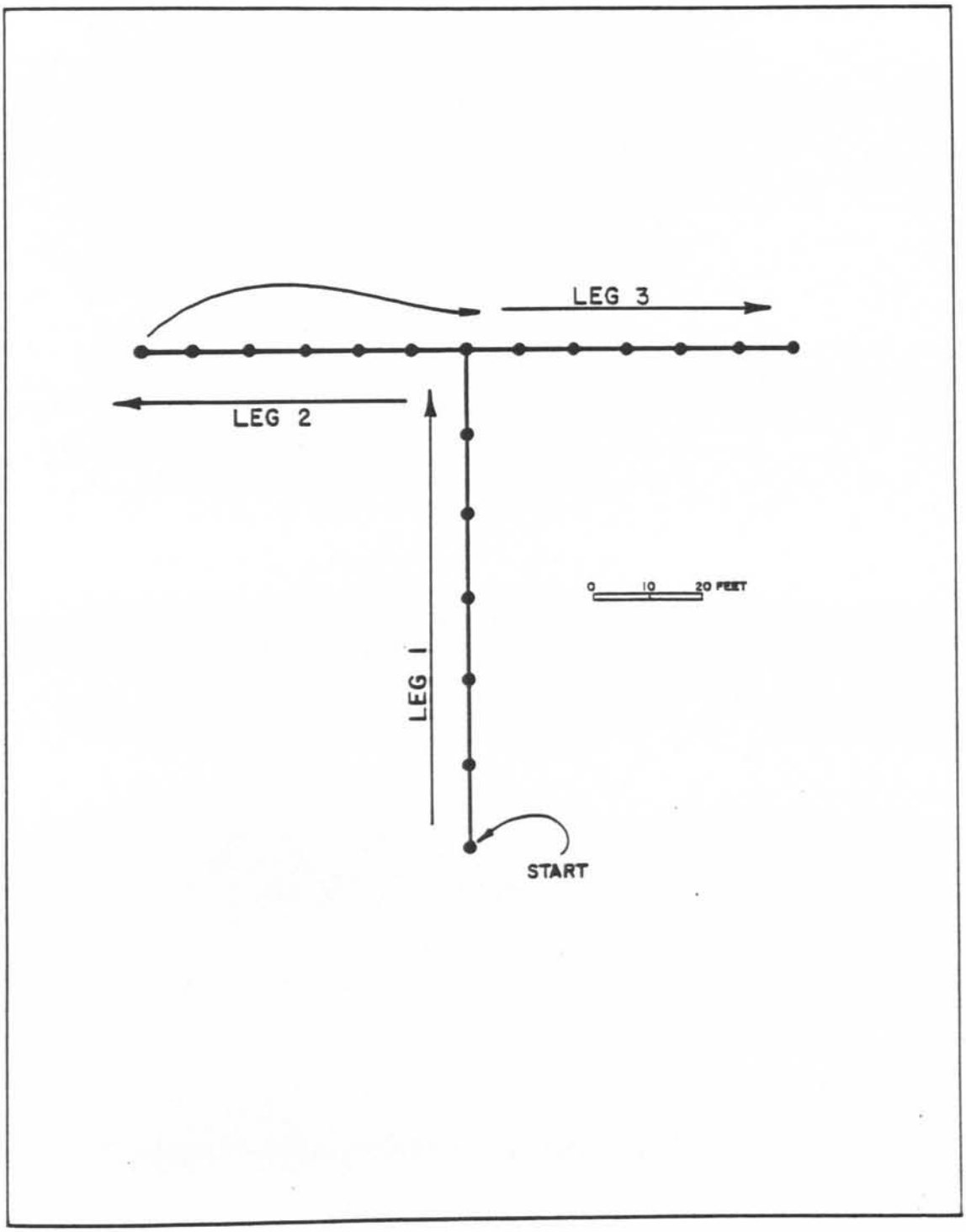

Fig. 11. Mobile station reading pattern.

FIELD PROCEDURES

Introduction

The field area was chosen to cover the major portion of the producing zone. The survey station locations were constrained by the roads in the area. The stations were spaced at ½ mile east-west and 1 mile north-south intervals wherever possible. In areas where access was difficult, coverage was not as dense. The survey made use of a procedure whereby two magnetometers were employed. The instruments were designated the mobile and base station magnetometers. The magnetometers were never exchanged. The operators of the magnetometers were in constant radio contact, using the mobile station automobile driver as an intermediary. Time synchronization was always maintained within 1 second and the watches were checked daily.

This procedure should have detected any rapid variations in the magnetic field as long as their periods were greater than 1 second. Also, diurnal and slow secular variations could be subtracted out. Hartman et al. (1971) studied the magnetic field variation in parts of Canada. They found significant differences in the diurnal variation of the magnetic field between 2 stations as close as 85 miles (136 km.). Because the maximum station separation in this survey was approximately 4 miles, the time variations should have been identical within survey accuracy. The synchronized reading procedure allowed operation on days when magnetic activity was relatively high.

Station Location

The stations were located using 1:62,5000 scale USGS topographic maps. A 1 cm. coordinate system was superimposed on the maps, and the southwest corner was designated 0.0. Stations were located using visual fixes on these maps, and the X,Y location was recorded for each station. Enclosure 1 is a copy of the mosaic of topographic maps with the superimposed grid system.

Mobile Station Procedure

The mobile stations were located within radio communication range of the base station. This formed an area of approximately 16 square miles, with the base station in the center. Two people operated the mobile station. The driver first located a field with as little cultural interference as possible. A minimum distance of 1,000 feet was allowed for major pipelines and high tension power lines. In areas near the oil fields, where oil wells are numerous, readings could not be taken. Once a suitable open area was found, the driver would relay a starting time to the base station. The readings were then taken using the standardized 'T', or a similar convenient pattern. A minimum distance of 100 feet was maintained from north-south fence lines, and no less than 200 feet was allowed between the car and the mobile operator. If the operator detected any excessive gradients, where 10 gammas/leg was considered excessive, the station was abandoned. Usually these unused stations had obvious local interference.

Base Station Procedure

The initial base stations were located along a north-south line bisecting the area. Later stations were located parallel to this line. Enclosure 1 shows the base station locations. Care was maintained in choosing station locations, and they were located in inactive and easily locatable areas. Topographic highs were used wherever possible, since this aided radio communication. Trees were used as magnetometer staff supports at nearly every base, and the location of the sensor head was marked. A check for local gradient was made at each prospective base, and in most cases where the gradient was excessive that location was not used. During the readings, the base operator would read the magnetometer, using the standardized timing procedure.

Summary of Field Operations

The majority of the data were collected from June 12, 1980 to August 12, 1980. One additional day, November 8, 1980 was used for later coverage.

Listed in Table A are other pertinent data:

Table A. Survey Operation Data

Total Number of Stations	695
Total Number of Field Days	38
Total Mobile and Base Station Readings	19,928
Average Number of Stations Per Day	17.3
Average Number of Readings Per Station	14.3
Average Base Station Standard Deviation	1.0
Average Mobile Station Standard Deviation	1.6

DATA REDUCTION

Introduction

Several corrections must be applied to the magnetic data before it can be analyzed. A correction must be made for the time variation of the field, along with a correction for the regional gradient. These corrections were performed using several computer programs. The basic approach in the reduction process was to first place the data into a computer file, and then apply the diurnal correction followed by the subtraction of the regional gradient.

Field Data

Because a large amount of data were collected, a computer program was written to organize the data into a digital file. This program, MAGDAT, accepts the base and mobile readings, mobile station location, base station location, time of the reading, station operator number, and the number of readings. The actual field readings are typed in by first typing all 5 digits of the magnetic value. With the subsequent values, only the digits that differ from the original number need be typed. The program also contains safeguards that prevent the mixing of improper mobile and base station data, and check for other errors in data entry.

Corrections for Time Variations

A program MAGRED was devised to correct for the normal time variation in the magnetic field. This program uses the computer file generated from program MAGDAT. Since each mobile station value has a corresponding base station within ±1 second, the program simply subtracts the corresponding values. After all 16 values are subtracted, a mean and standard deviation are calculated. The output of the program consists of the mobile and base station coordinates, the data and time of each reading, the number of stations used, the standard deviation of the station readings used, and the resultant mean magnetic value.

Determination of Base Station Values

A datum of 57,650 gammas was chosen for the survey. This was the average value of the first series of readings at Base 1. All base values were then corrected to this datum. Table B lists the base values. The base stations were linked using the mean difference of a series of 10 simultaneous readings. The original ties were accomplished as the survey progressed. At the end of the survey, a single day was devoted exclusively to repeating base ties. During this day all but two of the base stations were rechecked. Most of the bases were joined twice using a leapfrog method. This was carried out in both directions with each operator occupying opposite stations on the second pass.

Table B . Calculated Base Station Values

(refer to enclosure 1 for locations)

(values are in gammas)

Base No.	Base Value
1	57650.0
2	57655.0
3	57666.0
4	57653.5
5	57710.5
6	57686.5
7	57676.5
8	57669.3
9	57665.2
10	57675.0
11	57670.5
12	57638.3
13	57685.2
14	57644.1
15	57639.3
16	57667.4
17	56773.0
18	57697.4
19	57436.4
20	57731.6
21	57784.3

Because two base station values were normally obtained, the error had to be distributed between the values. This was accomplished by simply averaging the absolute value of the difference obtained between bases. Some discrepancy was noted with the earlier base values. The more recent values were used as they proved to be more accurate upon closure. A long loop using 14 different ties along the primary line of base stations closed within 3.6 gammas. Other loops were more accurate, and the maximum discrepancy within a loop

was 3.8 gammas. Also, all the base ties were completed at least twice in one day. If any discrepancies existed at base locations, these would have been detected.

Determination of The Contour Interval

A statistical evaluation of the data was carried out. A 't' test was used to determine the accuracy of the magnetic values. With 95% confidence, the true mean will be located within $\bar{X} \pm \frac{tS}{\sqrt{N}}$ where N (degrees of freedom) is the number of readings less one, t = 2.160 with 13 degrees of freedom, S is the standard deviation of the station value, and $\bar{X}$ is the calculated average. From this, it can be seen that for the true mean to be within ± 1.5 of the calculated mean, the standard deviation must be less than or equal to 2.60. Using this criterion, a contour interval of 3 gammas was determined to be reasonable.

Removal of Erratic Readings

Many of these stations had readings that deviated significantly from the mean station value. A procedure was implemented within the program MAGRED that eliminated these inconsistent data. During the initial stage of data reduction, this procedure deleted data greater than ±2 standard deviations from the mean. An average of 1.2 data points per station were rejected. After this first pass, 13% of the stations had standard deviations greater than the chosen limit of

2.60 gammas. Using these data, the preliminary 'Ground Magnetic Map of Homer and Spring Arbor 15' Quadrangles, Michigan' was produced (Hoin et al., 1981). The regional gradient was not subtracted from this map.

During the final data processing stage, a different data testing procedure was implemented. In this case, an arbitrary range of ±4 gammas around the mean was used, and any data outside this range were deleted. An average of 1.7 data points per station were eliminated. After this second pass, all but 0.4% of the mean station values fit within the desired statistical confidence.

Removal of the Regional Gradient

Even though the regional magnetic variation in the survey area is small because of the limited north-south extent of the area, removal of this gradient should aid in interpreting the more subtle anomalies. The regional field was calculated using the program GFIELD. This program was developed by Cain et al. (1967) and modified by Sauck (1975). The program calculated the geomagnetic reference field at any position on or above the earth's surface, at any time during the designated epoch. The field was calculated using 12 degrees of spherical harmonic expansions, with coefficients (AWC/75) calculated by Fabiano and Peddie (1975). The field was calcualted for 1000 feet (305 meters) above mean sea level. Figure 12 is a contoured map of the values calculatd at .125 degree intervals over

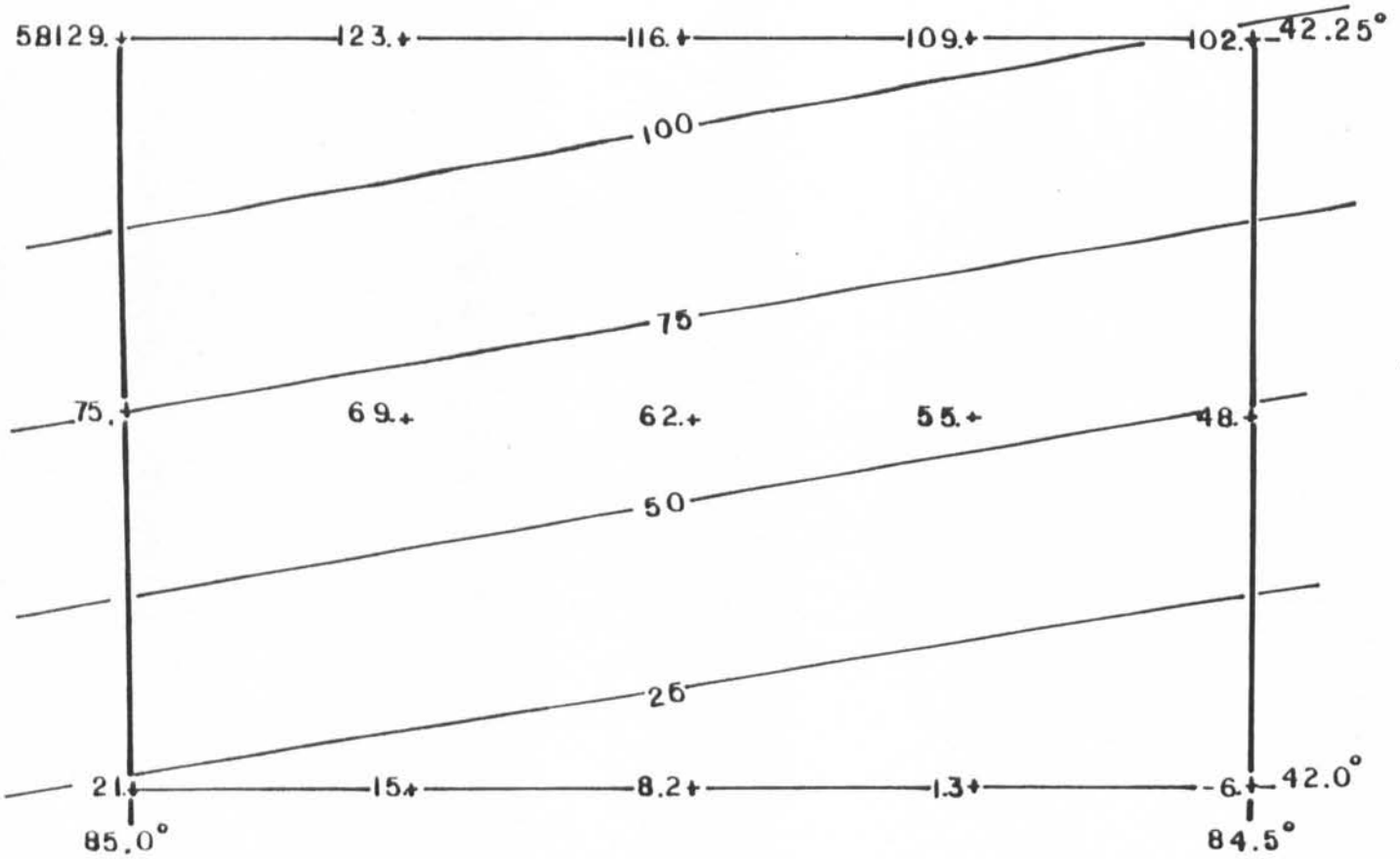

Fig. 12. Geomagnetic Reference Field in the study area.

the survey area. Upon inspection of the data, it can be seen that the gradient can be considered linear over the small area used. A linear euqation (Correction = .40625x - 2.391169Y) was determined to fit the slope of the regional field assuming an arbitrary datum. This equation fits the data when X and Y are in centimeters, and 0,0 is located at 42.0 north latitude, 85.0 west longitude. A computer program REGMAG was created to make this correction.

Data Plotting

The corrected values obtained from REGMAG were then plotted on a California Computer Products (CALCOMP) 906 drum plotter. The computer program MAGPLT was written to plot the data, showing both location and magnetic value of each station. The data were then hand contoured, and two maps were produced. These are, 'Interpretive Residual Ground Magnetic Map of the Albion-Scipio Trend' (Enclosure 3), and the 'Residual Ground Magnetic Map of the Albion-Scipio Trend' (Enclosure 2).

INTERPRETATION

Introduction

Methods of interpreting magnetic maps and data are both numerous, and variable in complexity. Most interpretations have been and still are qualitative in nature. Survey techniques vary depending upon objectives. In mining exploration for example, small wavelength, high amplitude anomalies are sought, since these are in many cases caused by ore bodies or associated structures. The usual goal of the petroleum industry on the other hand is to map the depths of sedimentary basins. Thus, most of the magnetic information consists of relatively large wavelength anomalies. The objective of this survey was to delineate basement structure in a sedimentary basin. Therefore, anomalies with wavelengths of a few miles would likely be needed to define the structures.

The Albion-Scipio Trend is clearly a linear structure. If the trend is basement controlled, this linear structure should appear on a magnetic map as a linear discontinuity or trend. This characteristic of magnetic maps makes the qualitative portion of this interpretation critical. Quantitative detection of a fault with limited vertical displacement associated with the trend is unlikely. The anomaly generated by a fault with approximately 600 feet (183 meters) of vertical displacement in the vicinity of the

trend, would commonly be between 1 and 20 gammas depending on the susceptibility of the basement (Reford and Sumner, 1964). Also a depth estimation accuracy of 10% is all that can be expected from quantitative methods. Thus, only under ideal conditions could an anomaly generated by a small-displacement vertical fault in the basement below the Albion-Scipio Trend be detected.

Anomaly Characteristics

The average magnetic field inclination in the survey area is approximately 71.6 degrees. The average declination is approximately 2.9 degrees west of true north. Assuming induction as the only anomaly source, this magnetic field orientation will generate distinct anomalies. The anomaly shape will be dependent on the shape and orientation of the geologic body. An equidimensional prismatic body with infinite depth extent will produce a teardrop-shaped positive high, with a corresponding negative low of approximately 5% of the maximum value, to the north. The geologic center of the body will be located just north of the anomaly maximum. A tabular thin sheet-like body with vertical or near vertical dip, and north-south strike will appear as a symmetric positive linear high. The geologic center of the body will be located beneath the anomaly center. This same body striking east-west will produce a slightly asymmetric anomaly with a linear positive high, and a parallel negative low to the north. The body will be located slightly north of the maximum. Vacquier et al. (1951) illustrates many of these anomaly types.

Sources of Anomalies

Before any interpretation can be attempted, some previous knowledge of possible anomaly sources is needed. The source of nearly all magnetic anomalies is fine-grained magnetite or related minerals. The amount of magnetite present in a rock determines the magnetic susceptibility of the rock. Table C shows the average magnetic susceptibility of some rock types. This table shows that most sedimentary rocks have little or no magnetic susceptibility when compared with igneous and metamorphic rocks. Carbonate rocks, which predominate in the Michigan Basin, have the lowest susceptibilities. This indicates that the source of the large magnetic anomalies in the survey area originate in the basement rocks.

In general, magnetic highs are correlated with intrusive and extrusive mafic rocks, and magnetic lows are associated with metasediments and felsic rocks. The ambiguity in this generalization is seen when sources of magnetic anomalies on the periphery of the Michigan Basin are studied. In the Canadian Shield Mclaren and Charbaneau (1968), found that magnetic lows generally correlate with volcanic rocks and low grade gneisses, and magnetic highs are associated with granitiod rocks and highly altered gneisses. O'Hara and Hinze (1972), after Dutton and Bradley (1970), found positive magnetic anomalies in southern Wisconsin associated with rhyolite, granite, and quartzite. The Central Province, which underlies the survey area (Kellogg, 1971), is characterized by granites, rhyolites,

granite gneisses, and metasedimentary rocks. From the preceding discussion it can be seen that any attempt to assign specific lithologies to anomalies is speculative, unless other geological or geophysical evidence is available.

Table C. Magnetic Susceptibilities of Some Common Rock Types

(values are in CGS units * 10-6)

Rock Type	Number of Samples	Range	Average
Dolomite a	66	1-75	8
Limestone a	66	2-280	23
Sandstone a	230	1-1665	32
Shale a	137	5-1478	52
Ryolite b	44	40-1120	280
Granite a,b	31	28-2700	470
Felsic Igneous a	58	3-6527	647
Gabbro a,b	37	68-5610	990
Diabase b	19	64-4200	2590
Mafic Igneous a	78	44-9711	2596
Basalt b	37	480-10000	2950

a. Dobrin (1976, p. 270)
B. Grant and West (1965, p. 266)

The effect of basement topography on magnetic anomalies has been thoroughly studied. Hinze and Merritt (1969) developed some simulated magnetic profiles for a model representing the Michigan basin. They showed that basement relief of over 15% of the total depth would generate an anomaly of less than 20 gammas. Reford and Sumner (1964) estimate that small magnetic anomalies, which appear as noses or gradient breaks against the stronger features, and are less than 50 gammas are usually indications of structure.

Another possible anomaly source in this survey is glacial till. The till near the survey area has been shown to have a rather high magnetic susceptibility, as previously discussed. The fine grid test of the magnetic response of glacial terrains (Figure 10) shows an anomaly of over 30 gammas in a boulder till over a distance of less than 25 feet. The error generated by this source would generate short-wavelength noise. This noise is present on nearly all of the residual magnetic map (Enclosure 2). The northeastern and central portions of the residual map show this noisy character most clearly. The general shape of the long-wavelength basement-derived anomalies is preserved.

Uncertainties in the Interpretation

As in most applied geophysical methods, the interpretation of magnetic data is hindered by some fundamental uncertainties. The presence of remanent magnetization in magnetic rocks presents a difficult obstacle in magnetic interpretation. Many of the early depth determination methods assume induction as the only cause of rock magnetization. Also, because magnetic anisotropy is common, it is difficult to accurately determine the major parameters of a magnetic body, even though data may be available on the remanent magnetic vector direction. Another difficulty in magnetic interpretations is the inherent ambiguity in potential field data. That is, an infinite number of subsurface configurations can fit an anomaly. Also, most interpretation methods are based on isolated anomalies with no

interference from surrounding anomalies, yet anomaly interference is the rule rather than the exception.

Quantitative Interpretation

Introduction

The quantitative aspect of this interpretation consists primarily of depth determinations. There are many techniques available. Each has advantages and disadvantages. Because of the mathematical complexity of total field calculations, most quantitative interpretation methods are based on anomalies caused by simple subsurface bodies. More recently developed methods apply computer programs to previously cumbersome methods. The magnetic depth determination methods used in this analysis were developed by Hartman et al. (1971), Koulomzine et al. (1970), and Vaquier et al. (1951).

Depth Determinations

Hartman et al. (1971) expanded upon the Werner method. The method is designed for rapid depth determinations along profiles, and it has many advantages over other methods. Some of these advantages are: 1) The method is valid for any semi-infinite thin sheet regardless of dip, strike, remanent magnetization, or latitude, 2) It is objective, in that the computer program automatically separates the anomalies that fit the model, and 3) Interference from adjoining anomalies can be filtered out.

Werner first developed the method using the following approach: The total field caused by a thin tabular body of infinite extent at a distance X along a profile can be defined as:

$$T(x) = \frac{A(X-Xo) + BZ}{(X-Xo)^2 + Z^2} \qquad (1)$$

Where X is the distance to a point over the center of the body, Z is the depth to the top and A and B are functions of the field strength, dip, strike, and magnetic inclination and declination of the body. The equation can be put into the form:

$$a_o + a_1 X + b_o F + b_1 X F = X^2 F \qquad (2)$$

Where

$$a_o = -AX_o + BZ,\ a_1 = A,\ b_o = X^2 - Z^2, \text{ and } b_1 = 2X_o$$

and

$$F = T(X)$$

from this

$$X = \frac{1}{2} b_1, \text{ and } Z = \pm \frac{1}{2} \sqrt{4b_o - b_1^2}$$

Now it is simply a matter of substituting T(X) at four different positions to obtain

a_o, a_1, b_o, b_1, and then solve for X_o and Z

Hartman et al. (1971) expanded on this solution, and assumed that anomaly interference could be written as a polynomial. Werner's original equation now becomes:

$$T(X) = \frac{A\,(X-X_o) + BZ}{(X-X_o)^2 + Z^2} = C_o + C_1\,X + \ldots\ldots + C_n X^n \qquad (3)$$

If a second degree polynomial is used, the equation is:

$$FX^2 = B_1 + B_2 + B_3\,F + B_4\,XF + B_5\,X^2 + B_6\,X^3 + B_7\,X^4 \qquad (4)$$

Where $B_4 = 2X$, and $B_3 = X - Z$, and from this

$$X = \frac{1}{2}\,B_4 \text{ and } Z = \pm\frac{1}{2}\sqrt{-4B_3 - B_4^2}$$

Hartman et al. (1971) also noted that the magnetic anomaly due to a dipping thin sheet is precisely the same as the horizontal derivative of the anomaly caused by a similarly positioned interface. This can be demonstrated by differentiating the equation for the magnetic effect of a contact. First, the equation for an anomaly caused by a north-south striking thin sheet is:

$$-Z_t = 2kt\,\frac{Z_o\,(\cos\alpha\,(X + d\cot\alpha) - d\sin\alpha}{d^2 + (X + d\cot\alpha)^2} \qquad (5)$$

(Telford et al., 1976).

Where k is the susceptibility of the thin sheet, t = the thickness, α = the dip and d = the depth, Z = the vertical component of the field.

Now simplify the equation by setting $\alpha = 90°$.

The equation now is:

$$Z_t = 2k_t\,Z_o\,\frac{d}{d^2 + X^2} \qquad (6)$$

The equation for a north-south striking vertical contact is:

$$Z_c = 2\,kZ_o\ \mathrm{Tan}^{-1}\frac{x}{d} \quad \text{(Telford et al., 1976)} \tag{7}$$

where k = the susceptibility contrast.

The horizontal derivative of Z_c is:

$$\frac{dz}{dX} = 2\,kZ_o\,\frac{d}{d^2+x^2} \tag{8}$$

where

$$dX\ \ \mathrm{Tan}^{-1}\frac{x}{d} = \frac{1}{1+\frac{x^2}{d^2}} * \frac{1}{d} \tag{9}$$

Thus the horizontal derivative of the magnetic effect of a contact (Equation 8) is equivalent to the magnetic effect of a thin sheet body (Equation 6). Using this idea, Hartmen expanded the method into the interpretation of depths for individual interfaces, as well as thin sheets. Thus depths can be calculated for all semi-infinite homogeneous, thin sheet bodies, contacts, faults, or slope changes, assuming the bodies strike perpendicular to the profile.

In practice, this method appears to work well. First some linear anomaly was chosen, where the linear extent is at least five times the depth. The horizontal derivative was manually calculated at 0.1 mile intervals along the profile. These data were then digitized. A program (WERNER) was then used to examine four successive equally spaced points, solve the resulting linear equations, and

calculate a depth and location. The points were then advanced by 0.1 mile and the caluclations were repeated. This process was complete when a profile had been covered. The distance between each of the four points was then varied and the program rerun. Optimum results were obtained when a point spacing of .5 miles was used. The next step was to examine the location and depth values. If three or more successive calculations gave depths and locations within 5%, the average was taken. This value was considered a valid depth. In practice, these groupings occurred with 5 or more points giving close solutions.

The solutions of the linear equations were obtained using the LINPAC Subroutine Package (Dongarra et al., 1979). This software package is designed to solve matrix equations. In this case a process of gaussian elimination is used. This involves first the factorization of the matrix into lower and upper triangular matrices. A solution is then generated from these two matrices. The program also calculates a condition number. The condition number indicates whether the matrix is singular or nonsingular, it also can be used to estimate the accuracy of the output. Only 4 data points were used when solving the matrices. When a polynomial was added to the original equation, many of the matrices approached singularity, thus the accuracy of the solutions was lowered. Therefore 'groupings' of locations and depths did not fit the 5% criteria. Since only 4 data points were used, the program was successful in determining depths only when magnetically isolated anomalies were used.

Two depths were obtained using this method. The depths were calculated for profile 'A' and 'B' of Enclosure 3. Profile 'A' yielded a depth of 4500 feet (1372 m.) below MSL, and the southwestern edge of the body was located 3.8 miles (6.1 km.) from the southwestern end of the profile. On profile 'B' a depth of 5100 feet (1555 m.) below MSL and a location of 3.3 miles (5.3 km.) from the southwestern end of the profile were calculated.

A second depth determination method was applied to anomaly 'A' of Enclosure 3. The method was developed by Koulomzine et al. (1970) for tabular bodies of infinite length and depth, and any orientation and magnetization. The method is an improvement over prior methods, in that no assumptions need be made about the zero datum level or the location of the center of the body. The field curve is decomposed into two components, the Arctangential and Logarithmic, or in graphical terms, the Symmetric (S) and Antisymmetric (A) components (Figure 13). The procedure consists of first graphically locating the position X=0. This location corresponds to the maximum position on the 'S' curve, and the zero position of the 'A' curve. Following this, the 'S' and 'A' curves are drawn. The symmetrical curve is defined as the locus of the midpoints between F(X) nad F(-X). The antisymmetrical curve is drawn by plotting 1/2 D as ordinates, where 1/2 D is the distance between the anomaly curve and the summetric curve. The depths are then determined using various abscissae ($X1/2$, $X3/4$, X_e) of the separated curves. These abscissae are

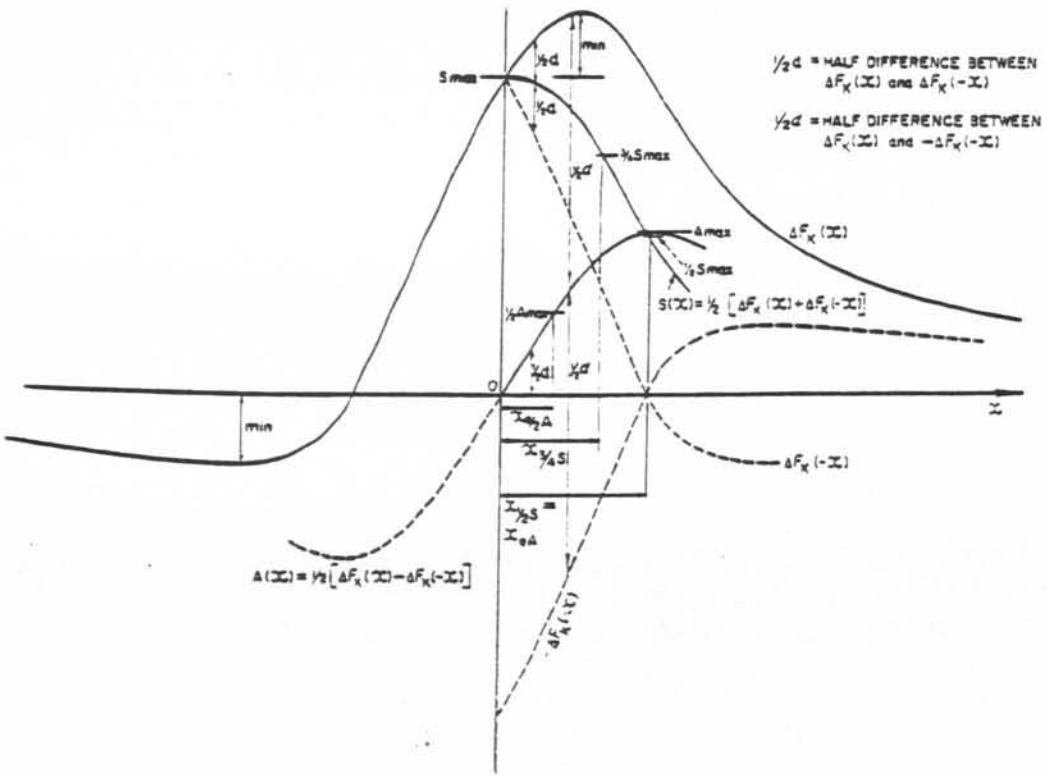

Fig. 13. Separation of a field curve into symmetric and antisymmetric components, from Koulomzine et al. (1970).

plotted on a set of 6 master curves relating the abscissae to the depth and width of the tabular body. A depth estimate of 3800 feet (1160 m.) below MSL, and a width of 2.3 miles (3.7 km.) were calculated. The center of the body was located at 4.75 miles (7.7 km.) along profile 'A'. This places the southwest edge of the tabular body at 3.6 miles (5.8 km.). This agrees with the value calculated using the method of Hartman et al. (1971). The depth estimates differ by 700 feet (16%).

The depth determination of Vaquier et al. (1951) was applied to anomaly 'B' of Enclosure 3. The method is based on the comparison of observed anomalies with anomalies computed from idealized bodies. These bodies are rectangular or square prisms with infinite vertical sides. The models apply only to the case of induced magnetization, or remanent magnetization in the same direction as the earth's field. The process consists of first selecting a model that is compatible with the chosen anomaly. The horizontal extent of the steepest gradient at characteristic positions on the contour map is measured. In this case the E (south) and F (east) positions were used since these positions showed the lease anomaly interference. The gradient distances are then compared to applicable 'Depth' indices, which are basically proportionality constants. The depth is estimated by dividing the measured horizontal gradient distance by the depth indices of the model. These depths were then averaged and a resultant depth of 5200 feet (1585 m.) below MSL was

calculated. Following the depth determinations, a susceptibility contrast was calculated. This is computed using the following formula:

$$k = \triangle T_m / \triangle T_c \quad T$$

Where k is the minimum susceptibility contrast, T_m is the amplitude of the observed anomaly in gammas, T_c is the amplitude of the model anomaly, and T is the intensity of the earth's magnetic field. The result is:

$$k = \frac{110}{4.0 \times 57560} = .005 \text{ CGS}$$

The depths generated in this analysis represent maximum depths, since the magnetic bodies may not be located at the basement surface. Basement drill hole data in Branch County, roughly 12 miles west of the southwest corner of the survey area, encountered basement at approximately 4500 feet (1370 m.) below MSL. This indicates that the depth estimate using the method of Hartman et al. (1971) is likely the more accurate value. The two depth estimates in the center of the survey are comparable. These depth estimates seem to indicate a general change in dip starting at the negative linear anomaly. The estimates calculated in this analysis are approximately 700 feet (213 meters) shallower than previous estimates (Kellogg, 1971).

Qualitative Interpretation

Introduction

The qualitative portion of the interpretation consists of visual analysis of anomaly types, and anomaly amplitudes. Linear anomalies are characterized by parallel gradients, alignment of contours, or linear discontinuities. They reflect strike lines of linear intrusives or faults. Faulting commonly produces abrupt lateral changes in anomaly character, or anomaly offsets or discontinuities. Much of the qualitative analysis is based on know geology or prior experience in similar terrains. Thus, in areas of sparse geologic control many of the conclusions generated are speculative.

Interpretation

The Residual Magnetic Anomaly Map (Enclosure 3) contains strong negative anomalies, as well as positive anomalies. This indicates that remanent magnetization is present in the basement rocks below the survey area. The magnetic intensity varies over a range of about 500 gammas. The southwestern portion of the map is characterized by a northwest-southeast trend direction. Anomaly 'A', a large negative anomaly, dominates this portion of the map. The negative character of the anomaly indicates that the body is remanently magnetized, and this magnetization appears to be nearly opposite the field direction. Quantitative analysis shows that this body is tabular. The regularity

of the contour lines also indicates that the body is relatively homogeneous. This anomaly is prominent on the Total Intensity Magnetic Map of Michigan (Kellogg, 1971), and Hinze et al. (1975) have attributed this anomaly to a mafic dike with associated feeder pipe. Books (1968) and Dubois (1962) have studied igenous intrusions in the Upper Peninsula of Michigan. Both found many dikes with reversed magnetization. Books (1968) found that most of the reversely magnetized dikes were lower Keweenawan. Pesonen and Halls (1979) also studied the paleomagnetic character of dikes in Michigan's northern peninsula. They associate the reversely magnetized dikes with a magmatic pulse during early rifting in the Lake Superior region. The northern Michigan dikes occur around the periphery of the basin, and trend parallel to the rift axis (Halls, 1978). Anomaly 'A' could be caused by a lower Keweenawan diabase dike associated with early rifting in southern Michigan. The two elongate magnetic highs paralleling anomaly 'A' to the northeast are most likely not part of anomaly 'A'. Depth analyses on the northeast flank of anomaly 'A' were unsuccessful, indicating that these anomalies are probably caused by a flanking magnetic body. Parallel to these anomalies and to the north is another linear negative anomaly. This anomaly is not as large as anomaly 'A', and it is also discontinuous. It may be caused by a similarly magnetized small dike parallel to anomaly 'A'. Anomaly 'B' is an equidimensional positive anomaly. Calculations show that the susceptibility is near the average value for granite (Table C). Some authors, Steeples et al. (1981) in

Kansas, and Lidiak (1972) in Nebraska, have shown that many of these equidimensional positive anomalies are associated with granitic or felsic plutonic rocks. O'Hara and Hinze (1972) extended a magnetic zone from Wisconsin across Lake Michigan into southwestern Michigan. Drill hole data in this zone in Wisconsin penetrated granite and quartzite. There is a good possibility that anomaly 'B' is caused by a granitic intrustion whose top is located approximately 5200 feet (1585 meters) below MSL. Anomaly 'C' is an equidimensional negative anomaly. It may be associated with anomaly 'A', since the direction of remanent magnetization appears to be the same. Anomaly 'D' is a prominent positive anomaly in the northwest corner of the survey area. This anomaly appears as the nose of a larger anomaly on the total intensity magnetic anomaly map of Michigan (Figure 3). The central part of the anomaly has an abrupt gradient increase. This may be caused by a feeder pipe associated with the igneous body.

The Albion-Scipio Trend has been superimposed on Enclosure 3. There are definite discontinuities associated with the trend. The feature marked 'E' on Enclosure 3 shows a deflection of a linear gradient. The deflection also appears to have separated anomalies 'F' and 'G' with left-lateral motion. The northeast-southwest gradient in the southeast portion of the survey area is disrupted in the vicinity of the trend. The nose-like anomaly 'H' is deflected in the same direction as the other anomalies. Another on-trend discontinuity exists between anomalies 'B' and 'C'. Depth calculations

using the method of Hartman et al. (1971) indicate the presence of an interface at this position.

These discontinuities are evidence of apparant left lateral strike-slip displacement in the basement rocks. The apparent horizontal fault displacement can be estimated at approximately 2.5 miles (4.0 km.). This relative large displacement basement fault associated with indistinct Paleozoic structures indicates that the original faulting occurred during the Pre-Cambrian. Subsequent minor reactivation of the fault during the Paleozoic, followed by the migration of fluids, formed the present trend structures and lithologies.

The magentic map also shows a definite change in trend directions from west to east. The trend direction changes from northwest in the western half of the map, to northeast in the eastern half of the map. The anomaly character in the eastern portion of the magnetic map also changes slightly. The eastern section displays a smoother character, with much less relief. This difference in magnetic character is probably due to a lithologic change. The Albion-Scipio Trend may be located on some basement lithologic boundary, and thus could have been a pre-existing zone of weakness along which recurrent movement took place until middle Silurian time.

CONCLUSION

A detailed high-resolution ground magnetic survey was carried out over the central portion of the Albion-Scipio Trend. The survey method successfully eliminated much of the magnetic noise associated with ground surveys. The resulting magnetic map indicates that the basement rocks consist of dike-like and plutonic, mafic and felsic rocks. These basement rocks exhibit two distinct trend directions, and several discontinuities are associated with the Albion-Scipio Trend.

The survey supports the postulate of a basement fault directly beneath the trend. The apparent left-lateral fault displacement has been estimated at about 2.5 miles (4.0 km.) for basement rocks. Major faulting occured during the Pre-Cambrian, with reactivation of the fault during the Paleozoic, terminating in middle Silurian time. The magnetic map also exhibits an anomaly character change across the trend. This is indicative of a possible lithologic boundry. The linear negative anomaly in the southwest is most likely caused by a Keweenawan dike. Other anomalies on the map appear to be caused by rocks associated with the Pre-Cambrian Central Province. Depth estimates show an increase in depth of basement toward the northeast, but are otherwise inconclusive.

APPENDIX A

Listing of some of the computer programs used in this study.

```
      PROGRAM MAGDAT
C*****************************************************************
C
C       UTILITY PROGRAM
C       DESIGNED TO ACCEPT FIELD DATA INTO A PERMANENT FILE.
C
C       FOR USE WITH THE WMU DEC SYSTEM 10
C       JUNE 1980
C
C*****************************************************************
      DIMENSION MAG(24)
      INTEGER BMAG(24)
      DATA BIG,MOB,IBAS/-999.,'MOBIL','BASE'/
      OPEN(UNIT=21,DEVICE='DSK',FILE='ALBMG.RAW',
     1 ACCESS='APPEND',PROTECTION=122)
      GO TO 89
    5 WRITE(5,100)
      WRITE(21,1100)BIG
  100 FORMAT(10X,'ENTER DAY, MO,YR, & BASE VAL.AS 14'
     1 , ',06,80,57481.2')
   10 READ(5,*) IDAY,MO,IYR,BASVAL
   80 WRITE(21,1000) IDAY,MO,IYR,BASVAL
 1000 FORMAT(3I3,2X,F8.1)
   15 WRITE(5,200)
  200 FORMAT(10X'ENTER X,Y,TIME(HR,MN,SC),MAG#, OP#, '
     1 , '& # OF RDNGS FOR MOBILE')
   20 READ(5,*) X,Y,IHR,IMIN,ISEC,NMAG,NOP,N
   25 WRITE(5,300)
  300 FORMAT(10X,'ENTER  STRING OF MAG RDNGS FOR MOBILE MAG.')
   30 READ(5,*) (MAG(I), I=1,N)
   35 WRITE(5,400)
  400 FORMAT(10X,'ENTER X,Y,START TIME,MAG.NO., OP.NO.'
     1 , ' ,& NO. OF RDNGS FOR BASE')
   40 READ(5,*) XB,YB,IHRB,IMINB,ISECB,NMAGB,NOPB,NB
      IF(IHR.NE.IHRB) GO TO 60
      IF(IMIN.NE.IMINB) GO TO 60
      IF(IABS(ISEC-ISECB).GT.5) GO TO 60
      IF(NMAGB.EQ.NMAG.OR.NOPB.EQ.NOP) GO TO 62
      IF(NB.EQ.N) GO TO 70
      WRITE(5,620)
  620 FORMAT(10X,'UNEQUAL NUMBERS OF MOBILE & BASE RDNGS')
      GO TO 61
   62 WRITE(5,640)
  640 FORMAT(10X'MAG OR OPERATOR ID'S IDENTICAL-ERROR')
      GO TO 61
  600 FORMAT(10X,'BASE AND STATION TIMES CONFLICT.')
   60 WRITE(5,600)
   61 WRITE(5,700)
  700 FORMAT(10X,'ENTER -1 TO RE-ENTER BASE DATA, 0 FOR'
     1 , ' MOBILE DATA, +1 TO STOP')
      READ(5,*) JJ
      IF(JJ) 35,15,99
   70 CONTINUE
   45 WRITE(5,500)
```

```
500   FORMAT(10X,'ENTER STRING OF MAG RDNGS FOR  BASE MAG.')
 50   READ(5,*) (BMAG(I), I=1,NB)
      WRITE(21,1100)X,Y,IHR,IMIN,ISEC,NMAG,NOP,N,MOB
1100  FORMAT(2F8.2,2X,3I3,I6,2I3,5X,A5)
      DO 85 I=1,N
      IF(MAG(I).LT.100) GO TO 82
      IHUN=(MAG(I)/100)*100
      GO TO 85
 82   MAG(I)=MAG(I) + IHUN
 85   CONTINUE
      WRITE(21,1200) (MAG(I),I=1,N)
1200  FORMAT(12I6)
      WRITE(21,1100)XB,YB,IHRB,IMINB,ISECB,NMAGB,NOPB,NB,IBAS
      DO 88 I=1,NB
      IF(BMAG(I).LT.100) GO TO 86
      IHUN=(BMAG(I)/100)*100
      GO TO 88
 86   BMAG(I)= BMAG(I) + IHUN
 88   CONTINUE
      WRITE(21,1200) (BMAG(I), I=1,NB)
 89   WRITE(5,800)
800   FORMAT(10X'ENTER -1 FOR NEW DAY OR NEW BASE,'
     1 ,' 0 FOR NEW STA, +1 TO STOP')
      READ(5,*) IJ
      IF(IJ) 5, 15, 99
 99   CLOSE(UNIT=21,FILE='ALBMG.RAW')
      STOP
      END
```

```
C       PROGRAM MAGRED
C
C*************************************************************
C
C       UTILITY PROGRAM
C       DESIGNED TO DO PRELIMINARY REDUCTION OF ALBION-
C       SCIPIO GROUND MAGNETIC DATA.
C
C       WRITTEN FOR USE WITH THE WMU DEC SYSTEM 10
C       JUNE, 1980
C
C*************************************************************
C
C**********READS FROM 20 (ALBMG.RAW) AND WRITES ON 21
C                (A FILE NAMED  ALBMG.RED  )
        DIMENSION MAG(24),BMAG(24),IDIF(24)
        INTEGER BMAG
        OPEN(UNIT=20,FILE='ALBMG.RAW')
        OPEN(UNIT=21,FILE='ALBMG.RED',ACCESS='APPEND')
        READ(20,2000) CODE
        WRITE(5,100)
  100   FORMAT( 4X,'ENTER IDAY,MMO, AND IYR OF FIRST DATE &
     1 LAST DATE + 1 TO BE PROCESSED')
        READ(5,*) IDAY,MO,IYR,  IDAY2,MO2,IYR2
 1000   FORMAT(3I3,2X,F8.1)
        WRITE(5,200)
  200   FORMAT(4X,'STATION',8X,'BASE',7X,'DATE',
     1  5X,'START',1X,'BASE SDEV STA ',
     2  'SDEV STA.VALUE'/5X,'X',5X,'Y',7X,'X',5X,
     3  'Y',2X,'DA MO YR',3X,'TIME',2X,'RDGS BASE RDGS',
     4  ' STA. GAMMAS',/1X,14('-----'))
C----------SEARCH FOR FIRST DAY TO BE PROCESSED.---------C
    5   READ(20,1000,END=99) IDAYM,MOM,IYRM,BASVAL
        IF(IDAY.EQ.IDAYM.AND.MO.EQ.MOM) GO TO 10
    6   READ(20,2000)X,Y,IHR,MIN,ISEC,NMAG,NOP,N
        IF(X.EQ.-999.) GO TO 5
        READ(20,3000) (MAG(I), I=1,N)
        GO TO 6
C----------READ DATA FOR 1 STATION.----------C
   10   READ(20,2000,END=99) X,Y,IHR,MIN,ISEC,NMAG,NOP,N
 2000   FORMAT(2F8.2,2X,3I3,I6,2I3)
        IF(X.EQ.-999.) GO TO 50
   15   READ(20,3000) (MAG(I),I=1,N)
 3000   FORMAT(12I6)
        READ(20,2000) XB,YB,IHRB,IMINB,ISECB,NMAGB,NOPB,NB
        READ(20,3000) (BMAG(I), I=1,NB)
C----------PROCESS DATA FOR THIS STATION.---------C
        DO 20 I=1,N
   20   IDIF(I) = MAG(I) - BMAG(I)
        CALL SDEV(N,IDIF,DMEAN,DEV)
        II = 1
        DO 30 I=1,N
        IF(ABS(IDIF(I) - DMEAN).GT.(4.)) GO TO 30
        MAG(II) = IDIF(I)
```

```
      II = II+1
 30   CONTINUE
      II=II-1
      IF(II.EQ.N) GO TO 40
      CALL SDEV(II,MAG,DMEAN,DEV)
      CONTINUE
 40   CALL SDEV(NB,BMAG,BMEAN,BDEV)
      STA=BASVAL+DMEAN
      WRITE(5,4000)X,Y,XB,YB,IDAYM,MOM,IYRM,IHR,MIN,NB,BDEV,
     1 II,DEV,STA
4000  FORMAT(2X,2F6.2,2X,2F6.2,3I3,2X,2I3,2(I4,F4.1),F9.1)
      WRITE(21,4000)X,Y,XB,YB,IDAYM,MOM,IYRM,IHR,MIN,NB,
     1 BDEV,II,DEV,STA
      GO  TO 10
 50   READ(20,1000,END=99)  IDAYM,MOM,IYRM,BASVAL
      IF(IDAY2.EQ.IDAYM.AND.MO2.EQ.MOM) GO TO 99
      GO TO 10
 99   STOP
      END
      SUBROUTINE SDEV(N,IDAT,DMEAN,DEV)
      DIMENSION IDAT(24)
      SUM=0.
      SUM2=0.
      DO 10 I=1,N
 10   SUM=SUM+IDAT(I)
      DMEAN=SUM/N
      DO 20 I=1,N
 20   SUM2=SUM2+(DMEAN-IDAT(I))**2
      DEV=SQRT(SUM2/N)
      RETURN
      END
```

```
C       PROGRAM REGMAG

C*************************************************************
C
C       THIS PROGRAM SUBTRACTS THE REGIONAL FIELD FOR THE
C       ALBION-SCIPIO AREA.  IT USES A LINEAR APPROXIMATION
C       TO THE REGIONAL GRADIENT, WHICH IS OBTAINED BY
C       OTHER MEANS.  THIS METHOD IS ONLY VALID FOR
C       SMALL AREAS WHERE THE REGIONAL FIELD GRADIENT
C       IS APPROXIMATELY LINEAR.  THE EQUATION USED IS
C       VALID ONLY FOR THE SURVEY AREA.
C
C*************************************************************
C
        OPEN(UNIT=20,FILE='ALBMG.RED')
        OPEN(UNIT=22,FILE='ALBMG.COR')
C
 10     READ(20,500,END=99)XLOC,YLOC,XMAG
500     FORMAT(2X,2F6.2,47X,F9.1)
C
C       ADD CORRECTION TO THE MAG VALUE
C
        CORMAG=XMAG+((.40625*XLOC)-(2.397169*YLOC))
        WRITE(22,200)XLOC,YLOC,CORMAG
200     FORMAT(2X,2F6.2,10X,F9.1,10X,2PE15.2)
        GO TO 10
 99     STOP
        END
```

```
C       PROGRAM MAGPLT
C
C*************************************************************
C       THIS PROGRAM PLOTS THE MAGNETIC STATION VALUES.
C       ON A CALCOMP DRUM PLOTTER, USING THE WMU
C       COMPUTER CENTER DEC SYSTEM 10.
C
C       THE + SYMBOLS ARE LOCATED AT THE X, Y POSITION
C       OF EACH STATION.
C
C       THE TOTAL FIELD VALUE IS PLOTTED ABOVE EACH +.
C
C       THE EXECUTE STATEMENT IS
C       EX MAGPLT.FOR,PUB:CALCOM.REL/SEA
C
C       TO PLOT THE DATA, YOU MUST TYPE PLOT GRID.FOR
C       WHERE GRID.FOR IS A STORAGE FILE FOR THE
C       COMPILED PLOT PROGRAM.
C
        REAL XLOC(695),YLOC(695),CORVAL(695)
C
C       NOW ALLOW ACCESS TO THE PLOT DATA
C
        OPEN(UNIT=21,FILE='PLOT.DAT')
C
C       THIS WILL SEND OUTPUT TO GRID.FOR
C
        OPEN(UNIT=20,FILE='GRID.FOR')
C
C       INITIALIZE PLOT SUBROUTINE
C
        CALL PLOTS(5,-1,20)
C
C       NOW READ IN THE DATA
C
        DO 10 I=1,695
        READ(21,500)XLOC(I),YLOC(I),CORVAL(I)
500     FORMAT(2X,2F7.3,10X,E15.8)
 10     CONTINUE
C
C       DRAW AN OUTER SQUARE OUTLINE
C
        CALL PLOT(30.0,0.,2)
        CALL PLOT(30.0,21.5,2)
        CALL PLOT(0.0,21.5,2)
        CALL PLOT(0.0,0.0,2)
C
C       DRAW AN INNER SQUARE
C
        CALL PLOT(1.75,1.75,3)
        CALL PLOT(28.2,1.75,2)
        CALL PLOT(28.2,19.65,2)
        CALL PLOT(1.75,19.65,2)
        CALL PLOT(1.75,1.75,2)
```

```
C
C       DRAW LAT. AND LONG. MARKERS
C
        CALL SYMBOL(2.0,2.0,.8,3,0.0,-1)
        CALL SYMBOL(28.0,2.0,.8,3,0.0,-1)
        CALL SYMBOL(28.0,19.4,.8,3,0.0,-1)
        CALL SYMBOL(2.0,19.4,.8,3,0.0,-1)
        CALL SYMBOL(15.0,2.0,.8,3,0.0,-1)
        CALL SYMBOL(15.0,19.4,.8,3,0.0,-1)
C
        DO 20 I=1,695
C
C       NOW PLOT THE STATION MARKERS
C
        CALL SYMBOL(XLOC(I),YLOC(I),.125,3,0.0,-1)
C
C       NOW ADD A LITTLE ROOM FOR THE NUMBER
C
        XNEW=XLOC(I)-.1
        YNEW=YLOC(I)+.11
C
C       NOW PLOT THE STATION VALUE
C
        CALL NUMBER(XNEW,YNEW,.085,CORVAL(I),0.0,-1)
C
 20     CONTINUE
C
C       DRAW IN COUNTY LINES(DASHED)
C
        CALL DASHS(ARRAY,1)
C
        CALL PLOT(1.75,7.07,3)
        CALL PLOT(11.02,7.0,2)
        CALL PLOT(17.02,6.87,2)
        CALL PLOT(28.2,7.03,2)
        CALL PLOT(11.02,7.0,3)
        CALL PLOT(11.02,1.75,2)
        CALL PLOT(17.02,6.87,3)
        CALL PLOT(16.92,12.25,2)
        CALL PLOT(16.65,19.65,2)
C
C       END PLOTTING
C
        CALL PLOT(30.0,0.0,999)
        STOP
        END
```

```
C       PROGRAM WERNER
C
C*****************************************************************
C
C       THIS PROGRAM IS DESIGNED TO SOLVE A 4*4 MATRIX USING
C       THE LINPACK SUBROUTINE SOFTWARE PACKAGE. (DONGARRA
C       ET AL., 1979). TWO SUBROUTINES WERE USED, SGECO AND
C       SGESL.  THEY PERFORM GAUSSIAN ELIMINATION (LU
C       FACTORIZATION) ON THE MATRIX A OF AX=B, AND THEN
C       SOLVE FOR X.
C
C       FROM THE MATRIX SOLUTION, THE DEPTH AND LOCATION OF A
C       TABULAR BODY OR INTERFACE CAN BE FOUND(HARTMAN,1971)
C
C*****************************************************************
C
        REAL A(12,12),B(12),BSAVE(12,12),T,RCOND,Z(12)
     1  ,STOR(100,100),BSTOR(100,100),LOC(100),DEP(100)
        INTEGER IPVT(12),NR
        DATA LDA/12/,NR/4/
        OPEN (UNIT=21,FILE='EGRAD.DAT')
C
C       WRITE THE TITLE FOR THE SQUARE MATRIX A
C
        WRITE(5,400)
  400   FORMAT('1',19X,'MATRIX A'/)
C
        NCTR=0
        M=1
        K=M+3
        NCHECK=0
C
C       NOW READ IN THE POSITION AND TOTAL FIELD VALUES
C       AND CALCULATE THE 'A' MATRIX VALUES USING
C       B(1)+B(2)*X+B(3)*(F)+B(4)*(X*F)=X**2*F, WHERE X
C       IS THE POSITION AND F IS THE TOTAL FIELD VALUE
C
        DO 20 I=1,100
        READ(21,300)X,F
  300   FORMAT(2E15.8)
        IF (F.EQ.999.)GO TO 110
        NCTR=NCTR+1
        STOR(I,1)=1.0
        STOR(I,2)=X
        STOR(I,3)=F
        STOR(I,4)=X*F
        BSTOR(I,5)=(X**2)*F
   20   CONTINUE
  110   N=M
        DO 50 I=1,4
C
        DO 45 J=1,4
        A(I,J)=STOR(N,J)
   45   CONTINUE.
```

```
          BSAVE(I,5)=BSTOR(N,5)
          N=N+10
   50     CONTINUE
C
   15     DO 10 I=1,4
          WRITE(5,350)(A(I,J),J=1,4)
  350     FORMAT(20X,4E15.8)
   10     CONTINUE
C
          WRITE(5,450)
  450     FORMAT(/,20X,'MATRIX B'/)
C
C         NOW WRITE THE MATRIX B OF AX=B
C
          DO 11 I=1,4
          WRITE(5,200)(BSAVE(I,5))
  200     FORMAT(20X,E15.8)
   11     CONTINUE
C
C         NOW TRANSFER BSAVE(I) INTO A ONE DIMENSIONAL ARRAY
C         FOR USE IN SGESL SUBROUTINE(SOLUTION SUBROUTINE)
C
          DO 30 I=1,4
          B(I)=BSAVE(I,5)
   30     CONTINUE
C
C*************************************************************
C
C         THIS SUBROUTINE IS PART OF THE LINPACK SERIES, IT
C         CALCULATES L AND U ,WHERE LY=B AND UX=Y,USING GAUSSIAN
C         ELIMINATION AND PARTIAL PIVOTING. A CONDITION NO. IS
C         ALSO GENERATED AND CAN BE USED TO DETERMINE WHETHER
C         THE MATRIX IS NON-SINGULAR.
C
          CALL SGECO(A,LDA,NR,IPVT,RCOND,Z)
          WRITE(5,500)RCOND
  500     FORMAT(/,20X,'THE INVERSE CONDITION NO.= ',E15.8/)
C
C         IF RCOND IS SMALLER THAN THE NO. OF SIGNIFICANT DIGITS
C         OF THE MACHINE, THE MATRIX IS CONSIDERED SINGULAR.
C         IF RCOND IS SMALL BUT DETECTABLE THE MATRIX SOLUTION
C         MAY BE INACCURATE.
C
          T=1.0+RCOND
          IF(T.EQ.1.0)GO TO 70
C
C*************************************************************
C
C         THIS SUBROUTINE SOLVES FOR X(AX=B) USING LY=B, AND
C         UX=Y. THE SOLUTION X IS PLACED INTO THE B(I) ARRAY
C
          CALL SGESL(A,LDA,NR,IPVT,B,0)
C
C         NOW WRITE THE SOLUTION MATRIX
```

```
C
      WRITE(5,650)
  650 FORMAT(20X,'THE SOLUTION FOR AX=B',/)
C
      DO 90 I=1,4
      WRITE(5,550)(B(I))
  550 FORMAT(20X,E15.8)
   90 CONTINUE
C
C     SOLVE FOR THE DEPTH AND LOCATION OF THE ASSUMED
C     DIKE USING WERNER'S EQUATIONS.
C
      XLOC=.5*B(4)
      DEPTH=SQRT((-4*B(3))-(B(4)**2))*.5

C
      WRITE(5,700)XLOC,DEPTH
      WRITE(23,700)XLOC,DEPTH
  700 FORMAT(10X,'LOCATION = ',E15.8,5X,'DEPTH = ',E15.8/)
C
C     NOW READ IN THE NEW VALUES AFTER SHIFTING 1 POSITION
C
      M=M+1
      NCHECK=NCHECK+1
      IF(NCHECK.GT.(NCTR-6))STOP
      GO TO 110
   70 WRITE(5,600)
  600 FORMAT(20X,'THE MATRIX IS COMPUTATIONALLY SINGULAR
     1 WITHIN MACHINE ACCURACY'/)
      M=M+1
      NCHECK=NCHECK+1
      IF(NCHECK.GT.(NCTR-6))STOP
   80 GO TO 110
C
      STOP
      END
```

APPENDIX B

Listing of the Reduced Data Files

Explanation.

Columns 1 and 2 give the X (east) and Y (north) coordinates in centimeters. The origin is located at 42° N 85° W.

Columns 3 and 4 are the base locations.

Columns 5, 6, and 7 are the day, month, and year.

Columns 8 and 9 give the time of the first reading of each station.

Column 10 is the number of base readings.

Column 11 is the standard deviation of the base readings.

Column 12 gives the number of readings used at each station site.

Column 13 is the standard deviation of the station values used.

Column 14 is the mean station value.

Note: The regional gradient has not been subtracted from these data.

STATION X	STATION Y	BASE X	BASE Y	DATE DA	DATE MO	DATE YR	START TIME	BASE RDGS	SDEV BASE	STA RDGS	SDEV STA.	STA.VALU GAMMAS
32.20	0.20	36.30	6.00	12	6	80	9 55	16	0.7	16	0.9	57672.9
34.70	0.10	36.30	6.00	12	6	80	10 29	16	0.8	16	1.3	57668.1
36.20	-0.10	36.30	6.00	12	6	80	10 46	16	0.5	16	1.1	57666.4
37.40	0.10	36.30	6.00	12	6	80	11 46	16	0.9	16	2.1	57657.6
38.50	-0.10	36.30	6.00	12	6	80	12 0	16	0.6	16	1.3	57661.4
40.00	0.10	36.30	6.00	12	6	80	12 12	16	0.9	16	1.8	57663.0
41.20	0.10	36.30	6.00	12	6	80	12 24	16	0.5	13	2.0	57663.2
41.00	2.70	36.10	7.70	12	6	80	1 45	16	1.4	16	1.9	57657.7
40.00	2.60	36.10	7.70	12	6	80	2 1	10	0.8	8	2.4	57658.4
38.40	2.80	36.10	7.70	12	6	80	2 20	16	0.9	14	1.1	57654.7
36.90	2.70	36.10	7.70	12	6	80	2 37	16	1.0	13	2.0	57664.4
36.20	3.20	36.10	7.70	12	6	80	2 48	16	1.6	12	2.2	57663.2
34.60	2.60	36.10	7.70	12	6	80	3 1	16	0.8	16	1.5	57670.3
33.60	2.60	36.10	7.70	12	6	80	3 12	16	0.8	16	1.0	57674.8
32.20	2.80	36.10	7.70	12	6	80	3 23	16	2.7	15	1.9	57679.3
32.30	5.50	36.10	7.70	12	6	80	4 0	16	2.8	15	1.1	57672.3
33.90	5.50	36.10	7.70	12	6	80	4 12	16	1.5	16	1.4	57670.8
36.20	4.80	36.10	7.70	12	6	80	4 29	16	2.1	16	2.1	57665.8
38.80	5.70	36.10	7.70	12	6	80	4 49	16	1.8	15	1.7	57649.5
40.30	5.20	36.10	7.70	12	6	80	5 5	16	1.0	16	1.6	57647.3
41.60	5.50	36.10	7.70	12	6	80	5 22	16	0.9	13	2.0	57640.6
42.30	5.50	36.10	7.70	13	6	80	10 53	16	1.2	12	2.0	57647.2
42.30	8.30	36.10	7.70	13	6	80	11 10	16	0.9	16	2.0	57633.8
41.10	7.60	36.10	7.70	13	6	80	11 22	16	0.9	16	1.4	57636.9
40.10	8.10	36.10	7.70	13	6	80	11 35	16	0.7	16	1.0	57641.9
38.40	8.00	36.10	7.70	13	6	80	11 46	16	1.0	14	2.4	57646.4
37.10	8.00	36.10	7.70	13	6	80	11 57	16	1.2	14	1.8	57651.7
35.80	7.80	36.10	7.70	13	6	80	12 8	16	0.7	16	2.1	57655.1
34.70	7.80	36.10	7.70	13	6	80	12 20	16	1.5	15	2.0	57657.5
33.60	7.80	36.10	7.70	13	6	80	12 33	16	1.4	12	2.0	57658.5
32.50	10.40	36.10	7.70	13	6	80	2 6	16	1.1	16	1.4	57663.3
33.60	10.80	36.10	7.70	13	6	80	2 18	16	1.5	16	1.8	57658.6
35.00	10.40	36.10	7.70	13	6	80	2 30	16	0.8	16	1.0	57655.3
36.20	10.70	36.10	7.70	13	6	80	2 43	16	0.9	15	1.1	57650.5
37.40	10.70	36.10	7.70	13	6	80	2 55	16	1.9	16	1.9	57647.9
38.70	10.70	36.10	7.70	13	6	80	3 8	16	0.6	6	1.2	57641.0
39.90	10.60	36.10	7.70	13	6	80	3 20	16	0.7	16	1.5	57647.8
41.10	10.70	36.10	7.70	13	6	80	3 33	16	1.2	16	1.2	57639.4
42.60	10.80	36.10	7.70	13	6	80	3 45	16	1.8	16	2.0	57643.1
32.30	12.60	36.10	7.70	16	6	80	10 34	16	1.3	16	1.3	57664.0
36.20	13.90	36.10	7.70	16	6	80	11 35	10	0.5	10	1.0	57665.3
33.50	12.80	36.20	13.90	16	6	80	12 28	16	1.2	15	1.7	57671.4
35.20	12.80	36.20	13.90	16	6	80	12 48	16	0.4	16	1.1	57670.1
35.80	12.50	36.20	13.90	16	6	80	1 3	16	0.8	16	1.6	57660.6
36.30	12.80	36.20	13.90	16	6	80	1 14	16	0.6	15	2.1	57660.5
38.40	12.60	36.20	13.90	16	6	80	1 30	16	0.6	16	1.7	57653.8

39.40	12.70	36.20	13.90	16	6	80	1	41	16	0.7	15	1.7	57658.3
40.80	12.60	36.20	13.90	16	6	80	1	53	16	0.9	16	1.7	57652.9
40.70	15.30	36.20	13.90	16	6	80	2	18	11	0.6	11	1.4	57664.8
38.60	15.20	36.20	13.90	16	6	80	2	46	16	0.9	14	1.8	57674.9
38.40	17.30	36.20	13.90	16	6	80	2	59	16	1.0	10	2.1	57674.5
37.00	17.30	36.20	13.90	16	6	80	3	11	16	0.8	15	1.5	57677.9
34.30	15.40	36.20	13.90	16	6	80	3	39	16	1.3	2	2.0	57676.0
33.10	15.50	36.20	13.90	16	6	80	3	51	16	0.7	14	1.9	57676.1
32.20	15.20	36.20	13.90	16	6	80	4	2	16	0.9	16	1.3	57672.4
32.20	17.90	36.20	13.90	16	6	80	4	17	13	0.9	11	1.6	57694.5
34.30	18.10	36.20	13.90	16	6	80	4	47	16	0.8	16	0.9	57691.2
35.50	18.10	36.20	13.90	16	6	80	4	59	16	0.7	16	1.4	57688.9
39.40	17.70	36.20	13.90	16	6	80	5	17	16	1.1	16	1.8	57670.4
40.70	17.60	36.20	13.90	16	6	80	5	31	9	0.6	9	1.2	57666.0
42.10	12.50	36.20	13.90	16	6	80	5	52	16	0.6	16	1.3	57653.4
33.40	20.90	36.00	21.10	17	6	80	12	59	16	0.7	14	1.5	57714.2
34.70	20.70	36.00	21.10	17	6	80	1	11	16	0.7	12	2.3	57707.7
36.40	20.70	36.00	21.10	17	6	80	1	32	16	0.4	16	1.1	57698.8
38.70	20.30	36.00	21.10	17	6	80	2	1	16	1.0	16	1.9	57692.6
39.70	20.60	36.00	21.10	17	6	80	2	18	16	0.5	16	1.3	57685.6
38.30	22.80	36.00	21.10	17	6	80	2	41	11	0.6	11	1.5	57687.0
35.60	23.30	36.00	21.10	17	6	80	2	57	16	0.8	16	0.9	57697.6
34.40	23.30	36.00	21.10	17	6	80	3	13	16	0.9	16	1.4	57704.3
33.50	23.40	36.00	21.10	17	6	80	3	26	16	0.8	15	1.7	57711.6
39.70	22.80	36.00	21.10	17	6	80	5	12	16	0.8	11	1.4	57667.4
32.70	25.60	35.70	27.20	18	6	80	12	12	16	0.7	14	1.9	57685.5
35.00	25.80	35.70	27.20	18	6	80	12	28	16	0.8	16	1.7	57680.5
36.20	25.60	35.70	27.20	18	6	80	12	39	16	0.9	16	1.2	57687.4
37.20	25.50	35.70	27.20	18	6	80	12	52	16	0.9	16	1.8	57685.4
38.50	26.40	36.00	27.80	18	6	80	3	13	16	0.8	13	2.3	57689.7
41.10	25.70	36.00	27.80	18	6	80	3	30	15	0.7	5	3.0	57675.1
32.80	28.50	36.00	27.80	18	6	80	3	47	16	0.7	15	2.2	57655.4
34.50	28.70	36.00	27.80	18	6	80	4	0	16	0.7	16	1.9	57673.4
36.40	28.80	36.00	27.80	18	6	80	4	13	16	0.7	15	2.1	57699.2
38.70	29.00	36.00	27.80	18	6	80	4	30	16	0.6	16	1.1	57726.4
39.70	29.30	36.00	27.80	18	6	80	4	44	16	0.4	16	1.2	57745.6
41.00	28.50	36.00	27.80	18	6	80	5	12	16	0.6	15	2.4	57732.1
41.90	29.80	36.00	27.80	18	6	80	5	27	16	0.7	16	1.3	57752.7
31.90	31.20	35.30	34.30	23	6	80	10	12	16	1.0	13	1.8	57652.9
33.20	30.50	35.30	34.30	23	6	80	10	25	16	0.8	16	1.4	57664.0
35.90	30.60	35.30	34.30	23	6	80	10	39	16	0.6	6	2.3	57704.3
37.00	31.20	35.30	34.30	23	6	80	10	53	16	0.7	16	1.5	57716.3
39.30	31.20	35.30	34.30	23	6	80	11	8	16	0.5	13	1.8	57763.3
40.90	31.20	35.30	34.30	23	6	80	11	21	16	0.9	16	1.6	57764.8
42.20	31.30	35.30	34.30	23	6	80	11	38	15	0.7	15	1.3	57750.0
41.60	33.80	35.30	34.30	23	6	80	11	52	16	0.7	16	2.2	57749.9
40.40	33.80	35.30	34.30	23	6	80	12	10	16	0.8	16	1.7	57748.4
38.90	33.80	35.30	34.30	23	6	80	12	21	16	0.7	16	1.5	57747.6
38.00	33.70	35.30	34.30	23	6	80	12	32	16	0.8	16	1.0	57737.3
36.80	33.30	35.30	34.30	23	6	80	12	43	16	0.7	16	1.3	57718.9

35.00	33.80	35.30	34.30	23	6	80	1	27	16	1.2	14	1.7	57685.7
32.60	33.40	35.30	34.30	23	6	80	1	49	16	0.6	12	2.3	57648.1
32.00	33.50	35.30	34.30	23	6	80	2	3	16	0.9	13	1.5	57645.0
31.20	36.10	35.30	34.30	23	6	80	2	20	16	0.7	14	1.6	57650.5
33.90	36.40	35.30	34.30	23	6	80	2	37	16	1.1	16	2.1	57665.4
35.10	36.30	35.30	34.30	23	6	80	2	49	15	0.7	15	1.4	57687.2
36.60	36.30	35.30	34.30	23	6	80	3	3	7	0.7	7	1.5	57698.1
37.80	36.10	35.30	34.30	23	6	80	3	17	16	0.7	16	1.4	57716.2
39.20	36.00	35.30	34.30	23	6	80	3	30	16	0.7	15	1.5	57732.0
40.60	36.20	35.30	34.30	23	6	80	3	41	16	0.6	16	1.3	57736.9
42.30	36.10	35.30	34.30	23	6	80	3	53	16	0.8	15	1.5	57736.0
31.00	39.00	35.40	40.70	24	6	80	10	18	16	1.4	16	0.9	57660.0
33.70	39.00	35.40	40.70	24	6	80	10	31	16	1.1	16	1.8	57676.4
35.50	39.00	35.40	40.70	24	6	80	10	43	16	0.8	8	2.1	57687.8
36.50	39.10	35.40	40.70	24	6	80	10	54	16	0.8	7	1.5	57691.4
38.20	38.70	35.40	40.70	24	6	80	11	5	16	0.8	12	1.5	57702.5
39.20	38.70	35.40	40.70	24	6	80	11	16	16	1.3	16	1.4	57703.7
40.70	39.00	35.40	40.70	24	6	80	11	29	16	0.9	16	1.1	57713.0
41.70	39.00	35.40	40.70	24	6	80	11	43	16	0.8	16	1.6	57711.4
43.40	39.20	35.40	40.70	24	6	80	11	56	16	0.7	16	1.5	57711.6
40.80	41.40	35.40	40.70	24	6	80	12	9	16	1.3	16	1.4	57677.9
38.80	41.20	35.40	40.70	24	6	80	12	22	16	1.2	6	2.0	57672.3
37.50	41.20	35.40	40.70	24	6	80	12	37	16	0.8	16	1.6	57679.4
36.50	41.30	35.40	40.70	24	6	80	2	16	16	0.8	16	1.2	57676.8
35.00	41.80	35.40	40.70	24	6	80	2	28	16	0.8	15	1.7	57673.0
32.70	40.60	35.40	40.70	24	6	80	2	58	15	1.1	6	2.5	57677.1
36.20	43.60	35.40	40.70	24	6	80	3	33	9	0.5	7	1.8	57677.9
38.50	44.20	35.40	40.70	24	6	80	3	51	16	1.1	13	2.0	57665.5
40.20	44.10	35.40	40.70	24	6	80	4	14	14	1.1	13	2.0	57665.8
41.80	44.10	35.40	40.70	24	6	80	4	29	16	0.9	16	1.3	57660.9
42.90	44.40	35.40	40.70	24	6	80	4	40	16	1.5	16	1.2	57661.7
43.20	42.30	47.00	38.90	25	6	80	10	38	16	0.7	16	0.8	57674.8
44.70	44.30	47.00	38.90	25	6	80	10	53	14	0.9	14	1.7	57659.2
46.40	44.20	47.00	38.90	25	6	80	11	7	16	0.8	14	1.3	57660.4
48.60	43.90	47.00	38.90	25	6	80	11	20	15	0.7	15	2.0	57649.4
50.30	43.70	47.00	38.90	25	6	80	11	33	16	0.6	16	1.7	57646.2
51.80	44.00	47.00	38.90	25	6	80	11	47	15	0.7	14	1.8	57645.6
52.70	44.30	47.00	38.90	25	6	80	11	59	16	0.6	16	1.0	57644.9
55.00	43.30	47.00	38.90	25	6	80	12	13	16	0.7	16	1.5	57648.6
54.90	41.80	47.00	38.90	25	6	80	12	31	14	0.6	14	1.3	57648.8
53.50	41.00	47.00	38.90	25	6	80	12	45	15	1.0	15	1.1	57646.8
44.00	41.70	47.00	38.90	25	6	80	1	55	14	1.3	12	1.8	57678.8
45.00	41.60	47.00	38.90	25	6	80	2	7	16	1.1	15	2.0	57675.9
46.80	41.70	47.00	38.90	25	6	80	2	27	15	1.4	14	2.2	57663.6
49.80	40.90	47.00	38.90	25	6	80	2	52	16	0.6	14	1.6	57654.3
50.00	39.70	47.00	38.90	25	6	80	3	7	15	0.7	4	2.3	57657.7
52.00	38.80	47.00	38.90	25	6	80	3	25	16	1.3	16	1.5	57661.6
45.80	37.90	47.00	38.90	26	6	80	9	27	16	1.2	13	2.0	57704.8
45.40	38.90	47.00	38.90	26	6	80	9	38	16	1.0	16	1.7	57697.0
46.50	39.20	47.00	38.90	26	6	80	9	50	16	0.7	16	1.8	57679.9

47.80	38.90	47.00	38.90	26	6	80	10	2	16	0.9	15	2.0	57676.7
48.60	37.40	47.00	38.90	26	6	80	10	15	16	1.0	16	1.7	57687.3
50.50	37.20	47.00	38.90	26	6	80	10	32	16	1.1	13	1.7	57677.5
53.80	39.10	47.00	38.90	26	6	80	10	53	14	1.0	13	1.7	57645.4
55.10	35.60	47.00	38.90	26	6	80	11	11	16	1.6	16	2.1	57661.3
53.60	35.20	47.00	38.90	26	6	80	11	22	16	0.9	13	2.3	57665.5
52.10	34.30	47.00	38.90	26	6	80	11	32	16	1.0	15	2.3	57671.9
50.50	34.90	47.00	38.90	26	6	80	11	48	16	0.8	16	1.4	57679.7
48.70	35.30	47.00	38.90	26	6	80	12	0	16	0.8	15	1.8	57687.5
47.10	35.20	47.00	38.90	26	6	80	1	14	16	1.0	15	2.1	57710.5
45.30	34.80	47.00	38.90	26	6	80	1	25	16	1.1	16	1.3	57736.5
46.10	33.90	47.00	38.90	26	6	80	1	50	16	1.9	10	1.5	57722.8
44.10	33.90	47.00	38.90	26	6	80	2	3	16	0.6	15	1.7	57739.5
45.00	31.00	48.30	25.30	26	6	80	4	43	11	0.9	8	2.3	57709.6
49.20	30.70	48.30	25.30	26	6	80	5	3	16	1.3	15	1.9	57666.1
51.50	30.90	48.30	25.30	26	6	80	5	15	16	0.9	16	1.9	57657.8
52.50	32.70	48.30	25.30	26	6	80	5	27	16	0.7	15	1.8	57670.1
54.20	32.80	48.30	25.30	26	6	80	5	39	16	1.2	15	1.6	57659.5
55.90	33.60	48.30	25.30	26	6	80	5	58	16	1.2	16	1.4	57661.4
49.30	33.30	48.30	25.30	26	6	80	6	16	16	1.1	15	1.3	57675.7
47.60	32.90	48.30	25.30	26	6	80	6	28	16	1.0	16	1.1	57685.0
44.40	29.00	48.30	25.30	27	6	80	8	57	16	1.0	16	1.3	57707.4
44.00	26.90	48.30	25.30	27	6	80	9	10	16	0.9	16	1.1	57678.4
44.00	25.60	48.30	25.30	27	6	80	9	22	12	0.6	12	1.4	57666.7
46.00	25.40	48.30	25.30	27	6	80	9	35	16	0.6	16	1.4	57655.3
47.20	25.50	48.30	25.30	27	6	80	9	47	16	0.8	14	1.8	57656.1
49.10	26.00	48.30	25.30	27	6	80	9	59	16	0.7	16	1.5	57643.6
48.30	27.30	48.30	25.30	27	6	80	10	18	16	0.8	16	1.5	57662.4
47.60	29.40	48.30	25.30	27	6	80	10	38	16	0.5	15	2.3	57666.0
50.10	29.30	48.30	25.30	27	6	80	11	18	16	0.8	16	1.1	57651.1
52.80	30.10	48.30	25.30	27	6	80	11	36	16	0.7	15	1.8	57658.5
54.20	30.10	48.30	25.30	27	6	80	11	48	16	0.7	16	1.3	57661.9
55.80	30.10	48.30	25.30	27	6	80	12	1	16	0.5	15	2.1	57666.0
51.10	27.30	48.30	25.30	27	6	80	12	33	16	0.6	16	1.3	57645.3
51.20	25.50	48.30	25.30	27	6	80	12	45	16	0.6	11	1.7	57636.4
51.30	23.70	48.30	25.30	27	6	80	12	57	16	0.6	16	1.2	57643.9
54.20	23.40	48.30	25.30	27	6	80	1	11	16	0.8	16	1.2	57641.0
55.50	23.40	48.30	25.30	27	6	80	1	27	16	0.5	9	1.3	57647.9
55.70	25.80	48.30	25.30	27	6	80	1	39	16	0.5	16	1.1	57652.2
54.90	27.20	48.30	25.30	27	6	80	1	53	16	0.6	15	2.1	57660.8
53.10	27.20	48.30	25.30	27	6	80	2	6	16	0.7	16	1.2	57652.8
54.00	25.30	48.30	25.30	27	6	80	2	22	16	0.6	16	1.4	57649.3
43.10	22.80	46.90	17.80	30	6	80	10	53	16	1.0	14	1.8	57645.6
44.50	22.80	46.90	17.80	30	6	80	11	5	16	0.8	16	1.8	57643.6
45.60	22.80	46.90	17.80	30	6	80	11	16	16	0.6	16	1.2	57641.4
47.70	22.50	46.90	17.80	30	6	80	11	36	16	0.7	15	1.3	57635.5
49.80	23.10	46.90	17.80	30	6	80	11	54	16	0.7	16	1.5	57639.9
44.20	20.40	46.90	17.80	30	6	80	12	30	16	0.5	16	1.3	57647.2
45.90	20.40	46.90	17.80	30	6	80	12	41	16	0.7	14	2.0	57644.2
49.30	21.20	46.90	17.80	30	6	80	1	1	16	0.8	16	1.6	57632.9

50.90	20.80	46.90	17.80	30	6	80	2	12	16	0.7	16	1.2	57635.2
53.00	20.50	46.90	17.80	30	6	80	2	26	16	2.3	15	1.1	57638.6
55.60	21.00	46.90	17.80	30	6	80	2	38	16	0.5	16	1.5	57647.9
55.80	18.30	46.90	17.80	30	6	80	2	51	15	0.6	15	1.9	57656.4
54.60	17.90	46.90	17.80	30	6	80	3	11	16	0.7	16	1.2	57639.6
53.00	17.90	46.90	17.80	30	6	80	3	23	15	1.1	15	1.4	57640.2
51.30	18.30	46.90	17.80	30	6	80	3	42	16	1.2	13	1.4	57636.5
49.40	18.20	46.90	17.80	30	6	80	4	5	16	0.7	3	1.2	57634.2
48.50	17.90	46.90	17.80	30	6	80	4	18	16	0.9	16	1.5	57638.7
46.50	17.80	46.90	17.80	30	6	80	4	31	16	0.8	14	1.8	57645.8
45.50	17.80	46.90	17.80	30	6	80	4	42	16	0.8	15	1.0	57648.5
41.80	18.10	46.90	17.80	30	6	80	5	7	10	1.0	9	2.0	57654.9
43.60	10.10	50.90	5.50	2	7	80	10	39	16	0.8	16	1.3	57638.0
44.80	10.70	50.90	5.50	2	7	80	10	51	16	0.9	14	2.1	57632.6
46.00	10.30	50.90	5.50	2	7	80	11	6	13	0.7	12	0.9	57636.9
49.60	11.40	50.90	5.50	2	7	80	11	24	16	1.2	16	1.3	57652.7
51.80	10.50	50.90	5.50	2	7	80	11	43	16	0.7	16	1.9	57656.9
54.40	10.50	50.90	5.50	2	7	80	12	1	16	0.5	16	1.1	57654.3
56.30	10.20	50.90	5.50	2	7	80	12	18	16	1.1	15	1.4	57646.6
56.20	8.20	50.90	5.50	2	7	80	1	29	14	0.9	14	1.3	57656.7
55.00	8.20	50.90	5.50	2	7	80	1	41	16	0.8	14	1.8	57654.6
52.80	7.80	50.90	5.50	2	7	80	1	53	16	0.9	16	1.3	57659.5
51.30	7.70	50.90	5.50	2	7	80	2	18	16	0.9	16	1.7	57662.3
47.90	7.70	50.90	5.50	2	7	80	2	32	16	0.8	16	1.7	57647.8
56.00	15.70	46.90	17.80	1	7	80	9	31	16	0.9	16	1.1	57649.1
54.30	15.70	46.90	17.80	1	7	80	9	42	16	0.7	16	0.7	57644.1
52.70	15.60	46.90	17.80	1	7	80	9	53	16	0.7	16	1.2	57644.8
51.30	15.70	46.90	17.80	1	7	80	10	5	16	0.6	16	1.6	57648.1
48.30	15.60	46.90	17.80	1	7	80	10	18	16	0.9	15	1.9	57651.9
50.10	15.70	46.90	17.80	1	7	80	10	30	16	0.5	16	1.4	57652.2
47.20	15.60	46.90	17.80	1	7	80	10	42	16	0.8	16	1.0	57652.6
46.00	15.70	46.90	17.80	1	7	80	10	54	16	0.6	16	1.4	57649.4
42.90	15.50	46.90	17.80	1	7	80	11	17	16	0.8	15	1.7	57657.9
42.30	14.50	46.90	17.80	1	7	80	11	34	16	0.8	16	1.5	57664.1
48.40	13.10	46.90	17.80	1	7	80	12	1	16	0.6	16	1.5	57651.1
44.50	13.00	46.90	17.80	1	7	80	12	22	16	0.6	16	1.1	57643.4
49.90	12.60	46.90	17.80	1	7	80	12	49	16	0.8	15	1.6	57661.0
51.30	12.40	46.90	17.80	1	7	80	1	6	16	1.0	14	1.9	57658.6
53.90	13.00	46.90	17.80	1	7	80	1	29	16	0.7	11	1.7	57646.9
56.60	13.30	46.90	17.80	1	7	80	1	46	16	0.8	15	1.6	57655.6
46.10	7.70	50.90	5.50	2	7	80	2	44	16	0.6	14	2.0	57645.8
45.20	7.70	50.90	5.50	2	7	80	2	54	16	0.6	16	1.6	57639.2
43.50	7.70	50.90	5.50	2	7	80	3	10	16	0.7	16	1.5	57637.7
44.00	5.10	50.90	5.50	2	7	80	3	24	16	0.8	16	1.9	57654.7
45.40	5.60	50.90	5.50	2	7	80	3	39	16	0.7	16	1.1	57655.1
47.00	5.60	50.90	5.50	2	7	80	3	52	16	1.2	16	1.1	57664.9
49.30	5.10	50.90	5.50	2	7	80	4	5	16	0.6	16	1.7	57671.1
52.00	5.80	50.90	5.50	2	7	80	4	28	16	0.6	15	2.1	57665.0
54.40	6.00	50.90	5.50	2	7	80	4	43	15	0.9	15	1.5	57656.3
55.70	5.70	50.90	5.50	2	7	80	5	1	15	0.5	15	1.5	57663.5

56.80	5.50	50.90	5.50	2	7	80	5	14	16	0.8	16	1.6	57668.7
42.30	2.60	50.90	5.50	3	7	80	9	42	16	0.7	16	0.9	57654.2
44.00	2.50	50.90	5.50	3	7	80	9	53	16	0.6	16	0.9	57664.5
45.10	3.00	50.90	5.50	3	7	80	10	3	16	0.8	16	1.9	57668.7
46.10	3.00	50.90	5.50	3	7	80	10	14	16	0.6	16	1.4	57675.9
48.30	2.50	50.90	5.50	3	7	80	10	29	16	0.6	14	1.6	57673.2
49.80	2.50	50.90	5.50	3	7	80	10	42	16	0.7	15	1.5	57662.2
53.00	3.00	50.90	5.50	3	7	80	11	2	14	0.6	13	1.7	57654.2
55.00	3.00	50.90	5.50	3	7	80	11	14	16	0.8	16	1.4	57661.2
56.70	0.20	50.90	5.50	3	7	80	11	49	16	0.8	16	1.8	57678.5
50.40	0.10	50.90	5.50	3	7	80	12	56	16	0.6	11	2.2	57668.2
52.50	-0.50	50.90	5.50	3	7	80	1	9	15	0.7	12	2.1	57675.6
55.50	0.20	50.90	5.50	3	7	80	1	21	16	0.5	15	1.4	57663.6
47.60	-0.30	50.90	5.50	8	7	80	9	59	13	1.1	9	2.3	57683.4
43.90	0.00	50.90	5.50	8	7	80	10	19	16	0.6	16	1.2	57679.2
44.90	0.00	50.90	5.50	8	7	80	10	48	16	0.7	9	1.8	57686.9
58.10	-0.10	61.80	6.70	8	7	80	1	53	16	0.6	14	1.0	57690.1
59.70	-0.10	61.80	6.70	8	7	80	2	4	16	0.8	14	1.9	57686.3
61.30	0.20	61.80	6.70	8	7	80	12	15	16	1.6	9	2.1	57691.9
62.80	0.10	61.80	6.70	8	7	80	2	38	15	1.8	13	1.2	57686.0
64.50	-0.10	61.80	6.70	8	7	80	2	53	16	0.9	9	1.2	57690.5
65.50	0.30	61.80	6.70	8	7	80	3	12	16	0.6	14	1.3	57690.5
65.50	2.90	61.80	6.70	8	7	80	3	28	5	0.6	5	2.3	57696.4
63.00	2.90	61.80	6.70	8	7	80	3	40	16	0.7	16	1.8	57696.9
61.60	2.90	61.80	6.70	8	7	80	3	56	16	1.3	16	1.9	57694.2
60.30	2.70	61.80	6.70	8	7	80	4	6	16	0.9	14	1.5	57691.6
58.90	2.90	61.80	6.70	8	7	80	4	18	16	1.0	13	1.9	57686.6
59.10	5.40	61.80	6.70	8	7	80	4	34	15	1.0	15	1.3	57686.5
57.90	8.20	61.80	6.70	8	7	80	4	48	16	1.0	15	1.5	57669.1
59.00	8.30	61.80	6.70	8	7	80	5	1	16	0.8	16	1.2	57666.7
60.80	7.80	61.80	6.70	8	7	80	5	17	16	0.6	13	2.4	57678.0
61.90	5.20	61.80	6.70	10	7	80	9	52	16	0.9	16	1.3	57684.8
63.30	5.60	61.80	6.70	10	7	80	10	3	16	0.8	16	1.2	57678.1
65.00	5.20	61.80	6.70	10	7	80	10	15	16	0.8	16	1.2	57675.4
66.50	5.50	61.80	6.70	10	7	80	10	27	16	0.7	16	1.9	57682.9
62.70	8.30	61.80	6.70	10	7	80	10	44	16	0.8	16	1.4	57683.8
64.40	8.00	61.80	6.70	10	7	80	11	0	16	1.1	7	1.9	57680.4
66.00	8.10	61.80	6.70	10	7	80	11	13	16	0.8	14	2.0	57672.9
61.40	10.70	61.80	6.70	10	7	80	11	33	16	0.9	16	1.6	57672.7
59.00	10.50	61.80	6.70	10	7	80	11	52	16	0.7	16	1.1	57660.8
57.90	10.00	61.80	6.70	10	7	80	12	9	16	0.8	16	1.4	57658.1
58.00	13.00	61.80	6.70	10	7	80	12	24	16	0.6	15	1.5	57655.2
59.90	12.70	61.80	6.70	10	7	80	12	37	16	0.9	8	2.0	57679.7
64.10	11.30	61.80	6.70	10	7	80	2	1	16	0.7	14	1.7	57695.4
64.40	13.30	61.80	6.70	10	7	80	2	12	16	1.1	16	1.8	57692.0
66.00	13.60	61.80	6.70	10	7	80	2	26	16	1.2	13	1.9	57698.2
62.60	13.20	61.80	6.70	10	7	80	2	40	16	1.1	10	2.4	57695.5
60.00	15.60	61.20	20.60	10	7	80	4	9	16	1.0	12	1.8	57677.5
60.90	15.70	61.20	20.60	10	7	80	4	21	15	0.7	15	1.6	57683.5
62.30	15.70	61.20	20.60	10	7	80	4	35	16	0.5	12	1.3	57685.9

64.50	15.70	61.20	20.60	10	7	80	4	55	15	0.8	12	2.4	57689.2
65.90	15.80	61.20	20.60	10	7	80	5	10	16	1.3	16	1.4	57691.6
57.30	18.00	61.20	20.60	11	7	80	9	31	16	0.8	15	1.7	57664.1
61.30	18.00	61.20	20.60	11	7	80	9	45	16	1.3	16	1.2	57673.7
63.10	18.00	61.20	20.60	11	7	80	9	59	16	0.9	14	1.2	57682.2
64.70	18.40	61.20	20.60	11	7	80	10	11	16	1.1	13	2.1	57694.6
66.60	18.20	61.20	20.60	11	7	80	10	23	16	1.2	16	1.7	57688.2
66.20	21.00	61.20	20.60	11	7	80	10	43	16	1.9	16	1.9	57690.2
64.70	21.00	61.20	20.60	11	7	80	10	59	16	1.0	14	1.5	57683.5
63.30	21.00	61.20	20.60	11	7	80	11	10	16	1.1	15	1.9	57673.6
61.40	20.90	61.20	20.60	11	7	80	11	23	16	1.0	15	1.9	57673.8
60.00	20.60	61.20	20.60	11	7	80	11	38	16	0.5	14	1.5	57673.4
59.00	20.90	61.20	20.60	11	7	80	11	52	16	0.7	13	1.5	57666.6
57.20	20.80	61.20	20.60	11	7	80	12	7	15	0.9	8	2.2	57654.6
56.50	23.50	61.20	20.60	11	7	80	12	55	16	1.1	16	1.4	57660.2
58.00	24.00	61.20	20.60	11	7	80	1	17	10	1.1	10	1.0	57651.6
59.30	22.70	61.20	20.60	11	7	80	1	42	16	0.7	16	1.1	57664.5
61.10	23.50	61.20	20.60	11	7	80	1	54	16	0.8	16	0.9	57653.9
62.90	23.60	61.20	20.60	11	7	80	2	5	16	1.0	13	1.1	57661.7
64.20	23.20	61.20	20.60	11	7	80	2	18	16	1.3	16	1.3	57683.7
66.40	26.10	61.20	20.60	11	7	80	2	36	16	1.1	14	2.0	57680.7
65.00	26.20	61.20	20.60	11	7	80	2	48	16	0.9	16	1.2	57667.5
62.90	25.90	61.20	20.60	11	7	80	3	3	16	1.3	16	1.4	57670.9
61.00	26.80	61.20	20.60	11	7	80	3	16	16	0.9	16	1.1	57672.7
59.00	27.20	61.20	20.60	11	7	80	3	28	16	1.5	15	1.7	57665.4
57.00	27.20	61.20	20.60	14	7	80	2	17	16	1.3	14	2.0	57656.3
57.40	30.20	61.20	20.60	14	7	80	2	36	16	1.1	16	2.0	57669.2
59.00	30.20	61.20	20.60	14	7	80	2	51	16	0.6	11	2.4	57667.4
60.40	29.40	61.20	20.60	14	7	80	3	3	16	0.8	16	1.8	57673.0
62.00	30.10	61.20	20.60	14	7	80	3	15	16	1.1	15	2.0	57677.6
63.50	29.80	61.20	20.60	14	7	80	3	30	16	0.7	15	1.9	57674.1
64.80	30.10	61.20	20.60	14	7	80	3	43	16	0.8	14	2.3	57673.9
66.10	29.90	61.20	20.60	14	7	80	3	58	16	0.8	16	1.5	57673.9
65.90	37.50	64.00	38.90	15	7	80	10	10	16	0.5	16	1.5	57679.0
66.10	35.20	64.00	38.90	15	7	80	10	23	16	0.8	15	1.8	57671.1
63.70	34.20	64.00	38.90	15	7	80	10	53	16	7.0	5	1.4	57673.7
61.40	35.60	64.00	38.90	15	7	80	11	28	16	0.7	15	1.4	57671.6
59.20	34.40	64.00	38.90	15	7	80	11	43	16	0.7	15	2.0	57672.1
56.80	34.30	64.00	38.90	15	7	80	12	0	16	1.0	15	1.6	57661.0
56.70	37.30	64.00	38.90	15	7	80	12	16	16	1.1	16	1.3	57645.0
58.60	37.80	64.00	38.90	15	7	80	12	40	15	1.0	12	1.7	57639.0
61.20	37.60	64.00	38.90	15	7	80	1	59	15	0.7	14	1.7	57667.9
62.40	37.80	64.00	38.90	15	7	80	2	17	16	0.6	15	1.9	57663.8
63.80	37.20	64.00	38.90	15	7	80	2	35	16	0.8	11	1.6	57674.5
66.50	32.00	64.00	38.90	15	7	80	2	55	16	0.6	16	2.1	57671.8
65.00	32.40	64.00	38.90	15	7	80	3	11	16	0.8	15	1.6	57672.9
63.60	32.20	64.00	38.90	15	7	80	3	27	16	0.9	16	1.9	57672.9
62.10	31.60	64.00	38.90	15	7	80	3	40	16	0.6	16	1.9	57674.5
58.40	31.80	64.00	38.90	15	7	80	3	54	16	0.9	16	1.3	57669.6
60.20	31.80	64.00	38.90	15	7	80	4	11	16	0.8	16	1.3	57670.9

56.50	40.10	64.00	38.90	15	7	80	5	3	16	0.9	16	1.5	57637.7
66.80	41.70	64.00	38.90	16	7	80	11	29	16	0.8	16	1.4	57671.3
64.00	41.90	64.00	38.90	16	7	80	11	44	15	0.7	15	0.9	57652.1
63.00	41.40	64.00	38.90	16	7	80	11	56	16	0.7	16	1.6	57649.4
61.40	40.50	64.00	38.90	16	7	80	12	10	16	0.8	16	1.6	57642.2
58.70	41.40	64.00	38.90	16	7	80	12	22	16	1.1	16	1.1	57639.7
64.30	44.20	64.00	38.90	16	7	80	12	41	16	0.8	16	0.9	57661.6
61.70	44.20	64.00	38.90	16	7	80	1	0	16	0.9	11	1.9	57637.0
59.00	44.20	64.00	38.90	16	7	80	1	14	16	0.7	16	1.1	57633.0
57.00	44.10	64.00	38.90	16	7	80	1	30	16	1.0	16	1.4	57625.3
24.50	39.00	24.50	39.40	17	7	80	11	43	15	0.7	13	2.3	57647.7
23.20	39.50	24.50	39.40	17	7	80	11	56	16	0.4	14	1.5	57669.3
21.50	39.00	24.50	39.40	17	7	80	12	9	16	0.8	12	2.0	57667.3
20.50	39.20	24.50	39.40	17	7	80	12	38	16	0.7	16	1.8	57683.5
20.20	41.60	24.50	39.40	17	7	80	12	50	15	0.7	12	1.8	57692.7
21.60	41.60	24.50	39.40	17	7	80	1	1	16	0.8	16	1.5	57689.4
23.20	41.30	24.50	39.40	17	7	80	1	13	16	0.7	16	1.8	57683.3
24.80	41.50	24.50	39.40	17	7	80	1	24	16	0.8	14	2.2	57681.3
25.90	41.80	24.50	39.40	17	7	80	1	36	16	0.4	15	1.8	57683.9
28.00	41.80	24.50	39.40	17	7	80	1	53	16	0.7	16	2.0	57674.8
26.30	38.60	24.50	39.40	17	7	80	2	10	16	1.0	16	1.7	57648.8
27.50	38.70	24.50	39.40	17	7	80	4	8	13	0.9	7	1.8	57651.0
26.50	36.40	24.50	39.40	17	7	80	4	52	15	0.9	15	1.7	57624.7
25.00	36.10	24.50	39.40	17	7	80	5	8	15	1.1	11	1.3	57592.9
23.60	36.10	24.50	39.40	17	7	80	5	20	16	1.8	13	1.5	57619.3
29.20	42.40	24.50	39.40	18	7	80	9	47	16	0.6	15	2.5	57674.9
28.20	43.80	24.50	39.40	18	7	80	10	1	16	0.7	13	1.9	57686.6
26.60	43.70	24.50	39.40	18	7	80	10	13	16	0.8	13	2.2	57685.9
25.20	44.20	24.50	39.40	18	7	80	10	26	16	0.6	14	1.6	57683.6
23.60	43.90	24.50	39.40	18	7	80	10	40	16	0.8	16	1.6	57686.7
21.90	44.10	24.50	39.40	18	7	80	10	52	16	0.7	14	1.7	57684.0
20.60	44.10	24.50	39.40	18	7	80	11	4	15	0.4	15	1.6	57691.4
19.20	43.90	24.50	39.40	18	7	80	11	16	15	0.7	15	1.2	57691.5
18.00	41.30	24.50	39.40	18	7	80	11	38	16	0.7	16	1.5	57701.8
18.00	38.90	24.50	39.40	18	7	80	11	55	16	0.8	12	1.7	57695.8
19.30	38.90	24.50	39.40	18	7	80	12	10	9	0.8	9	1.3	57690.4
17.40	36.50	24.50	39.40	18	7	80	12	32	16	0.7	16	1.5	57689.6
20.00	36.70	24.50	39.40	18	7	80	12	50	15	0.7	14	1.6	57679.7
21.50	36.10	24.50	39.40	18	7	80	1	4	16	1.1	16	1.0	57651.1
28.40	36.10	24.50	39.40	18	7	80	2	19	16	0.6	14	1.4	57639.5
29.80	36.40	24.50	39.40	18	7	80	2	33	16	0.6	16	1.5	57652.1
30.20	33.30	24.50	39.40	18	7	80	2	54	16	1.2	15	1.2	57646.1
28.80	33.80	24.50	39.40	18	7	80	3	10	16	1.1	14	1.6	57641.5
26.80	33.70	24.50	39.40	18	7	80	3	22	16	0.6	16	1.5	57626.2
24.60	32.40	24.50	39.40	18	7	80	3	40	16	2.9	15	1.9	57643.4
21.60	33.10	24.50	39.40	18	7	80	4	4	16	1.0	14	2.7	57656.1
20.30	33.70	24.50	39.40	18	7	80	4	16	16	1.8	16	1.7	57682.0
18.50	33.50	24.50	39.40	18	7	80	4	28	15	3.6	14	1.9	57700.0
16.70	33.80	24.50	39.40	18	7	80	4	39	16	1.9	16	2.1	57704.1
23.70	26.20	24.50	39.40	21	7	80	10	53	16	0.9	16	0.9	57705.4

21.70	26.10	24.60	25.50	21	7	80	11	8	15	0.7	15	0.9	57712.7
20.50	25.60	24.60	25.50	21	7	80	11	20	16	0.9	16	0.9	57714.6
19.50	25.80	24.60	25.50	21	7	80	11	31	16	0.9	16	1.2	57714.1
17.60	26.80	24.60	25.50	21	7	80	11	45	16	0.8	16	1.0	57726.6
18.00	28.20	24.60	25.50	21	7	80	11	58	16	0.9	13	1.3	57717.2
19.40	28.20	24.60	25.50	21	7	80	12	9	16	1.5	16	0.7	57714.4
20.80	28.50	24.60	25.50	21	7	80	12	21	16	1.1	16	1.1	57708.0
22.20	28.20	24.60	25.50	21	7	80	12	34	16	0.9	16	1.5	57696.8
23.90	28.60	24.60	25.50	21	7	80	12	46	16	0.7	16	1.8	57685.3
25.00	28.00	24.60	25.50	21	7	80	1	1	16	1.1	15	1.3	57684.4
27.10	28.20	24.60	25.50	21	7	80	1	16	16	0.9	16	0.8	57678.5
30.20	28.60	24.60	25.50	21	7	80	2	58	16	0.8	15	1.4	57664.9
30.20	30.80	24.60	25.50	21	7	80	3	20	12	0.9	9	2.3	57648.9
28.70	30.80	24.60	25.50	21	7	80	3	33	16	1.5	16	1.5	57652.5
28.70	30.80	24.60	25.50	21	7	80	3	54	16	0.5	15	1.8	57651.0
25.20	30.80	24.60	25.50	21	7	80	4	11	13	0.8	11	1.6	57657.5
23.90	30.80	24.60	25.50	21	7	80	4	28	13	0.8	13	2.1	57665.0
21.60	30.80	24.60	25.50	21	7	80	4	39	16	1.1	16	2.1	57678.1
18.80	30.80	24.60	25.50	21	7	80	4	55	15	0.9	13	1.4	57709.4
17.20	30.80	24.60	25.50	21	7	80	5	8	16	1.3	15	1.8	57718.8
28.80	28.60	24.60	25.50	21	7	80	5	27	16	0.8	14	1.8	57667.1
27.00	26.30	24.60	25.50	22	7	80	9	13	15	0.7	12	2.2	57691.6
28.30	25.90	24.60	25.50	22	7	80	9	24	15	0.6	15	1.5	57695.2
31.80	23.30	24.60	25.50	22	7	80	10	7	16	0.6	15	1.7	57695.5
30.60	23.30	24.60	25.50	22	7	80	10	19	16	0.7	14	2.1	57693.6
31.30	20.60	24.60	25.50	22	7	80	10	43	16	1.2	16	1.0	57699.7
29.70	21.30	24.60	25.50	22	7	80	10	59	16	0.8	16	1.4	57702.8
29.00	23.50	24.60	25.50	22	7	80	11	16	16	1.3	4	1.2	57696.0
26.90	23.10	24.60	25.50	22	7	80	11	31	11	1.1	4	1.7	57704.5
25.80	23.10	24.60	25.50	22	7	80	11	42	14	0.7	14	1.4	57702.8
24.00	23.20	24.50	25.50	22	7	80	11	55	16	0.9	16	1.2	57712.1
23.00	23.10	24.60	25.50	22	7	80	12	6	16	1.0	16	1.3	57712.6
18.30	23.20	24.60	25.50	22	7	80	12	23	16	0.6	16	1.4	57721.5
19.70	23.60	24.60	25.50	22	7	80	12	34	16	0.6	16	1.2	57716.2
16.70	20.50	24.60	25.50	22	7	80	1	42	15	0.8	15	1.3	57721.2
19.40	20.60	24.60	25.50	22	7	80	1	58	16	0.5	16	0.7	57703.6
21.40	20.50	24.60	25.50	22	7	80	2	12	16	0.7	16	1.1	57707.2
23.30	20.60	24.60	25.50	22	7	80	2	22	16	1.0	16	1.0	57702.3
24.80	20.60	24.60	25.50	22	7	80	2	32	16	1.0	16	1.1	57702.8
27.90	20.50	24.60	25.50	22	7	80	2	53	16	0.7	16	0.9	57697.6
28.00	17.80	24.60	25.50	22	7	80	3	4	16	0.9	16	2.6	57684.5
30.30	17.50	24.60	25.50	22	7	80	3	24	16	0.6	16	0.8	57691.3
25.80	17.80	24.60	25.50	22	7	80	3	45	16	0.8	16	1.4	57694.3
24.00	18.00	24.60	25.50	22	7	80	3	56	16	1.0	16	1.5	57693.2
22.60	18.00	24.60	25.50	22	7	80	4	6	16	0.8	16	1.6	57680.6
21.30	18.40	24.60	25.50	22	7	80	4	16	16	0.7	16	0.8	57685.3
19.40	18.00	24.60	25.50	22	7	80	4	27	16	1.0	16	1.6	57662.6
18.00	17.90	24.60	25.50	22	7	80	4	40	16	0.5	16	0.8	57681.7
30.90	15.20	24.00	8.80	23	7	80	9	39	16	0.9	16	1.5	57670.0
29.40	15.30	24.00	8.80	23	7	80	9	50	16	0.7	16	1.5	57672.1

25.70	15.60	24.00	8.80	23	7	80	10	6	16	0.9	15	0.9	57678.7
23.60	15.70	24.00	8.80	23	7	80	10	22	15	0.6	15	0.7	57671.6
20.80	15.00	24.00	8.80	23	7	80	10	38	16	0.8	15	1.1	57686.6
19.10	15.70	24.00	8.80	23	7	80	10	53	16	0.9	16	0.9	57682.9
17.80	15.50	24.00	8.80	23	7	80	11	14	16	0.7	16	1.1	57692.1
19.00	12.80	24.00	8.80	23	7	80	11	59	16	0.9	16	1.2	57705.7
20.70	13.30	24.00	8.80	23	7	80	12	11	16	0.7	16	0.9	57698.0
22.50	12.80	24.00	8.80	23	7	80	12	22	16	1.0	16	1.3	57688.5
24.80	12.80	24.00	8.80	23	7	80	12	34	16	0.9	15	1.4	57674.1
29.00	13.00	24.00	8.80	23	7	80	1	3	16	0.9	16	1.6	57664.2
30.50	13.00	24.00	8.80	23	7	80	1	13	16	1.0	14	1.7	57657.0
30.80	10.40	24.00	8.80	23	7	80	1	28	16	1.1	16	1.3	57667.1
29.60	10.40	24.00	8.80	23	7	80	1	40	16	0.9	16	1.1	57672.1
28.10	10.70	24.00	8.80	23	7	80	1	51	16	0.9	16	2.2	57668.2
26.00	10.70	24.00	8.80	23	7	80	2	3	16	1.2	15	1.2	57675.1
23.30	8.80	24.00	8.80	24	7	80	11	24	16	0.7	15	1.4	57706.1
21.40	10.40	24.00	8.80	24	7	80	11	39	16	0.7	16	2.0	57702.5
20.50	10.40	24.00	8.80	24	7	80	1	53	16	0.7	16	1.4	57694.0
19.10	9.60	24.00	8.80	24	7	80	12	44	9	0.6	6	2.4	57686.1
17.70	10.80	24.00	8.80	24	7	80	1	0	16	0.7	15	1.7	57692.3
17.70	7.80	24.00	8.80	24	7	80	1	12	16	0.8	10	1.7	57681.4
19.40	8.00	24.00	8.80	24	7	80	1	25	16	1.0	12	1.6	57685.8
20.60	7.50	24.00	8.80	24	7	80	1	37	16	0.9	12	2.2	57702.0
21.70	7.80	24.00	8.80	24	7	80	1	51	16	1.0	12	1.8	57708.2
23.30	7.70	24.00	8.80	24	7	80	3	17	16	1.2	16	1.8	57706.3
24.50	7.70	24.00	8.80	24	7	80	3	33	16	0.9	16	1.0	57709.4
25.80	8.10	24.00	8.80	24	7	80	3	46	16	0.7	16	1.9	57703.3
27.00	7.70	24.00	8.80	24	7	80	3	59	16	1.2	14	1.6	57704.1
28.50	7.80	24.00	8.80	24	7	80	4	20	16	0.8	16	1.8	57691.8
30.40	6.80	24.00	8.80	24	7	80	4	34	16	1.0	14	1.7	57698.4
30.10	5.60	24.00	8.80	24	7	80	4	44	16	1.3	15	1.5	57701.9
29.00	5.60	24.00	8.80	24	7	80	4	57	16	0.8	16	2.1	57702.3
27.80	5.60	24.00	8.80	25	7	80	10	17	16	0.9	15	2.1	57704.9
26.50	5.60	24.00	8.80	25	7	80	10	37	16	1.9	16	1.8	57712.5
25.00	5.60	24.00	8.80	25	7	80	10	50	16	3.0	15	1.6	57716.1
23.40	5.20	24.00	8.80	25	7	80	11	20	16	1.3	12	1.0	57709.2
22.00	5.50	24.00	8.80	25	7	80	11	32	8	2.7	7	1.4	57717.3
20.60	5.80	24.00	8.80	25	7	80	11	47	16	7.0	9	1.6	57701.1
19.20	5.80	24.00	8.80	25	7	80	12	0	16	1.3	16	1.1	57672.0
17.90	5.10	24.00	8.80	25	7	80	12	13	16	1.6	14	1.9	57637.3
17.10	0.20	24.00	8.80	25	7	80	12	30	16	3.1	16	1.0	57430.1
18.30	0.20	24.00	8.80	25	7	80	12	45	16	1.6	16	1.4	57451.7
19.80	0.00	24.00	8.80	25	7	80	12	59	16	0.9	15	1.7	57500.9
21.90	-0.10	24.00	8.80	25	7	80	1	12	16	1.6	16	1.7	57564.9
23.10	0.50	24.00	8.80	25	7	80	1	25	16	1.9	16	1.2	57626.8
24.30	-0.10	24.00	8.80	25	7	80	1	39	16	1.4	16	1.7	57634.8
30.80	0.30	24.00	8.80	25	7	80	2	51	16	1.8	14	1.9	57682.7
29.50	0.30	24.00	8.80	25	7	80	3	4	16	2.5	14	2.0	57687.2
28.40	0.40	24.00	8.80	25	7	80	3	16	16	1.7	13	1.4	57687.4
26.90	0.30	24.00	8.80	25	7	80	3	28	16	2.4	15	2.2	57679.1

25.70	0.30	24.00	8.80	25	7	80	3	41	16	1.8	16	1.8	57670.0
17.50	2.90	24.00	8.80	25	7	80	4	12	12	3.0	12	1.3	57526.7
18.80	2.70	24.00	8.80	25	7	80	4	23	16	1.2	13	1.8	57579.2
20.80	3.30	24.00	8.80	25	7	80	11	2	8	2.3	8	2.1	57660.6
21.80	2.70	24.00	8.80	25	7	80	11	15	16	0.8	11	2.2	57664.1
23.10	2.70	24.00	8.80	25	7	80	11	27	16	0.8	15	2.0	57682.5
24.50	2.90	24.00	8.80	25	7	80	11	39	16	0.5	13	2.4	57703.5
25.80	2.80	24.00	8.80	25	7	80	11	51	15	0.9	14	1.1	57704.1
27.00	2.70	24.00	8.80	25	7	80	12	8	12	0.6	11	1.3	57702.0
28.50	2.70	24.00	8.80	25	7	80	12	32	16	0.8	16	1.8	57705.1
29.70	2.90	24.00	8.80	25	7	80	12	43	16	0.7	14	1.3	57697.9
30.90	2.70	24.00	8.80	25	7	80	12	55	16	0.9	14	2.3	57690.4
15.70	-0.10	8.90	4.60	29	7	80	4	26	16	1.2	15	1.7	57423.3
14.70	0.30	8.90	4.90	29	7	80	4	38	16	1.1	13	1.4	57416.9
13.50	-0.10	8.90	4.90	29	7	80	4	49	16	0.7	15	1.0	57442.8
11.70	0.20	8.90	4.90	29	7	80	5	1	16	1.3	13	1.4	57460.1
10.00	0.40	8.90	4.90	29	7	80	5	12	16	0.9	16	1.8	57498.3
8.00	-0.10	8.90	4.90	29	7	80	5	24	16	0.6	16	1.6	57572.0
6.50	0.20	8.90	4.90	29	7	80	5	34	16	0.9	16	1.4	57591.6
5.00	0.40	8.90	4.90	29	7	80	5	46	16	0.7	16	1.9	57605.1
4.20	0.20	8.90	4.90	29	7	80	5	59	16	1.0	16	1.7	57612.8
2.20	0.20	8.90	4.90	29	7	80	6	14	16	1.1	16	1.5	57625.1
0.40	-0.10	8.90	4.90	29	7	80	6	25	16	0.8	10	2.2	57638.8
14.80	2.60	8.90	4.90	30	7	80	9	40	16	0.7	15	1.8	57454.9
12.80	2.60	8.90	4.90	30	7	80	9	55	16	0.7	16	1.1	57422.2
11.00	2.50	8.90	4.90	30	7	80	10	6	16	0.7	16	0.7	57428.8
9.40	2.50	8.90	4.90	30	7	80	10	17	16	1.0	16	1.3	57453.6
8.00	2.50	8.90	4.90	30	7	80	10	28	16	1.4	16	1.3	57485.4
6.40	2.50	8.90	4.90	30	7	80	10	40	16	0.8	16	1.2	57529.2
4.10	2.90	8.90	4.90	30	7	80	10	51	16	0.7	16	1.2	57576.3
2.30	2.90	8.90	4.90	30	7	80	11	11	16	0.4	16	0.9	57604.6
0.50	2.80	8.90	4.90	30	7	80	11	21	16	0.9	16	0.7	57620.0
1.10	5.20	8.90	4.90	30	7	80	11	41	16	0.8	16	1.1	57565.5
3.70	5.50	8.90	4.90	30	7	80	11	52	16	1.1	16	1.1	57503.6
7.00	5.60	8.90	4.90	30	7	80	1	14	10	1.1	7	2.4	57448.5
9.40	5.20	8.90	4.90	30	7	80	1	25	16	1.0	15	1.8	57440.8
11.00	5.50	8.90	4.90	30	7	80	1	37	7	0.5	7	1.6	57459.3
13.00	5.70	8.90	4.90	30	7	80	1	49	16	0.8	14	1.7	57510.6
14.30	5.20	8.90	4.90	30	7	80	2	3	13	0.7	13	1.7	57531.9
15.60	5.70	8.90	4.90	30	7	80	2	14	14	0.7	12	1.3	57585.2
15.20	7.70	8.90	4.90	30	7	80	2	26	16	1.0	16	1.7	57652.8
13.50	8.70	8.90	4.90	30	7	80	2	40	16	1.0	11	1.8	57649.5
12.10	8.70	8.90	4.90	30	7	80	2	51	16	0.9	16	1.8	57631.4
10.40	8.50	8.90	4.90	30	7	80	3	6	15	0.8	11	2.0	57569.1
8.90	8.10	8.90	4.90	30	7	80	3	23	13	0.7	9	1.9	57502.0
7.60	7.70	8.90	4.90	30	7	80	3	35	15	0.6	12	1.6	57468.1
5.50	8.20	8.90	4.90	30	7	80	3	46	16	1.0	14	1.7	57453.1
3.90	8.40	8.90	4.90	30	7	80	4	2	16	0.8	13	2.1	57437.9
-0.20	7.70	8.90	4.90	30	7	80	4	27	13	0.7	10	2.3	57530.4
10.70	10.70	8.90	4.90	31	7	80	11	40	16	0.9	16	1.8	57674.9

9.00	10.30	8.90	4.90	31	7	80	11	52	16	0.7	16	1.9	57620.6
7.30	10.70	8.90	4.90	31	7	80	12	4	16	0.9	14	1.8	57586.5
5.50	10.30	8.90	4.90	31	7	80	12	15	16	0.8	16	2.1	57504.6
3.50	10.70	8.90	4.90	31	7	80	12	28	16	0.7	16	1.8	57466.6
2.00	10.30	8.90	4.90	31	7	80	12	40	16	1.1	15	1.3	57439.0
16.20	10.30	8.90	4.90	31	7	80	1	0	16	0.8	16	1.1	57698.5
14.30	10.40	8.90	4.90	31	7	80	1	11	16	0.7	16	1.8	57694.4
12.50	10.30	8.90	4.90	31	7	80	1	22	15	0.8	10	2.1	57686.7
16.30	14.40	9.10	18.90	31	7	80	3	27	16	0.7	16	1.1	57711.5
14.00	13.10	9.10	18.90	31	7	80	3	40	16	0.6	16	0.9	57723.0
12.00	12.80	9.10	18.90	31	7	80	3	52	16	0.8	16	0.9	57719.6
8.40	13.10	9.10	18.90	31	7	80	4	13	16	1.0	16	1.4	57705.9
6.60	12.80	9.10	18.90	31	7	80	4	24	16	1.0	16	1.4	57661.4
4.40	12.80	9.10	18.90	31	7	80	4	36	16	0.9	16	1.4	57582.0
0.90	13.20	9.10	18.90	31	7	80	4	54	16	0.8	14	2.5	57464.8
2.20	12.90	9.10	18.90	31	7	80	5	7	16	0.9	16	1.8	57503.6
14.80	15.70	9.10	18.90	1	8	80	9	23	16	0.7	15	1.8	57716.3
13.20	14.10	9.10	18.90	1	8	80	9	40	16	0.7	16	1.1	57721.0
10.50	15.40	9.10	18.90	1	8	80	9	54	16	0.9	16	0.9	57731.4
8.70	16.40	9.10	18.90	1	8	80	10	5	16	0.8	16	1.4	57739.0
9.00	18.00	9.10	18.90	1	8	80	10	17	16	0.7	16	1.3	57734.5
7.20	15.90	9.10	18.90	1	8	80	10	30	16	0.8	16	1.1	57732.7
3.70	15.10	9.10	18.90	1	8	80	10	56	16	0.9	16	1.4	57665.2
2.30	15.50	9.10	18.90	1	8	80	10	57	15	1.1	15	1.7	57637.0
0.00	16.20	9.10	18.90	1	8	80	11	14	15	5.9	14	0.9	57549.9
0.10	18.60	9.10	18.90	1	8	80	11	32	16	0.7	16	1.0	57646.2
2.00	18.80	9.10	18.90	1	8	80	11	44	15	5.0	12	1.0	57711.7
3.80	18.00	9.10	18.90	1	8	80	12	17	16	1.0	15	1.3	57723.3
5.00	17.50	9.10	18.90	1	8	80	12	28	14	0.8	14	2.3	57735.2
6.00	18.30	9.10	18.90	1	8	80	12	41	16	0.9	15	1.7	57743.6
8.00	18.30	9.10	18.90	1	8	80	12	54	15	0.6	13	1.9	57734.0
10.10	18.00	9.10	18.90	1	8	80	1	6	15	0.7	13	1.5	57733.4
11.50	18.00	9.10	18.90	1	8	80	1	18	16	0.9	14	2.0	57724.6
13.20	18.30	9.10	18.90	1	8	80	1	32	15	0.8	14	1.8	57726.0
15.10	18.50	9.10	18.90	1	8	80	1	43	16	0.8	16	1.4	57719.5
16.40	18.30	9.10	18.90	1	8	80	1	55	14	0.7	13	1.5	57701.1
15.10	20.90	9.10	18.90	1	8	80	2	11	16	0.8	16	1.3	57719.9
13.40	21.30	9.10	18.90	1	8	80	2	22	15	0.6	15	0.9	57717.7
12.30	20.90	9.10	18.90	1	8	80	2	35	14	0.7	11	2.1	57713.3
11.10	20.60	9.10	18.90	1	8	80	2	49	16	0.7	16	1.9	57719.9
9.00	20.60	9.10	18.90	6	8	80	9	40	16	2.1	16	1.6	57727.1
6.70	20.50	9.10	18.90	6	8	80	9	54	16	1.1	16	1.6	57735.9
4.60	20.60	9.10	18.90	6	8	80	10	5	16	0.8	16	1.8	57731.5
3.20	21.00	9.10	18.90	6	8	80	10	18	16	0.8	15	2.4	57723.7
2.00	20.60	9.10	18.90	6	8	80	10	29	16	0.6	16	1.5	57721.6
0.80	20.60	9.10	18.90	6	8	80	10	40	13	1.2	8	1.9	57702.0
0.30	23.20	9.10	18.90	6	8	80	10	58	16	0.8	15	2.0	57711.9
2.60	23.10	9.10	18.90	6	8	80	11	13	16	1.4	16	1.5	57718.5
3.80	23.50	9.10	18.90	6	8	80	11	24	16	2.6	15	1.3	57715.5
5.50	23.50	9.10	18.90	6	8	80	11	36	15	0.9	13	1.3	57715.1

6.80	23.50	9.10	18.90	6	8	80	11	48	16 0.8	16 2.1	57719.4
8.20	23.20	9.10	18.90	6	8	80	11	59	16 0.7	16 1.4	57715.9
9.50	23.30	9.10	18.90	6	8	80	12	10	16 0.6	16 1.5	57715.0
11.70	23.40	9.10	18.90	6	8	80	12	23	16 0.6	14 1.6	57719.6
13.10	23.50	9.10	18.90	6	8	80	12	35	15 0.5	15 1.2	57723.2
14.30	23.50	9.10	18.90	6	8	80	12	48	15 1.5	15 1.4	57726.4
15.80	23.50	9.10	18.90	6	8	80	1	0	16 0.7	16 1.2	57724.7
16.70	25.70	9.10	18.90	6	8	80	1	43	16 1.5	15 1.4	57724.3
14.70	25.70	9.10	18.90	6	8	80	1	54	16 0.8	16 1.2	57730.4
13.20	26.10	9.10	18.90	6	8	80	2	6	15 1.0	15 1.2	57729.9
11.30	26.00	9.10	18.90	6	8	80	2	17	16 7.1	15 0.8	57720.1
8.70	26.00	9.10	18.90	6	8	80	2	33	15 1.0	14 1.2	57706.8
7.60	26.00	9.10	18.90	6	8	80	2	43	16 5.6	16 1.5	57704.1
6.30	26.00	9.10	18.90	6	8	80	2	54	16 2.7	15 1.3	57704.1
4.50	26.10	9.10	18.90	6	8	80	3	5	15 1.1	15 1.1	57702.7
2.70	26.50	9.10	18.90	6	8	80	3	30	12 2.2	10 2.3	57711.7
0.40	27.70	9.10	18.90	6	8	80	3	53	15 1.4	14 1.7	57712.8
1.00	28.70	8.50	34.80	7	8	80	12	36	16 0.8	7 1.2	57721.6
5.40	28.30	8.50	34.80	7	8	80	12	50	16 0.8	16 1.8	57704.6
6.60	28.30	8.50	34.80	7	8	80	1	18	15 1.0	14 1.6	57706.4
8.20	28.50	8.50	34.80	7	8	80	1	48	15 0.7	15 1.1	57710.0
9.50	28.50	8.50	34.80	7	8	80	1	59	16 0.9	14 2.3	57714.7
10.80	28.50	8.50	34.80	7	8	80	2	10	16 0.9	16 1.6	57722.3
12.30	28.30	8.50	34.80	7	8	80	2	21	15 0.7	14 1.9	57724.2
13.90	28.20	8.50	34.80	7	8	80	2	32	16 1.0	16 2.1	57726.8
15.30	28.50	8.50	34.80	7	8	80	2	47	16 1.3	16 1.6	57729.5
16.80	28.50	8.50	34.80	7	8	80	2	59	16 0.7	14 1.3	57723.0
15.80	31.10	8.50	34.80	7	8	80	3	12	15 0.9	15 1.8	57723.4
14.50	31.20	8.50	34.80	7	8	80	3	26	16 0.9	16 1.8	57722.7
10.00	31.10	8.50	34.80	7	8	80	4	2	16 1.0	14 1.3	57730.8
8.90	32.50	8.50	34.80	7	8	80	4	18	14 1.1	14 1.3	57750.9
4.60	30.90	8.50	34.80	7	8	80	4	55	15 0.6	14 2.7	57719.8
2.70	30.80	8.50	34.80	7	8	80	5	9	14 0.6	14 1.5	57721.9
1.10	31.20	8.50	34.80	7	8	80	5	23	13 0.9	10 2.1	57727.8
-0.30	31.20	8.50	34.80	7	8	80	5	35	15 0.8	14 1.8	57732.2
0.10	33.50	8.50	34.80	7	8	80	5	48	16 1.5	13 2.2	57756.8
1.70	32.70	8.50	34.80	7	8	80	6	3	16 0.9	16 1.3	57759.2
5.00	32.80	8.50	34.80	8	8	80	10	7	15 0.6	10 2.3	57731.6
6.50	33.40	8.50	34.80	8	8	80	10	21	16 1.1	15 1.7	57753.6
7.60	33.70	8.50	34.80	8	8	80	10	32	16 1.2	16 1.3	57769.4
8.70	33.60	8.50	34.80	8	8	80	10	42	14 0.8	13 1.7	57774.4
9.30	36.20	8.50	34.80	8	8	80	10	55	15 1.3	13 1.8	57832.5
10.80	36.20	8.50	34.80	8	8	80	11	12	16 0.8	16 2.1	57799.7
12.00	36.30	8.50	34.80	8	8	80	11	25	14 0.7	12 1.3	57767.0
13.20	35.90	8.50	34.80	8	8	80	11	36	16 0.7	16 1.8	57743.6
14.90	36.10	8.50	34.80	8	8	80	11	48	14 0.7	14 1.9	57709.3
16.80	36.40	8.50	34.80	8	8	80	11	59	16 0.8	15 2.0	57695.0
13.50	34.40	8.50	34.80	8	8	80	12	15	15 0.9	11 2.0	57730.8
9.90	33.80	8.50	34.80	8	8	80	12	31	16 0.9	13 1.6	57771.6
7.60	36.50	8.50	34.80	8	8	80	12	47	16 0.9	12 1.6	57855.5

6.40	36.40	8.50	34.80	8	8	80	1	1	16	1.1	15	1.9	57846.4
5.00	35.50	8.50	34.80	8	8	80	1	12	16	0.7	14	1.9	57820.9
3.70	36.40	8.50	34.80	8	8	80	1	30	16	0.9	12	2.2	57837.4
2.00	36.50	8.50	34.80	8	8	80	1	43	16	0.8	14	2.1	57859.7
0.20	35.70	8.50	34.80	8	8	80	1	55	16	0.9	15	1.5	57803.8
0.10	39.40	8.50	34.80	8	8	80	2	11	16	0.8	14	2.2	57926.1
1.70	39.30	8.50	34.80	8	8	80	2	55	16	0.7	15	0.9	57999.2
5.20	39.10	8.50	34.80	8	8	80	2	45	16	1.0	13	1.6	57886.2
7.50	38.70	8.50	34.80	8	8	80	3	3	16	1.1	13	1.6	57861.9
9.10	38.70	8.50	34.80	8	8	80	3	14	12	0.8	9	2.5	57841.7
10.30	38.60	8.50	34.80	8	8	80	3	26	13	0.9	11	2.0	57820.7
12.00	39.00	8.50	34.80	8	8	80	3	38	16	0.9	16	1.3	57788.6
13.50	39.30	8.50	34.80	11	8	80	11	3	11	1.2	8	1.5	57755.0
14.80	38.90	8.50	34.80	11	8	80	11	16	16	0.8	16	1.8	57729.3
16.30	38.70	8.50	34.80	11	8	80	11	31	16	0.8	16	1.7	57710.5
7.80	41.20	8.50	34.80	11	8	80	11	49	16	0.5	16	1.5	57814.9
9.30	41.50	8.50	34.80	11	8	80	12	1	15	0.8	15	2.3	57802.2
10.50	41.70	8.50	34.80	11	8	80	12	13	15	0.7	14	1.2	57789.8
12.40	41.50	8.50	34.80	11	8	80	12	27	15	0.7	12	1.7	57776.7
13.80	41.20	8.50	34.80	11	8	80	12	40	16	0.7	16	1.5	57760.3
16.50	41.30	8.50	34.80	11	8	80	1	3	14	0.6	8	1.5	57728.4
2.90	39.00	8.50	34.80	12	8	80	9	34	11	0.6	9	1.4	57920.1
2.90	41.50	8.50	34.80	12	8	80	9	55	16	0.7	14	2.2	57909.4
5.10	41.50	8.50	34.80	12	8	80	10	7	16	0.6	16	1.6	57860.2
5.20	44.50	8.50	34.80	12	8	80	10	21	15	1.2	14	1.5	57816.9
2.70	43.70	8.50	34.80	12	8	80	10	35	16	1.3	16	1.9	57892.5
1.90	44.60	8.50	34.80	12	8	80	10	48	16	0.7	16	2.4	57874.3
-0.10	44.30	8.50	34.80	12	8	80	11	7	16	0.7	16	0.9	57900.7
0.10	42.20	8.50	34.80	12	8	80	11	23	16	1.1	16	1.6	57963.8
2.00	41.00	8.50	34.80	12	8	80	11	38	16	0.7	16	1.9	58012.2
8.70	43.70	8.50	34.80	12	8	80	12	7	13	0.8	9	1.8	57783.3
10.00	43.50	8.50	34.80	12	8	80	12	20	16	0.8	12	2.1	57774.5
17.90	43.80	8.50	34.80	12	8	80	12	48	15	0.9	15	1.8	57697.8
16.70	44.00	8.50	34.80	12	8	80	1	0	12	0.8	11	2.0	57700.4
15.00	44.00	8.50	34.80	12	8	80	1	22	15	0.9	15	1.7	57720.9
13.40	43.80	8.50	34.80	12	8	80	1	39	15	0.8	11	1.9	57743.5
33.40	26.90	24.60	25.50	8	11	80	11	18	16	0.7	16	2.0	57668.0
23.30	22.10	24.60	25.50	8	11	80	11	42	16	0.8	16	1.8	57705.7
20.40	17.50	24.60	25.50	8	11	80	12	31	16	0.7	15	1.6	57668.0
25.70	14.00	24.60	25.50	8	11	80	12	5	14	0.5	11	1.3	57668.2
12.00	16.80	24.60	25.50	8	11	80	1	9	16	0.9	16	1.5	57731.9
11.50	14.50	24.60	25.50	8	11	80	1	30	16	0.8	13	2.0	57732.2
13.10	29.40	24.60	25.50	8	11	80	2	0	16	0.7	15	1.6	57725.0
49.50	21.20	47.00	17.70	8	11	80	3	16	16	0.7	16	1.6	57634.7
43.00	20.60	47.00	17.70	8	11	80	3	36	16	0.6	13	1.7	57650.4
46.40	13.70	47.00	17.70	8	11	80	3	55	16	7.4	12	1.6	57652.8
49.50	13.00	47.00	17.70	8	11	80	4	16	16	0.7	12	1.9	57657.2
49.60	24.60	47.00	17.70	8	11	80	4	36	16	0.6	14	1.1	57645.7
28.40	39.00	35.30	40.70	8	11	80	5	19	13	0.8	13	1.2	57649.9
31.50	41.80	35.30	40.70	8	11	80	5	45	16	0.8	14	1.6	57674.9

BIBLIOGRAPHY

Beghini, V. G., and Conroy, T. R., 1966, A history of the Albion-Scipio Trend of Michigan; IN Ontario Petroleum Institute, v. 5, Technical Session No. 1, Nov. 2, 1966.

Books, K. G., 1968 Magnetization of the Lowermost Keweenawan lava flows in the Lake Superior area; U. S. Geol. Surv., Prof. Pap. 600-D, pp. 248-254.

Buehner, J. H., and Davis, S. H. Jr., 1968, Albion-Pulaski-Scipio Trend Field; IN Mich. Basin Geol. Soc. Oil and Gas Field Symposium.

Cain, J. C., Hendricks, S. J., Langel, R. A., and Hudson, W. V., 1967: A proposed model for the International Geomagnetic Reference Field-1965; Jour. Geomag. and Geoelectricity; 19(4), pp. 335-355.

Cambray, F. W., 1979, The Pre-Cambrian basement of Michigan: IN The Hydrocarbon Potential of the Michigan Basin, The Way Ahead; Michigan Basin Geol. Soc. Sym., p. 16.

Catacosinos, P. A., 1973, Cambrian lithostratigraphy of the Michigan Basin; Am. Assoc. of Petroleum Geologists Bull., v. 57, pp. 2404-2418.

Cohee, G. V., and Landes, K. K., 1958, Oil in the Michigan Basin: IN Weeks, L. G. (Ed), Habitat of Oil; Am. Assoc. Petroleum Geologists, v. 42, pp. 473-493.

Dobrin, M. B., 1976, Magnetic Measurements On Land: IN Introduction To Geophysical Prospecting; Edition No. 2, McGraw-Hill Book Co., Inc., New York, pp. 304-320.

Dongarra, J. J., Moler, C. B., Bunch, J. R., and Stewart, G. W., 1979, LINPAC Users' Guide; Society For Industrial and Applied Mathematics, Philadelphia, Pa.

Dubois, P. M., 1962, Paleomagnetism and Correlation of Keweenawan rocks; Geol. Sur. Can. Bull., v. 71, p. 75.

Dutton, C. E., and Beadley, R. E., 1970, Lithologic, Geophysical and Mineral Commodity Maps of Pre-Cambrian Rocks in Wisconsin; U. S. Geological Service and Univ. of Wisc., Map 1-631.

Ells, G. D., 1962, Structures Associated with the Albion-Scipio Field Trend; Mich. Geol. Surv. Rept., 86 p.

Ells, G. D., 1969, Architure of the Michigan Basin: IN Stonehouse, H. B. (Ed.), Studies of the Pre-Cambrian of the Michigan Basin; Mich. Basin Geol. Soc. Ann. Excursion, pp. 60-88.

----------, 1980, Developments in Michigan in 1979; Am. Assoc. Petroleum Geologists Bull., v. 64, p. 1377.

----------, and Champion, B. L., 1975, Developments in Michigan in 1974; Am. Assoc. Petroleum Geologists Bull., v. 59, p. 1364.

----------, and Layton, F., 1968, Developments in Michigan in 1967; Am. Assoc. Petroleum Geologists Bull., v. 52, p. 976.

Fisher, J. H., 1969, Early Paleozoic history of the Michigan basin, IN Studies of the Pre-Cambrian of the Michigan basin: Michigan Basin Geol. Soc. Ann. Field Excursion, pp. 89-93.

Fabiano, E. B., and Peddie, N. W., 1975, U. S. World Chart Model Coefficients for 1975: Transactions, AGU, v. 56, No. 9, pp. 587-588.

Engel, A. E. J., 1963, Geologic evolution of North America; Science, v. 140, pp. 143-152.

Fowler, J. H., and Kuenzi, W. D., 1978, Keweenawan Turbidites in Michigan (deep borehole red beds): A foundered basin sequence developed during evolution of a protoceanic rift system; Jour. Geoph. Res., v. 83, pp. 5833-5843.

Geometrics, 1979, Operating Manual: Model G 816 portable proton magnetometer, Sunnyvale, CA.

Grant, F. S. and West, G. F., 1965, Interpretation Theory in Applied Geophysics; New York, McGraw-Hill, 584 pp.

Halls, H. C., 1978, The Late Pre-Cambrian Central North American Rift System - A survey of recent geological and geophysical investigations: IN Tectonics and Geophysics of Continental Rifts. Edited by E. R. Neumann and I. Ramburg, NATO Advanced Study Institute; Series C, Mathematics and Physical Sciences, v. 37, pp. 111-123.

Harding, T. P., 1974, Petroleum traps associated with wrench faults; Am. Assoc. Petroleum Geologists Bull., v. 58, pp. 1290-1304.

Hartman, R. R., Teskey, D. J., and Friedberg, J. L., 1971, A system for rapid digital aeromagnetic interpretation: Geophysics, v. 36, No. 5, pp. 891-918.

Hinze, W. J., 1963, Regional Gravity and Magnetic anomaly maps of the southern peninsula of Michigan: Mich. Geol. Surv. Rept. Inv. 1, 26 p.

----------, Kellog, R. L., and O'Hara, N. W., 1975, Geophysical Studies of basement geology of the southern peninsula of Michigan: Am. Assoc. Petroleum Geologists Bull., v. 59, pp. 1562-1584.

----------, and Merritt, D. W., 1969, Basement rocks of the southern peninsula of Michigan: IN Stonehouse, H. B. (Ed.), Studies of the pre-Cambrian of the Michigan Basin: Mich. Basin Geol. Soc. Ann. Field Excursion, pp. 28-59.

----------, Merritt, D. W., and Kellogg, R. L., 1971, Gravity and Aeromagnetic anomaly maps of the southern peninsula of Michigan; Mich. Geol. Surv. Rept. Inv. 14, 16 p.

Hoin, S. J., Sauck, W. A., and Parker, B. K., 1981, Ground Magnetic Map of Homer and Spring Arbor 15' Quadrangles, Michigan; Michigan Geol. Surv., OFM 81-1.

Honnorez, J. J., 1979, Preliminary petrological study of the lower metadiabase from the basement of the Michigan Basin; Jour. Geophys. Res., v. 84, pp. 3664-3670.

Ives, R. E., and Ells, G. D., 1958, Developments in Michigan in 1957; Am. Assoc. Petroleum Geologists Bull., v. 42, p. 1194.

Jenny, W. P., 1961, Regional magnetic isogam map, Albion area, Calhoun-Jackson Cos., Michigan; Unpublished map.

Jensen, L. W., Steiner, D., and Brown, L. R., 1979, COCORP deep crustal seismic reflection studies in the Michigan Basin: IN The hydrocarbon potential of the Michigan Basin, The Way Ahead; Mich. Basin Geol. Soc. Sym., p. 16.

Kellogg, R. L., 1971, An aeromagnetic investigation of the southern peninsula of Michigan; Unpub. Ph.D Thesis, Michigan State University, East Lansing, Michigan.

King, E. R., and Zeitz, I., 1971, Aeromagnetic study of the Mid-Continent Gravity High of Central United States; Geol. Soc. Am. Bull., v. 82, No. 8. pp. 2187-2208.

Koulomzine, T. H., LaMontagne, Y., and Nadeau, A., 1970, New methods for direct interpretation of magnetic anomalies caused by inclined dikes of infinite length; Geophysics, v. 35, pp. 812-918.

Lidiak, G. E., 1972, Pre-Cambrian rocks in the subsurface of Nebraska; Nebraska Geol. Surv. Bull., v. 26, 41 p.

----------, Marvin, R. F., Thomas, H. H., and Bass, M. N., 1966, Geochronology of the Mid-Continent Region, United States, part 4, Eastern area; Jour. Geophys. Res., v. 71., pp. 5427-5438.

Lindsley, D. H., Andreason G. E., and Balsley, J. R., 1966, Magnetic properties of rocks and minerals: IN Handbook of Physical Constants, Sydney P. Clark, Jr. (Ed.), Geol. Soc. Am., Memoir No. 97, pp. 545-552.

Lockett, J. R., 1947, Development of structures in Basin areas of Northeastern United States; Am. Assoc. Petroleum Geologists Bull., v. 31, pp. 429-446.

Lovan, N. A., 1977, Analysis of an interlobate boundary in the Wisconsinan drift of Kalamazoo County and adjacent areas in southwest Michigan; Unpub. M.S. Thesis, Western Michigan University, Kalamazoo, Michigan.

Martin, H. M., Bergquist, S. G., Terwilliger, F. W., Straight, M. T., Colubrn, W., and Campbell, J. M., 1955, Map of the Surface Formations of the Southern Peninsula of Michigan; Mich. Geol. Surv. Pub., No. 49.

McLaren, A. S., and Charbonneau, B. W., 1968, Characteristics of magnetic data over major subdivisions of the Canadian Shield; Geol. Assoc. Canada Prof., v. 19, pp. 57-65.

Merritt, D. W., 1968, A gravitational investigation of the Scipio Oil Field in Hillsdale County, Michigan, with a related study for obtaining a variable elevation factor; Unpub. Ph. D thesis, Michigan State University, East Lansing, Michigan.

Newcombe, R. B., 1933, Oil and gas fields of Michigan; Mich. Geol. Surv., Pub. 38.

O'Hara, N. W., and Hinze, W. H., 1972, Basement geology of the Lake Michigan Area from aeromagnetic studies; Geol. Soc. Am. Bull., v. 83, pp. 1771-1786.

Passero, R. N., Straw, W. T., Schmaltz, L. J., Curran, D. L., Leske, D. N., and Miller, L., 1981, Glacial Drift Thickness Map, Plate 15; Hydrogeologic Atlas of Michigan, Dept. of Geology, Western Michigan University, Kalamazoo, Michigan.

Pesonen, L. J., and Halls, H. C., 1979, The Paleomagnetism of Keweenawan dikes from Baraga and Marquette Counties, Northern Michigan; Canadian Jour. Earth Sci., v. 16, pp. 2136-2149.

Pirtle, G. W., 1932, Michigan Structural Basin and its relationship to surrounding areas; Am. Assoc. Petroleum Geologists Bull., v. 16, pp. 145-152.

Reford, M. S., and Sumner, J. S., 1964, Review article, Aeromagnetics; Geophysics, v. 29, pp. 482-516.

Rudman, A. J., Summerson, C. H., and Hinze, W. J., 1965, Geology of Basement in Midwestern United States; Am. Assoc. Petroleum Geol. Bull., v. 49, pp. 894-904.

Sauck, W. A., Program GFCALL; unpublished report.

Sharma, R. G., and Biswas, S. K., 1966, A portable proton procession magnetometer; Geophysical Prospecting, v. 16, p. 292.

Shaw, B., 1975, Geology of the Albion-Scipio Trend, Southern Michigan; unpub. M.S. thesis, University of Michigan, Ann Arbor, Michigan.

Shaw, R. M., 1971, Mobile ground magnetometer survey of a portion of the Southern Peninsula of Michigan; unpub. M.S. thesis, Michigan State University, East Lansing, Michigan.

Sleep, N. H., and Sloss, L. L., 1978, A deep borehole in the Michigan Basin; Jour. Geophys. Res., v. 83, p. 8515.

Steeples, D. W., and Bickford, M. E., 1981, Piggyback drilling in Kansas; An example for Continental Scientific Drilling Program; EOS, v. 62, No. 18, p. 473.

Telford, W. M., Geldhart, L. P., Sheriff, R. F., and Keys, D. A., 1976, Magnetic Methods, in Applied Geophysics; Cambridge University Press.

Theil, E., 1956, Correlation of gravity anomalies with Keweenawan geology of Wisconsin and Minnesota; Geol. Soc. Am. Bull., v. 67, No. 8, p. 1079-1100.

Vacquier, V., Steenland, N. C., Henderson, R. G., and Zietz, I., 1951, Interpretation of aeromagnetic maps; Geol. Soc. Am., Memoir 47.

Varga, L., and Samuelson, K., 1980, Total magnetic intensity maps over various glacial lithologies, unpublished report.

Vander Voo, R., and Watts, D. R., 1978, Paleomagnetic results from igneous and sedimentary rocks from the Michigan Basin Borehole; Jour. Geophys. Res., v. 83.

AREA SHOWING MAGNETOMTER BASE STATIONS

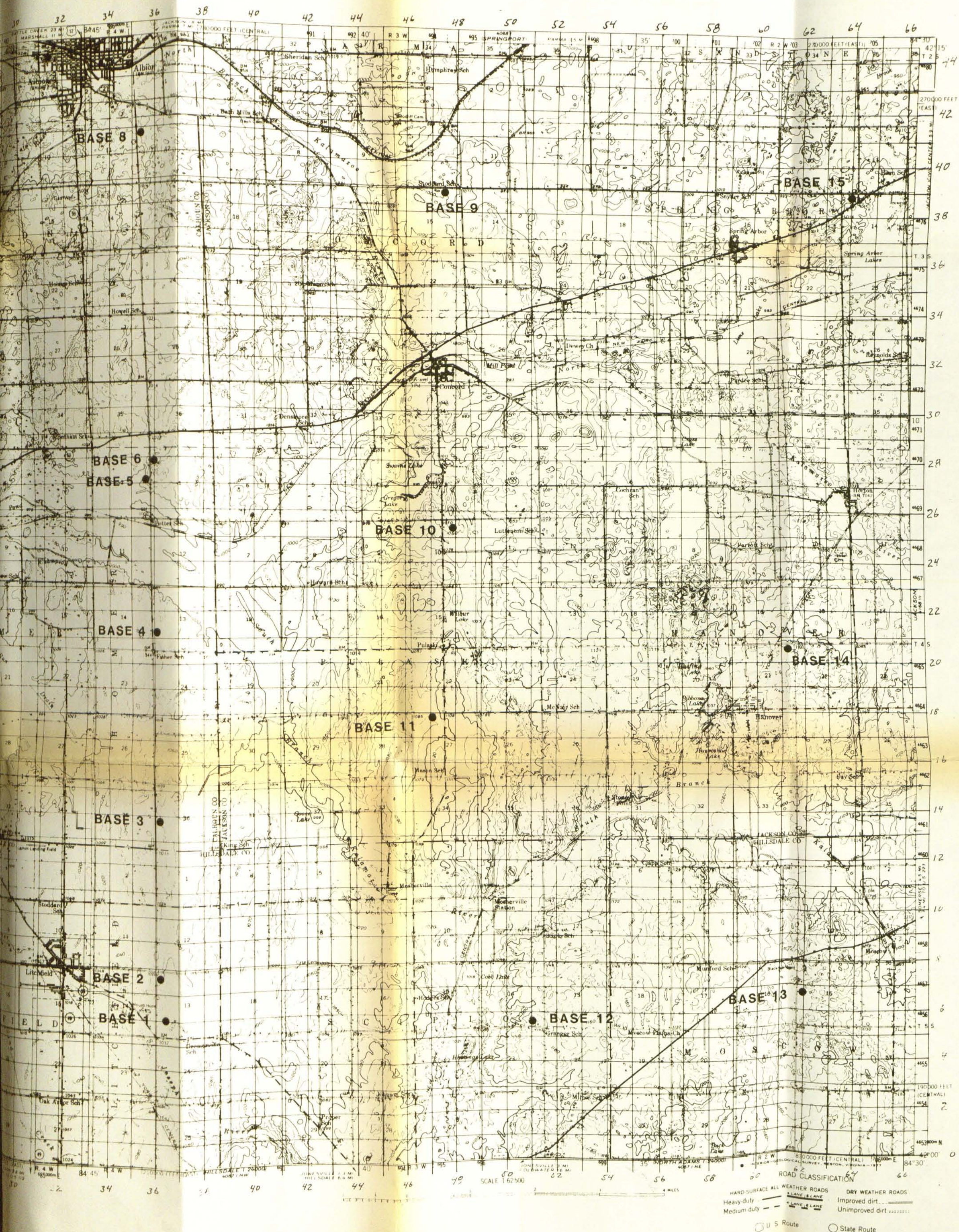

IETIC MAP OF THE ALBION–SCIPIO TREND

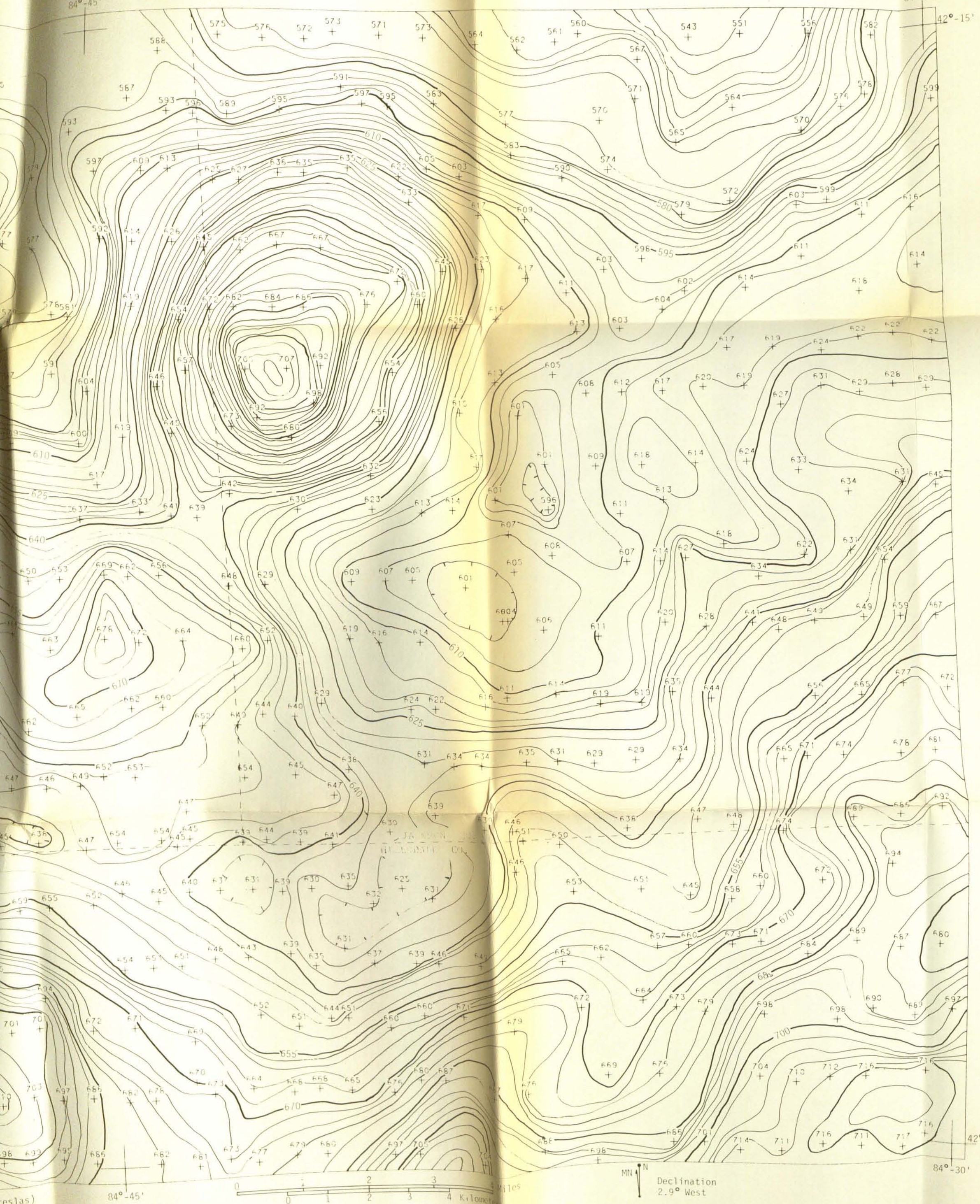

RESIDUAL GROUND MAGNETIC MAP O

85°-00' Total intensity magnetic values can be obtained by adding 57,000 gammas.

Contour interval 3 gammas (Nanoteslas)
15 gammas in zone of steep gradient

84°-45'

ENCLOSURE 2

D MAGNETIC MAP OF THE ALBION-SCIPIO TREND

84°-45'

84°-30'

42°-15'

42°-00'

PROFILE B

B

E

F

G

H

JACKSON CO.

HILLSDALE CO.

(Nanoteslas)
p gradient

0 1 2 3 4 Miles

0 1 2 3 4 Kilometers

MN N

Declination
2.9° West

INTERPRETIVE RESIDUAL GROUND MAGNETIC

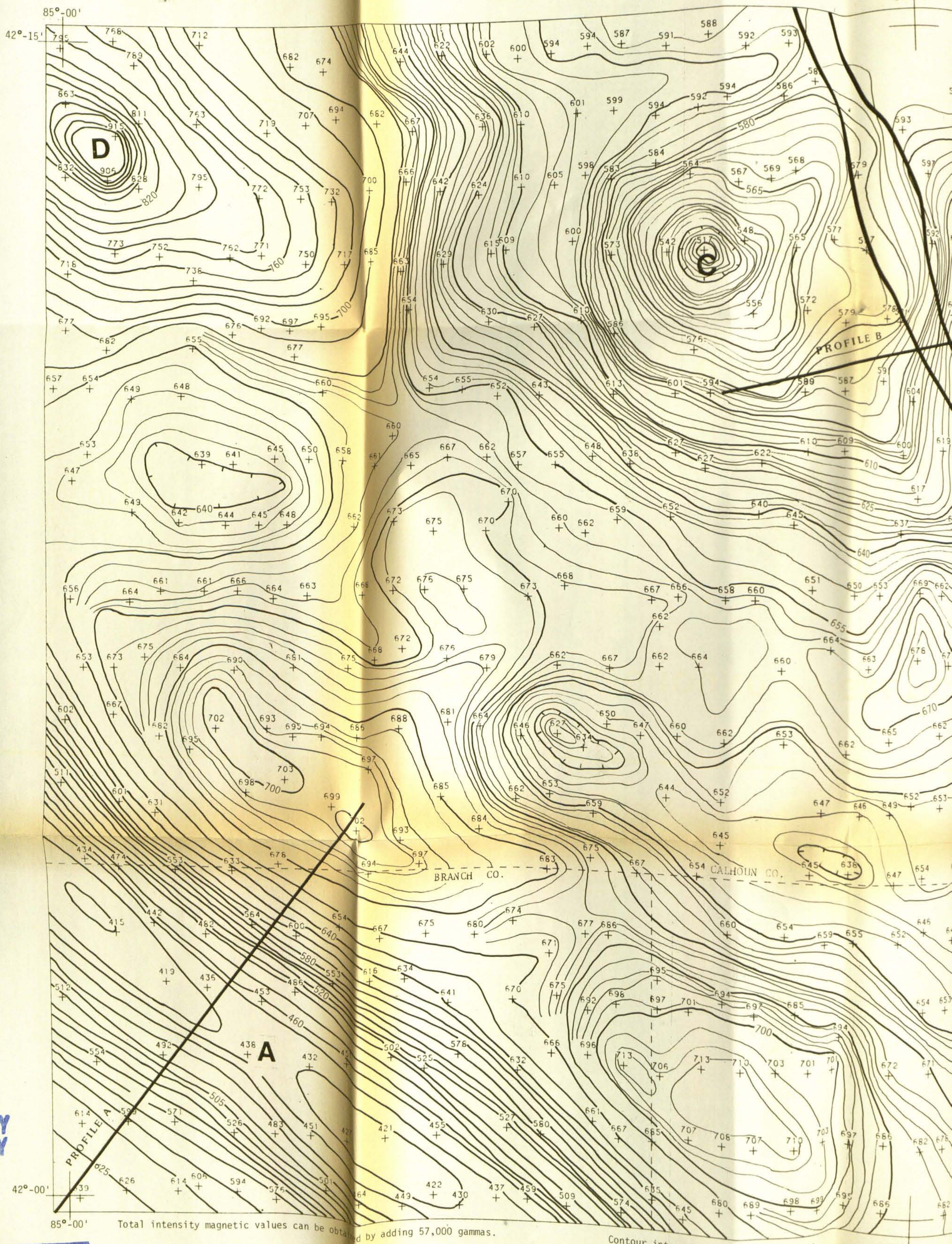

Total intensity magnetic values can be obtained by adding 57,000 gammas.

Contour interval 3 gammas (Nanoteslas)
15 gammas in zone of steep gradient

PRODUCING ZONE

MAGNETIC FEATURE

ENCLOSURE 3